Human Mobility Perturbation and Resilience in Natural Disasters

Qi Wang

Dissertation submitted to the faculty of the Virginia Polytechnic Institute and State University in partial fulfillment of the requirements for the degree of

Doctor of Philosophy
In
Civil Engineering

John E. Taylor, Chair
Michael J. Garvin
Ignacio T. Moore
Arika Ligmann-Zielinska

April 9th, 2015
Blacksburg, VA

Keywords: Human Mobility; Natural Disasters; Geo-Social Networks; Resilience; Big Data.

Human Mobility Perturbation and Resilience in Natural Disasters

Qi Wang

ABSTRACT

Natural disasters exert a profound impact on the world population. In 2012, natural disasters affected 106 million people, forcing over 31.7 million people to leave their homes. Climate change has intensified natural disasters, resulting in more catastrophic events and making extreme weather more difficult to predict. Understanding and predicting human movements plays a critical role in disaster evacuation, response and relief. Researchers have developed different methodologies and applied several models to study human mobility patterns, including random walks, Lévy flight, and Brownian walks. However, the extent to which these models may apply to perturbed human mobility patterns during disasters and the associated implications for improving disaster evacuation, response and relief efforts is lacking. My PhD research aims to address the limitation in human mobility research and gain a ground truth understanding of human mobility patterns under the influence of natural disasters. The research contains three interdependent projects. In the first project, I developed a novel data collecting system. The system can be used to collect large scale data of human mobility from large online social networking platforms. By analyzing both the general characteristics of the collected data and conducting a case study in NYC, I confirmed that the data collecting system is a viable venue to collect empirical data for human mobility research. My second project examined human mobility patterns in NYC under the influence of Hurricane Sandy. Using the data collecting system developed in the first project, I collected 12 days of human mobility data from NYC. The data set contains movements during and several days after the strike of Hurricane Sandy. The results showed that human mobility was strongly perturbed

by Hurricane Sandy, but meanwhile inherent resilience was observed in human movements. In the third project, I extended my research to fifteen additional natural disasters from five categories. Using over 3.5 million data entries of human movement, I found that while human mobility still followed the Lévy flight model during these disaster events, extremely powerful natural disasters could break the correlation between human mobility in steady states and perturbation states and thus destroy the inherent resilience in human mobility. The overall findings have significant implications in improving understanding and predicting human mobility under the influence of natural disasters and extreme events.

Dedicated to my wife Lily and my daughter Jasmine.

ACKNOWLEDGEMENT

My journey of PhD study has been an incredible though sometimes overwhelming experience. I resonate with Professor Robert Sampson's statement that conducting research in "interdisciplinary 'big science' was as painful as it was exhilarating." Fortunately, love, support and help accompanied me during my journey and allowed me to overcome the confusion, difficulties, and even pain.

I would like to thank my PhD advisor John Taylor for recruiting me into the Civil Engineering Network Dynamics Laboratory, giving me enormous support and freedom to initiate a new research area in the group, and guiding me through so many difficulties in my research, my services, my career development, and my life. I would like to thank Michael Garvin for providing me the opportunity to join the interdisciplinary BioBuild program and being an amazing mentor and friend. He and Professor Taylor together showed me how a professional life could be full of passion and fun as well. I also would like to thank my other committee members Arika Ligmann-Zielinska and Ignacio Moore for their insightful suggestions and comments, and tremendous support during my difficult times.

I was fortunate to be surrounded by some extremely intelligent and dynamic friends and colleagues. Without the many discussions and debates we shared over my research this dissertation would not have been possible. I would like to thank Josh Iorio for helping me shape my research ideas and define its scopes as well as advising on my writing. Special thanks to Rimas Gulbinas and Amy Tang for their suggestions on my research and their companionship during my difficult time. I also would like to thank Neda Mohammadi and Yilong Han for their unconditional and genuine support.

I would like to acknowledge several funding resources. This research was supported by the National Science Foundation under Grant No. 1142379 and by the Virginia Tech BioBuild Interdisciplinary Graduate Education Program (IGEP) grant. Additionally, open access publication of a journal article based on my PhD research was supported by Virginia Tech's Open Access Subvention Fund. The funders had no role in study design, data collection and analysis, decision to publish, or preparation of the manuscript. Any opinions, findings, and conclusions or recommendations expressed in this material are those of the author(s) and do not necessarily reflect the views of the financial sponsors.

Finally, I would like to thank my family for their support, patience and love. I want to thank my parents for supporting my dream to pursue a PhD degree even though it means their only son would have to move far away. Last but not least, I would like to thank my wife and my daughter. Their love, hugs, and laughter made my life whole, peaceful and passionate at the same time. Without those, this dissertation will never happen.

Table of Contents

List of Figures

List of Tables

CHAPTER 1: INTRODUCTION

1.1 A Global Challenge from Natural Disasters

The world is facing growing threats from natural disasters. From 2000 to 2012, natural disasters caused 1.7 trillion dollars of economic loss, killed 1.2 million people and affected half of the entire population on earth (UNISDR, 2013). Looking into the future, both the magnitudes and frequencies of natural disasters are expected to increase. Such increase is due to global environmental change. Human activities and fossil fuel consumption are causing global warming. Analysis shows that the global annual mean surface air temperature has increased during the last 65 years (Stocker et al. 2013). Almost all simulation models project that such a trend will continue for the next 20 years. The trend of global warming has caused the steady retreat of glaciers (Oerlemans 1994) and impacted sea levels (Meehl et al. 2005). Global warming also caused anomalous tropical sea surface temperatures and global aridity. Dry periods lasting for decades have occurred multiple times during the last millennium across the world (Dai 2013). While aridity will increasingly influence most of the regions in the world, the regions like the United States which have avoided prolonged droughts during the last 50 years due to natural climate variations may see persistent droughts in this century. Global warming is influencing tropical cyclones as well. Records show that the frequency of Atlantic tropical cyclones has increased for the last 100 years, and the increasing trend has accelerated since the 1980s (Landsea et al. 2010). By 2100, the intensity of tropical cyclones is predicted to increase by 2-11% (Knutson et al. 2010). Therefore, it is predicted to be a long-term, continuous issue for humans to prepare for and be resilient to natural disasters.

Urban areas, especially those in large cities and population centers, have developed different coping mechanisms to fight natural disasters. Among these mechanisms, top-down disaster response and evacuation plans are particularly prevalent. These plans evaluate possible risks brought by different disasters and attempt to control and minimize the consequences. However, the effectiveness of these top-down plans is often questioned due to their lack of sufficient understanding and consideration of human behaviors (Chakraborty et al. 2005; Drabek 2000; Wolshon and Marchive III 2007). Take New Yorkers' actions during Hurricane Sandy as an example. Only about one third of the population living in the mandatory evacuation zones left those areas (Schuerman 2013). Because of the inaccurate estimation of the flooding zones, even the evacuated residents could still be in severe danger (Rosenzweig and Solecki 2014)[1]. The unfortunate loss of lives shows that it is critical to gain a ground truth understanding of human behaviors during natural disasters.

1.2 Human Mobility and Natural Disasters

Understanding human mobility is a key component to gain a ground truth understanding of human travel behaviors during natural disasters. Research in this field can improve our understanding and prediction of human mobility during emergencies. Additionally, it can facilitate policy development and decision-making during natural disasters, resulting in less injuries, fatalities, and economic loss.

Research of human mobility originated from the research on animal movement patterns, which can be dated to over one hundred years ago. Pearson (1905) first proposed a mathematical model

[1] Detailed discussion of the situation of NYC under the influence of Hurricane Sandy can be found in section 3.4.

to capture human and animal movements. The model proposed that an individual moves consistently, and each move has a set distance through a randomly different angle from its previous movements. Such a model is called a random walk model. Later on, Lévy modified the model and made the distances of steps follow a heavy-tailed probability distribution such as power-law (Mandelbrot 1983). This model was called Lévy flight. Research has shown that the movements of many types of animals follow Lévy flight (Bartumeus 2007; Benhamou 2007; Viswanathan et al. 1996).

Lévy flight observed in animal movements has inspired studies in human mobility. Brockmann (2006) was the first researcher to study human mobility using a large quantity of empirical data. By tracking the travel distances of 464,670 one-hundred dollar bills, the study confirmed that human mobility follows Lévy flight model. This study also demonstrated that the truncated power-law distribution governs human mobility, and the exponent value was found to be around 1.59. Such findings have been supported by multiple following studies with exponent values ranging from 1.59 to 1.88 (Brockmann et al. 2006; Cheng et al. 2011; González et al. 2008; Hawelka et al. 2014).

While Lévy flight is confirmed to be a fundamental model to describe human mobility, researchers have also discovered some other important patterns of human mobility regarding its boundaries (González et al. 2008), visitation frequency (Song et al. 2010a), predictability (Song et al. 2010b), configuration (Schneider et al. 2013), periodicity (Cho et al. 2011), etc. These findings have greatly improved the understanding and prediction of human mobility in general and in urban settings.

While human mobility has attracted some researchers' attention, research in this area is still limited. One significant limitation is the lack of research on human mobility during natural disasters and

extreme events. Such research is of critical importance from both theoretical and practical perspectives. From the theoretical perspective, understanding and predicting human mobility requires profound knowledge on human mobility perturbation and resilience. From the practical perspective, human mobility determines the effectiveness of evacuations. As Pan et al. (2007) pointed out, overcrowding and crashing during emergency situations can cause incidents and thus injuries and loss of lives. Take the snow storming that pummeled Atlanta in December 2013 as an example. Alarmed by the approaching of a severe snow storm in December 2013, the city of Atlanta issued a blizzard warning and advised people to leave school and work early. Without foreseeing the consequence of such a warning, many people crammed in roads and highways at the same time, and this caused a city-scale traffic jam. People were still stuck in the roads or forced to abandon their vehicles to seek shelters when the snow storm arrived (Beasley 2014). A ground-up understanding of human mobility can help reduce the reoccurrences of such traffic jams during emergencies. Additionally, human mobility can determine the effectiveness of information communications during emergencies. Natural disasters could possibly damage and/or destroy communication infrastructures, and in that case human movements would determine the width of temporary communication networks built on portable devices (Chaintreau et al. 2007; Feeley et al. 2004; Kleinberg 2007). Furthermore, deep understanding and accurate prediction of human mobility can potentially save lives. In the case of Hurricane Sandy, if we could have identified and predicted susceptible individuals and provided critical information, lives might have been saved. The critical roles of human mobility in both the theoretical and practical perspectives call for more in-depth examinations on human mobility.

1.3 Research Question

While previous studies have unveiled some important properties of human mobility, the findings are based on a basic assumption, even though it is not often explicitly stated by the researchers. The assumption is that human mobility is stable and consistent, and it experiences no external influences. While such an assumption is appropriate in some situations, it can overly simplify the phenomenon in other ones. During natural disasters and extreme events, it is intuitive to think that the dynamics of human mobility can be severely perturbed. Until now, the perturbation in human mobility remains a limited topic of inquiry. A key research question that has not been answered with depth is: how human mobility perturbs during natural disasters and how such perturbation can be quantified. Humans are at their most vulnerable during the occurrences of disaster events; their properties, health, and even lives are under severe danger. Understanding, quantifying and predicting human mobility in these situations can potentially help avoid economic loss and improve safety.

1.4 Research Methodology and Dissertation Structure

To address this broad research question, my PhD study focuses specifically on human mobility perturbation and resilience under the influence of natural disasters. I conducted three interrelated studies. The three studies examined the underlying mechanisms of human mobility patterns across a broad spectrum of factors such as travel constraints, movement distribution, center and radius of movements, and resilience.

In the first effort, I developed a novel data collecting system to gather human movement data. Recent technological advancements have enabled the possibility to collect large quantities of human movement data. Researchers have used multiple venues to collect data. These venues

include currency circulation, GPS, cell phones, geo-social networking platforms, etc. The unprecedented data quantity and granularity has enabled human mobility research on both the aggregate and individual levels. This research has reported some fundamental patterns in human mobility. However, there is still a dearth of research on how human mobility is influenced by abrupt changes of the natural environment. The lack of research may be the results of limitations in the data resources concerning data quantity, accuracy, representativeness and open access. My first project thus took an initial step to address this problem by developing a data collecting system. The system allowed me to collect high quality large scale data of human movements around the world and study human movements. The system implemented Twitter, a massive online social-networking platform. I conducted multiple analyses and confirmed Twitter was a viable venue to study human mobility.

My second effort studied human mobility of NYC residents under the influence of Hurricane Sandy. Using the data collecting system I previously developed, I gathered a large quantity of high resolution data to analyze human mobility patterns during Hurricane Sandy. The study examined and quantified both the human mobility perturbation and resilience during the strike of Hurricane Sandy.

Building on my second effort, my third study extended my research to fifteen more disaster events. I examined whether the human mobility patterns observed in NYC still stood true at other locations under the influences of different disasters. This project adopted a comparative approach, investigating multiple disaster events. This strategy counterbalances the tendency in some of the human mobility literature to make a comparison based on single cases. The results of this study demonstrated a more general pattern of human mobility perturbation and resilience. Thus, through

my research, I gained a ground truth understanding of human mobility under the impact of natural disasters.

The dissertation structure follows a three-paper format. Chapter 2 describes the development of the data collecting system from my first research effort. This chapter includes a description of the system's technical architecture, the principles behind the design, and the validation efforts of the system. The article was co-authored with Professor John Taylor and was published in the *Journal of Computing in Civil Engineering* (Wang and Taylor 2015).

Next, Chapter 3 includes a journal article that describes the novel study of human mobility perturbation and resilience of NYC residents under the influence Hurricane Sandy. The chapter presents the design of the study, the attributes of the empirical human mobility data, and the analytical results. The article was co-authored with Professor John Taylor and was published in the peer-reviewed journal of *PLOS ONE* (Wang and Taylor 2014).

In Chapter 4, I describe my methodology of examining human mobility patterns under the influences of different types of natural disasters. It is a natural extension from Chapter 3 and examines human mobility data of fifteen disaster events. These events can be categorized into five types. The article presented in this chapter is in preparation to be submitted to a peer-reviewed journal.

In Chapter 5, I discuss how my research contributes to human mobility research. In the Chapter 6, I identify the limitations that current human mobility research suffers and what future research avenues my research has enabled. References and supplementary materials referred to in this dissertation can be found at the end of the dissertation.

CHAPTER 2: PROCESS MAP FOR URBAN-HUMAN MOBILITY AND CIVIL INFRASTRUCTURE DATA COLLECTION USING GEO-SOCIAL NETWORKING PLATFORM[2]

2.1 Abstract

Human mobility is central to our understanding of design, planning, and development of civil infrastructure in urban areas. Although researchers have spent considerable effort in studying human mobility patterns, there is still a lack of human movement data with satisfactory quantity and accuracy. This paper introduces an approach to collecting human mobility data and discusses analyses conducted. A comprehensive process map was developed to collect human movement data from Twitter. The map included four steps and multiple programmed modules, processes, and databases. Via the process map, human mobility data was collected, and a one-month subset from NYC was retrieved to use in a case study. Results from the case study aligned with findings from existing human mobility research, and thus Twitter was confirmed to be a viable resource for studying city-scale human mobility. Large-scale human mobility data will allow researchers to study the interdependence of human activity and civil infrastructure as a way to deepen understanding of important city-scale phenomena such as evacuation during extreme events and the spread of epidemics.

[2] This paper was co-authored with Professor John E. Taylor and was published in the Journal of Computing in Civil Engineering.
Wang, Q. and Taylor, J. (2015). "Process Map for Urban-Human Mobility and Civil Infrastructure Data Collection Using Geosocial Networking Platforms." *ASCE J. Comput. Civ. Eng.* , 10.1061/(ASCE)CP.1943-5487.0000469 , 04015004.

Keywords: *Geosocial networking; Human mobility; Infrastructure development; Twitter; Urban development*

2.2 Introduction

An increasing number of people are migrating to and living in urban areas. The urban population increased from 1.01 billion in 1960 to 3.69 billion in 2012 (World Bank 2013). This number surpassed the population of rural areas in 2009 for the first time in human history (United Nations 2009). A growing population has made urban areas more active and complex. A variety of infrastructure systems are built to accommodate the increasing number of urban dwellers and their movements. The coupling of human and infrastructure systems forms an interdependent sociotechnical system.

Although interactions and mutual influences of humans and infrastructure are prevalent in this sociotechnical system, human mobility plays vital roles in, and is influenced by, different aspects of the urban environment and civil infrastructure development (Estabrooks et al. 2003; Sandercock et al. 2010; Van Dyck et al. 2011). The influence of human mobility can be observed in transportation networks (Badland and Schofield 2005; Huang et al. 2013), energy and power supply (Gulbinas et al. 2014; Menassa et al. 2014), and other significant areas such as disaster evacuation and response (Bengtsson et al. 2011; González et al. 2008; Song et al. 2010a, b; Wang and Taylor 2014; Wesolowski et al. 2012). Human movements and activities determine the development and sprawl of civil infrastructures, but infrastructures also impact the means, schedules, paths, and configurations of human movements. The interaction and reciprocal influence of the two play a substantial role in shaping urban forms and functions (Du and Wang 2011; Fan and Khattak 2008). Therefore, understanding and predicting the patterns of human

mobility can promote understanding of and solutions to urban issues, and can drive policy making related to urban planning, disaster evacuation and response, and public health provisioning.

The importance of such understanding has drawn research interest from multiple fields for decades, yet research on human mobility is limited. The lack of research has several reasons, but a main one is the difficulty of collecting large quantities of human movement data with satisfactory precision and accuracy. Because of the scarcity of empirical data, human mobility was historically assumed to follow the same pattern observed in animal movements, although limited evidence existed to prove or disprove that assumption (Pearson 1905; Ramos-Fernandez et al. 2004). Owing to the breakthroughs in the field of information technology and geographical locating techniques, it is now possible for researchers to access large amounts of human movement data. Researchers have studied human mobility using currency circulation, global positioning systems, wireless services, and geosocial networking media (Brockmann et al. 2006; Cho et al. 2011; González et al. 2008; Noulas et al. 2012; Song et al. 2010a, b; Wang and Taylor 2014).

Researchers have begun using geosocial networking platforms to study human mobility in urban areas (Cho et al. 2011; Noulas et al. 2012; Noulas et al. 2011). These platforms, such as FourSquare, Gowalla, Brightkite, Twitter, and Facebook, allow users to self-report their locations by checking in. The open design of some of these platforms allows free and unlimited accesses to users' locations via open application programming interfaces (APIs) (Kwak et al. 2010; Russell 2011; Russell 2011). The strength of these platforms is that they not only record precise geographical information about a user's location but also provide opportunities to understand how geographical and social networks are interrelated.

Despite a number of recent advances in human mobility research, there are still several gaps. One of them is that research to date has been limited to small platforms (Cho et al. 2011; Lindqvist et

al. 2011; Noulas et al. 2012; Noulas et al. 2011), missing the opportunity to track mobility using more massive social networking platforms with larger numbers of users. Some of these more popular social media, such as Facebook, Twitter, and Google+, have integrated geosocial networking functions into their platforms. By September 2013, one of the most popular geosocial networking platforms, FourSquare, had over 45 million users (Smith 2014). Meanwhile, Facebook had attracted 1.23 billion (Smith 2014), Twitter, 600 million (Statistic Brain 2014), and Google+, 540 million (Isaac 2013). Unfortunately, there is a lack of research establishing these more massive online social networking platforms as venues for studying human mobility.

Despite its importance, a paucity of research has used geosocial networking to study the interactions of human mobility and civil infrastructure. Yet researchers have realized the value of empirical human mobility data in studying key civil infrastructure issues. Several studies have used cell phone data to study road usage in urban areas (Toole et al. 2014; Wang et al. 2012; Wang et al. 2014), even though data resources are usually of lower precision and lack open access. Researchers have also started using mobile computing and geosocial networking platforms for infrastructure development and assessment (Nik Bakht and El-Diraby 2013; Walker et al. 2014). Several recent studies examined the role of Twitter during and after disaster events (Bland and Frost 2012; Sutton et al. 2011; Sutton et al. 2013; Sutton et al. 2013; Sutton 2009; Sutton 2010; Wang and Taylor 2014), but these studies primarily focused on communication, broadcasting, and social networking functions. Studies that have incorporated the geosocial networking functionality of Twitter or other large-scale social media to explore challenging urban civil engineering problems have been few.

This paper proposes a comprehensive process map to collect human mobility data from Twitter. The reason Twitter was chosen is that it was designed to share public information and has an open

API to collect a large quantity of human mobility data. Several Python modules were developed to implement the process map. Then a case study was conducted and data from NYC were analyzed. The results were compared with existing studies and are discuss in detail. The paper concludes with a discussion of promising future research directions enabled by the use of Twitter to study human mobility.

2.3 Background

Collecting empirical data on human mobility is a difficult task. As mentioned previously, some early studies assumed that human movements had the same patterns as animal movements. Pearson (1905) first proposed the problem of random walks over a century ago. Although a purely mathematical problem at the beginning, this simple model has been used to capture the phenomenon of movements in different areas, especially biology and ecology (Bartumeus et al. 2005; Byers 2001; Kareiva and Shigesada 1983; Spitzer et al. 1964; Wang and Landau 2001). The random walk was an important discovery, but the lack of adequate and accurate data greatly limited its applicability in human mobility.

Researchers have also studied the reciprocal influences of human physical activities and the built environment (Badland and Schofield 2005; Bassett et al. 2000; Du and Wang 2011; Fan and Khattak 2008). Findings from such studies have expanded our understanding of human movements; however, they have predominantly relied on pedometers and/or surveys to collect data, neither of which provide accurate geographical information on locations and trajectories.

2.3.1 Information Technology and Human Mobility

For several years, researchers have been using information technologies to collect human movement data. For example, Brockmann et al. (2006) used the circulation of bank notes to study

human mobility. By analyzing more than a million individual displacements in the United States, they found that the distances of human travel follow a power law and that the fundamental distribution of human movements can therefore be captured by Lévy flight, a scale-free, heavy-tailed random walk model. Although such a finding was an important breakthrough, the study suffered from several limitations. First, the circulation of one bank note may have been composed from the movement trajectories of multiple persons. Also, it is unlikely that people limited their activities to areas in and around banks.

To address the aforementioned limitations, researchers began collecting data from mobile phones. When a person makes a phone call or receives/sends a text message, the nearest cell phone tower routes the communication, and its location—roughly the user's location—is recorded (González et al. 2008; Wesolowski et al. 2012). Connecting the location data reveals an individual's movement trajectory. Cell phone data naturally distinguish individuals because each cell phone is most likely to follow just one individual. Also, although bank notes diffuse, cell phones do not, so they are more suitable to recording people's primary locations. González et al. (2008) studied human mobility using two data sets, one of which contained data from 100,000 mobile phone users over a six-month period. They found that the distribution of incremental displacements of all individuals followed a truncated power law distribution, aligning with the findings from Brockmann et al. (2006). They also showed that individual trajectories were largely indistinguishable after rescaling using the radius of movement gyrations. This study discovered some fundamental laws of human mobility and provided important implications for large-scale agent-based human mobility models.

Song et al. (2010a, b) expanded this research, developing a human mobility model using cell phone data—that is, a three-month-long record of 50,000 mobile phone users—that adopted entropy as

the fundamental quantity to capture the movement of individuals and predict their locations. The study concluded that a person's daily movements exhibited inherent regularity. Predictability of movement could peak at 93% accuracy, although determining individuals' exact locations was beyond the model's capability. Later, Song et al. (2010a, b) investigated a larger data set that contained 1 million mobile phone users for a year-long period. They observed three unique characteristics of human mobility that both the Lévy flight model (Brockmann et al. 2006) and the continuous-time random walk model (Metzler and Klafter 2000; Montroll and Weiss 1965) failed to explain. These characteristics were (1) a person's decreasing tendency to visit new locations; (2) an uneven frequency of visits to different locations; and (3) ultraslow diffusion, meaning that people tended to return to the same locations (home, office, etc.). Based on these observations, Song et al. (2010a, b) developed a new individual mobility model by adding two unique generic mechanisms: exploration and preferential return. This new model was more representative of human mobility patterns compared with other models, but its strength was in capturing long-term spatial and temporal scaling patterns. It was less ideal for studying daily human movements in short periods within the boundaries of urban areas.

Despite having enabled important findings, cell phone data have their own limitations. First, the precision of the data is determined by the distributions and coverage areas of cell phone towers. Generally the coverage area of each cell phone tower is 1–3 km^2. Such precision has been instrumental in developing an understanding of general patterns of human mobility over larger scales (e.g., a state or a country), but it may not be able to capture human mobility at smaller scales (e.g., a district or a city). Second, most of the data are privately owned and proprietary, with virtually no open access to most researchers. Therefore, researchers have difficulty accessing

large-scale human mobility data and cannot verify/validate the findings from existing studies (Huberman 2012; Ravetz 2012). A detailed discussion can be found in Markoff (2012).

2.3.2 Geosocial Networking and Human Mobility

Now researchers are beginning to use geosocial networking platforms to study human mobility. These platforms provide a geo-locating function that can communicate with the GPS units inside devices such as cell phones, computers, and tablets. When a person uses these platforms or applications, his or her geographical location is recorded. Human mobility data collected from these platforms have several advantages. First, the data often have higher accuracy—3–8 m compared with the 1–3 km of cell phone data [National Coordination Office (NCO) 2014]—although accuracy is influenced by device quality. Such accuracy is more promising when studying human movements at smaller scales in urban areas. Second, other than movements, these platforms provide social relation information about users. The extra information sheds light on the causes of human movements and thus may improve the predictability of human mobility. Cho et al. (2011) used geosocial networking platforms to attempt to answer the question of how social relations influence mobility patterns. They collected empirical movement data from Gowalla and Brightkite, two online location-based social networking websites. These platforms not only provide more precise location information because they combine GPS signals with wireless networks; they also disclose social relationships among users. Using geographical movements, temporal dynamics, and social relations, the researchers developed both a periodic mobility model and a periodic and social mobility model. The latter showed up to 30% better predictive performance when compared with the former. Also, the models could predict the exact location of individuals with up to 40% accuracy. In another study, Noulas et al. (2012) used FourSquare to study human mobility in urban areas. Thirty-one large cities around the world were selected, and human movement data from

them were analyzed. The researchers found that global movements followed a power law distribution and that human mobility in all of the cities studied followed almost the same pattern.

Twitter has also been used to study geosocial networking. One of the largest online networking platforms, Twitter, adopts an open design to encourage information dissemination, broadcasting, and social networking. Taking advantage of this open access, researchers have used Twitter to study privacy (Hauff and Houben 2012; Hecht et al. 2011; Mao et al. 2011; Vicente et al. 2011), crowd behaviors (Lee and Sumiya 2010; Lee et al. 2011; Wakamiya et al. 2013), sociospatial properties of online social networks (Scellato et al. 2011; Scellato et al. 2010; Scellato et al. 2011), and global information cascades (Ikawa et al. 2012; Scellato et al. 2011; Scellato et al. 2011), among other phenomena. In addition, geotagged tweets (i.e., microblogs) are now being used to study human mobility.

Using Twitter data, Kinsella et al. (2011) developed a model to predict human locations and human behaviors at locations. They claimed that their model provides more accurate prediction of locations than current commercially available models. Hawelka et al. (2014) examined Twitter users as proxies to study global transportation. They found that global human mobility followed a power law distribution with a scale variance of 1.62. They also discovered Twitter to be a valuable proxy for human mobility at the country level despite the fact that the geographical coordinates embedded in geotagged tweets had far higher resolutions.

The studies just described led the way to employing geosocial networking websites in the study of human mobility, but there still remain some important research gaps. First, users' demographic information is unknown, and there is a lack of data confirming that the user bases from these platforms are representative of the general population. Without such confirmation, it is unclear

whether significant bias exists in these studies. Second, urban mobility research has mostly focused on small and medium-size geosocial networking platforms, with limited extension to some of the more massive and popular social networking platforms. Studies that adopted Twitter as their data source did not develop and publish systematic procedures for data collection that would guide others in pursuing similar data collection approaches. Third, additional research is necessary to resolve some contradictory findings from existing studies. For example, although research based on cell phone data showed that human mobility follows Lévy flight in general (Brockmann et al. 2006; González et al. 2008), Noulas et al. (2012) observed no such pattern from the movement data in urban areas using FourSquare.

These gaps highlight the need for research into human mobility using massive online geosocial networking platforms, particularly Twitter. Twitter's huge social network structures, broad user base, and rich communication data can enhance understanding of human mobility. Until now, the lack of a comprehensive and transferable data collection system hindered the academic community in its exploration of the full potential of Twitter. To overcome this lack, the current study proposed a methodology to collect and analyze data from online geosocial networking platforms. The focus of this study was Twitter, and a process map to collect human mobility data was developed. Also, the study compared the quantity of data collected from Twitter with quantities from other geosocial media used in previous studies. The data were analyzed and the results were compared with the findings from research based on both mobile data and data from relatively small-scale social networking platforms. This effort will promote the development of human mobility models to simulate and predict human mobility in populous cities in the future.

2.4 Data Representativeness and Collection

2.4.1 Representativeness of Twitter Users

Twitter is an online social networking medium that allows people to post text messages limited to 140 characters, called tweets. Users can also choose to let Twitter add location information, called a geotag, to each tweet they post. Each geotag contains the exact geographical coordinate of the tweet.

Before creating an approach to collecting Twitter data, the study first examined demographic information about Twitter users. As previously mentioned, Twitter has a tremendously large user base and an open design that together make it potentially an ideal platform to collect human mobility data. However, to confirm its applicability, the first step was to confirm that Twitter users are representative of the general population. Unfortunately, only limited data were available, of which most concentrated on U.S. users. Because of this data scarcity, the study examined the demographic information about U.S. Twitter users (Bennett 2013) and compared it with demographic information about the general U.S. population (Howden and Meyer 2010; USCB 2012; USCB 2012; USCB 2013; USCB 2014). The comparison and data sources can be found in Table 1, where it is observed that Twitter users are well distributed in different demographic groups in different categories. They are also representative of the general population in gender, race, age, and income. The main difference is that less of the general population has completed higher education. People with higher education are more likely to use Twitter.

Table 1: Demographics Comparison

Categories	Demographics	Twitter Users[1] (%)	U.S. Population (%)
Gender	Men	50.8	49.2[2]
	Women	49.2	50.8[2]
Race	White, Non-Hispanic	70.9	68.1[3]
	Black, Non-Hispanic	9.6	13.1[3]
	Hispanic	11.7	16.9[3]
Age	18-29	18.8*	22.0*[4]
	30-49	33.3*	36.1*[4]
	50-64	28.3*	25.0*[4]
	65+	19.6*	16.9*[4]
Education	High school grad or less	26.6	42.1[5]
	Some college	30.0	29.0[5]
	College+	42.8	28.9[5]
Income	Less than $30,000/yr	22.6	29.9[6]
	$30,000-$49,999	17.9	20.2[6]
	$50,000-$74,999	12.9	18.1[6]
	$75,000+	33.6	31.6[6]

1: (Bennett 2013); 2: (Howden and Meyer 2010); 3: (USCB 2014); 4: (USCB 2012); 5: (USCB 2013); 6: (USCB 2012)
*Since data from Twitter users only included those whose ages were above 18, we excluded people under 18 in the general population. Then we adjusted the values for the rest of the age groups such that the sum equals to 100 percent.

2.4.2 Process Map for Twitter Data Collection

Using the Twitter public API, a process map to collect public tweets was developed. The map contained four steps, as shown in Figure 1. Each step comprised a programmed module, several processes, and a database to store the data generated. The steps are described in the following sections.

2.4.2.1 Step 1: Collect Geotagged Tweets

The first step was to collect tweets that contained geotags. A geotagged tweets streaming module was developed establishing a continuous connection between a computer in the research lab and the Twitter server. The connection streamed every tweet containing a geotag. *Tweepy*, a Python package for implementing the Twitter API, was used to develop the module. In addition to the exact geographical coordinate, each streamed tweet contains its ID, place name, name and ID of the user who posted it, and a time stamp. The collected tweets were stored in a database called **GeoTweets**. A reconnecting mechanism was coded so that, if the continuous connection was lost for 30 seconds, a restart message was displayed and a new connection established.

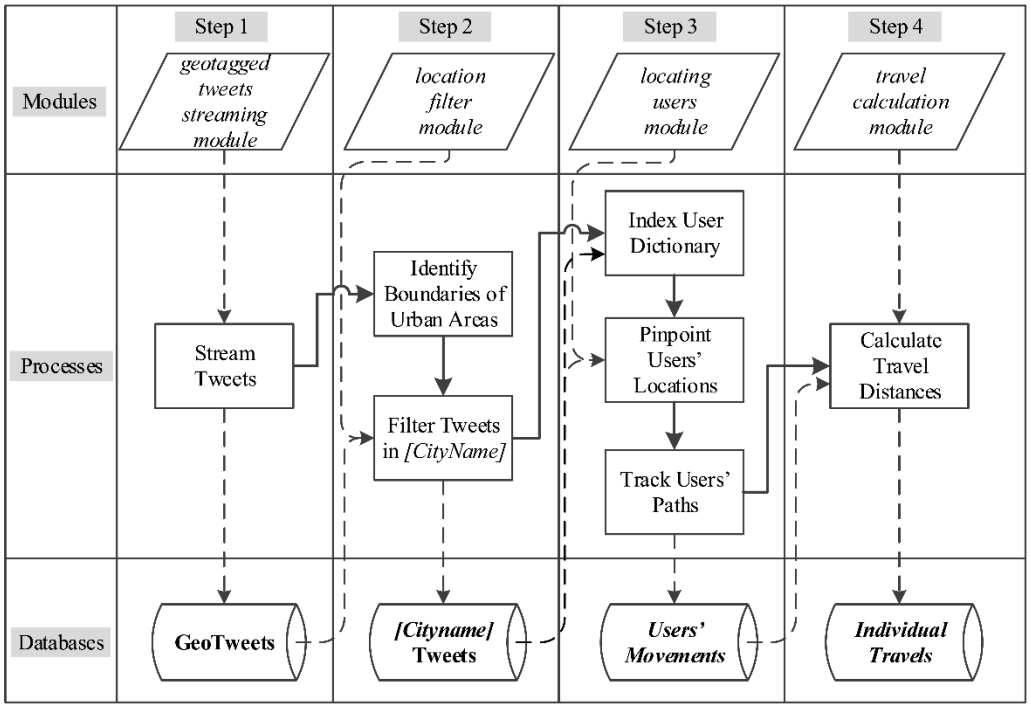

Figure 1: Process Map for Twitter Data Collection

2.4.2.2. Step 2: Filter Tweets in Specific Geographical Boundaries

In this step, the process map helped filter data in urban areas. The first process identified the geographical boundaries of urban areas. The boundaries depended on the research subjects. For example, to study how natural disasters influence urban areas, the boundaries should be set as the cities visited by natural disaster events. Although the boundaries can be simple boxes, they can also be detailed borderlines of cities. The next process tested whether the geographical coordinate of each tweet was within the boundary. As mentioned before, geospatial information is embedded in each tweet, so a *location filter module* was designed for this step. The module retrieved each tweet in the **GeoTweets** database and determined its geographical coordinate. If the coordinate fell within the city, the tweet was selected and imported into a second database called **[*CityName*]Tweets**.

2.4.2.3 Step 3: Retrieve Human Movement Data

In this step, each individual's locations and movement trajectories were identified. The first process was to retrieve the data stored in ***[CityName]*Tweets** and identify all unique individuals. All users were indexed into a dictionary, which was a data set comprising associated arrays and indexed by keys. Each array followed the data structure shown here:

$$Distionary = \begin{bmatrix} user1 : tweet1, tweet2, tweet3, \ldots \\ user2 : tweet1, tweet2, tweet3, \ldots \\ \ldots. \\ usern : tweet1, tweet2, tweet3, \ldots \end{bmatrix}$$

After the dictionary was created, the next process pinpointed the location of each tweet using the *locating users module*, which retrieved the geographical coordinate from each tweet. Then it

reestablished a user's movement path by connecting all the coordinates. All location and trajectory data were stored in a separate database called **Users' Movements**.

2.4.2.4 Step 4: Quantify Travel Distances

The last step was to quantify travel distances. Using the *travel calculation module*, the distance between two consecutive locations was determined according to the following formula (Robusto 1957):

$$d = 2r \times \sin^{-1}\left(\sqrt{\sin^2\left(\frac{\phi_2 - \phi_1}{2}\right) + \cos\phi_1\phi_2 \sin^2\left(\frac{\varphi_2 - \varphi_1}{2}\right)}\right)$$

Where r is the earth radius, which approximately equals to 6,367,000 meters, ϕ is the latitude, and φ is the longitude. The results are stored in the **Individual Travels** database.

2.5 Case Study: Tweets in NYC

To verify and validate the proposed process map, a case study was carried out in the NYC area. First, the *geotagged tweets streaming module* was set up to run for 30 days (October 1, 2013, to October 31, 2013). As mentioned before, a reconnecting mechanism was built into the module to prevent losing the stream; however, during the 30-day period no reconnection was observed. Approximately 121 million tweets were streamed into the **GeoTweets** database.

The second module, the *location filter module*, was then tested. The urban area was constrained within 74°15′W–73°40′W longitude and 40°30′N–40°57′N latitude, which covered NYC entirely. The module filtered every tweet by its embedded coordinate. If the coordinate was within the area, the tweet was selected and imported into the **NYCTweets** database. Then, via the third module,

the locations for each user were determined and the movement path for that user was retrieved. For users with at least two displacements, a connection was made for each individual's visited locations and his/her trajectory was extracted. Via the fourth module, all displacements were calculated from the coordinates embedded in the tweets. A displacement was the distance of two consecutive locations from the same individual. Human-based checking was conducted to ensure that the programming codes were accurate for each module. Also, the data collection process and the structure of the retrieved data were examined. Continuous data accumulation confirmed that human mobility data were streamed into the database. Finally, all the data from NYC were plotted into *ArcGIS* and it was confirmed that the distribution of sampled data fell within the boundaries of the city. All of these efforts were undertaken to verify that the data collection system was collecting data as it was designed to.

To validate that Twitter data can be used to study human mobility, the study used several methods to analyze the NYC data. These methods are discussed in the following sections.

2.5.1 Find Data Quantity

Data quantity is important in the study of human mobility. Big data can minimize statistical biases and potentially provide deep insights. For this reason, the study first calculated the quantity of data and compared the results with those from other popular geosocial networking platforms. After filtering, the **NYCTweets** database contained 1,168,961 tweets from 93,375 users. The geographical distribution of the tweets from 00:00:00 on October 1, 2013, to 23:59:59 on October 1, 2013 EST, is shown in Figure 2. There were 38,263 tweets collected, and each black point shows the location where each was posted.

A total of 1,075,586 displacements and a total of 61,576 individual movement trajectories were found. Figure 3 shows the movement trajectories on October 1, 2013. The study's data showed that most trajectories radiated from the Manhattan area to other places in NYC. It was also clear that, whereas some trajectories covered long distances, others spanned relatively short ones.

2.5.2 Fit Data to Power Law Distribution

As discussed before, it has been observed that the power law dominates human mobility, and so Lévy flight captures human movements (Clauset et al. 2009; González et al. 2008; Klaus et al. 2011). Therefore, the study first fitted the displacement data to a truncated power law distribution, which can be captured by the following equation:

$$P(\Delta r) \propto \Delta r^{-\beta} e^{-\lambda \Delta r}$$

Where Δr is the displacement, β is the scaling parameter, and λ is the exponential cutoff value. To test the goodness of fit, we conducted a Maximum Likelihood Estimation test to compare truncated power-law distribution to both exponential distribution and lognormal distribution. Maximum Likelihood Estimation is a statistical method to estimate which statistical model has higher goodness of fit to the empirical data (Johansen and Juselius 1990; White 1982). The Python package powerlaw was used for fitting and Maximum Likelihood Estimation.

After fitting the displacement data to truncated power law distribution, we found that the β value was 1.09, and λ value was 3.78×10-5, and x_{min} was 3.0m which is the smallest distance of displacements to be fitted in the distribution. The Maximum Likelihood Estimation reported that power law distribution can fit the data better compared to both exponential distribution and lognormal distribution (p-values <0.001).

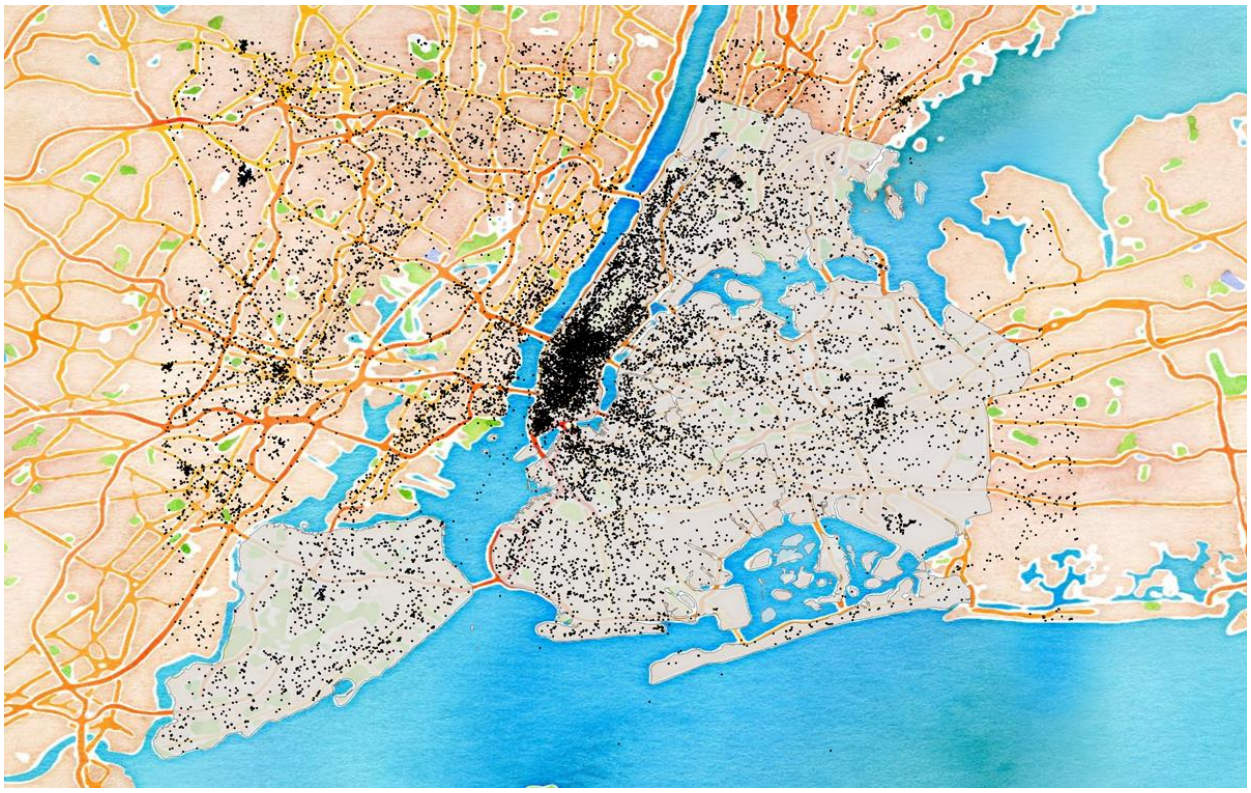

Figure 2: Tweets Locations in NYC on October 1, 2013
(© OpenStreetMap contributors)

2.5.3 Find Primary Locations

Using cell phone data, Schneider et al. (2013) showed that 7 locations can cover 90 percent of all the locations an individual visited. We analyzed human mobility data from Twitter to see whether such a trend existed in Twitter data. For each user, we retrieved all his/her geographical coordinates, then we identified all the locations he/she visited. Each location covered 0.01 km^2 (100 m*100 m). People's movements within this area were deemed trivial, and counted as multiple visitations to the same location. The number of locations covering 90% or more of all locations was then determined.

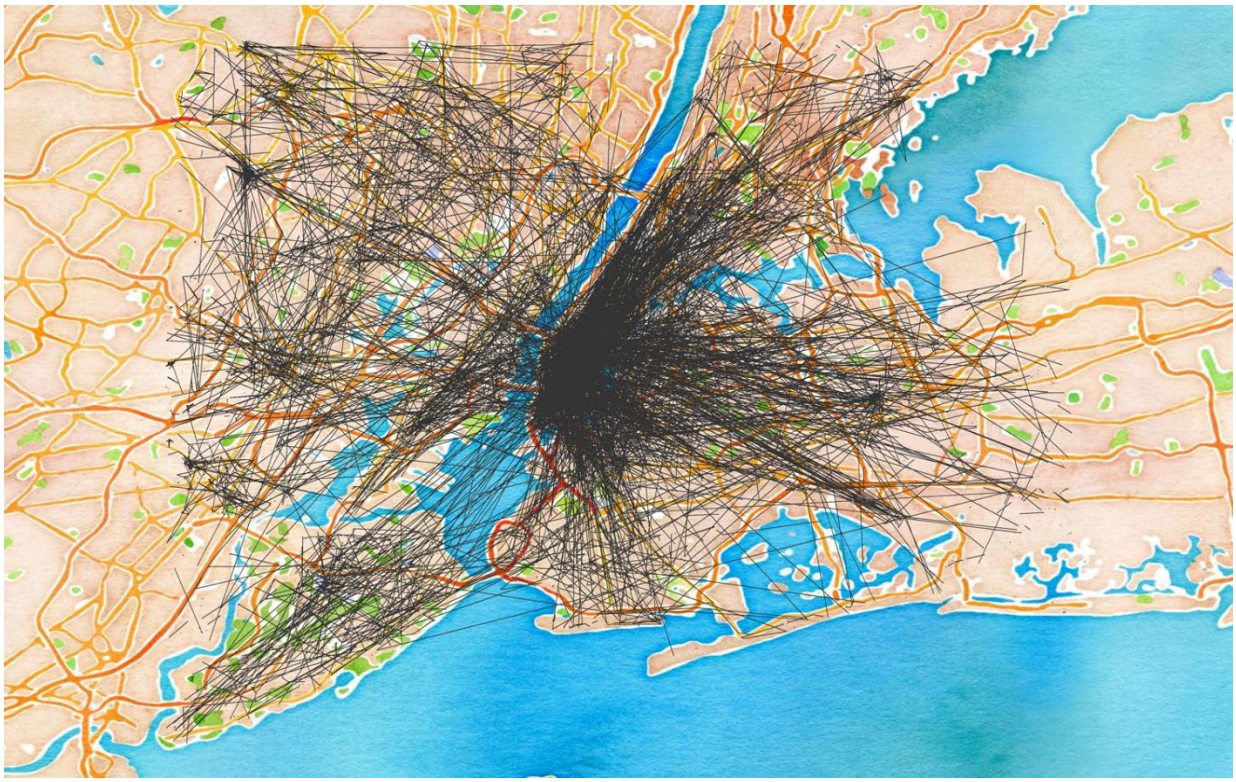

Figure 3: Movement Trajectories in NYC on October 1, 2013 (© OpenStreetMap contributors)

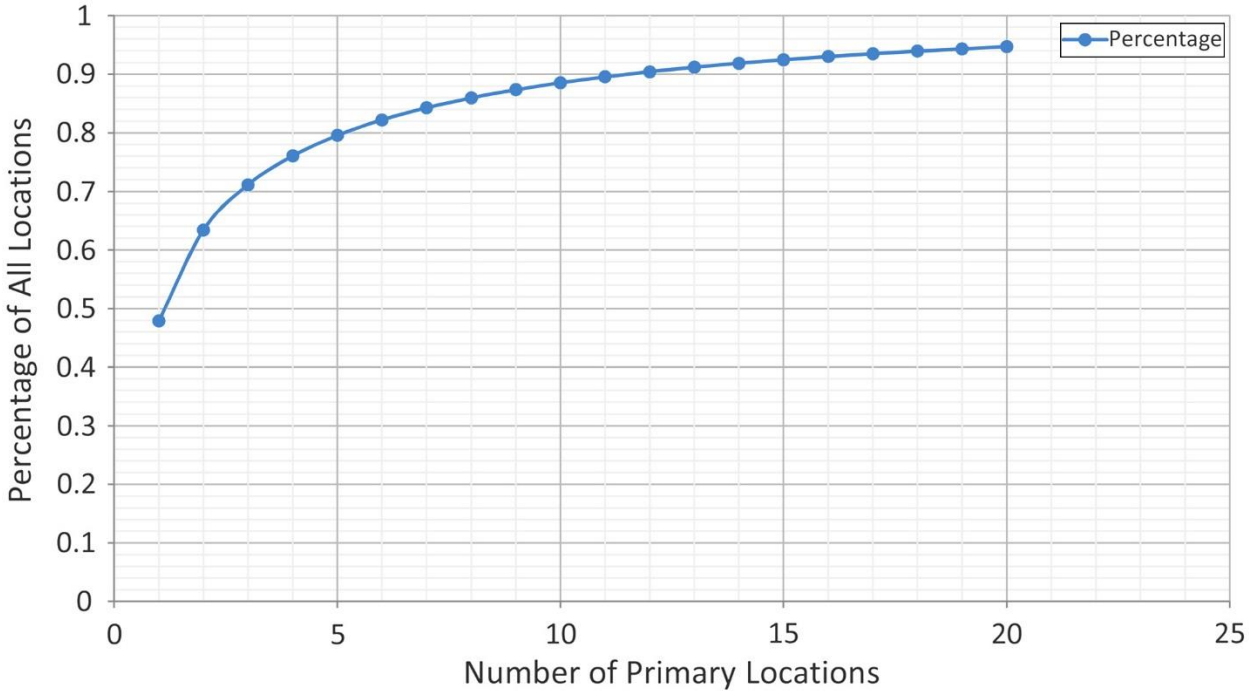

Figure 4: Primary Location and Their Coverage of All Locations

The results of primary location analysis are shown in Figure 4. A small number of primary locations can cover most of the places people visited. An individual spent almost half their time (47.87%) at his/her top primary location. 7 primary locations covered 84.27%of all the locations. When the number increased to 12, the coverage exceeded 90%, reaching to 90.42.

2.5.4 Identify Periodicity of Human Movements

As mentioned before, Cho et al. (2011) found that urban dwellers exhibited periodicity in their movement routines. To determine whether similar patterns existed in Twitter data, we mapped each user's locations and compared it to the temporal information. To examine one's periodicity, an individual must have enough data entries. Therefore, we ranked users based on the number of their tweets and only selected the top 1000 ones. Each of them had 174 or more data entries during the 31-day period. In other words, each individual has posted 5.6 or more tweets each day.

Each user's location distributions were mapped according to their temporal information. Figure 5a and Figure 5b show two user's distributions in different hours of the 31-day period. Each color represents the same hour period in different days. The analysis showed that human movements tend to converge at certain locations around certain periods of a day. These two users all tend to return to one single location between 10pm to 2am, but with different probabilities. After calculation, we found that user a tended to return to 73.86W, 40.85N with a probability of 0.89. However, one can only expected user b to show up at 74.00W, 40.79N with a probability of 0.35.

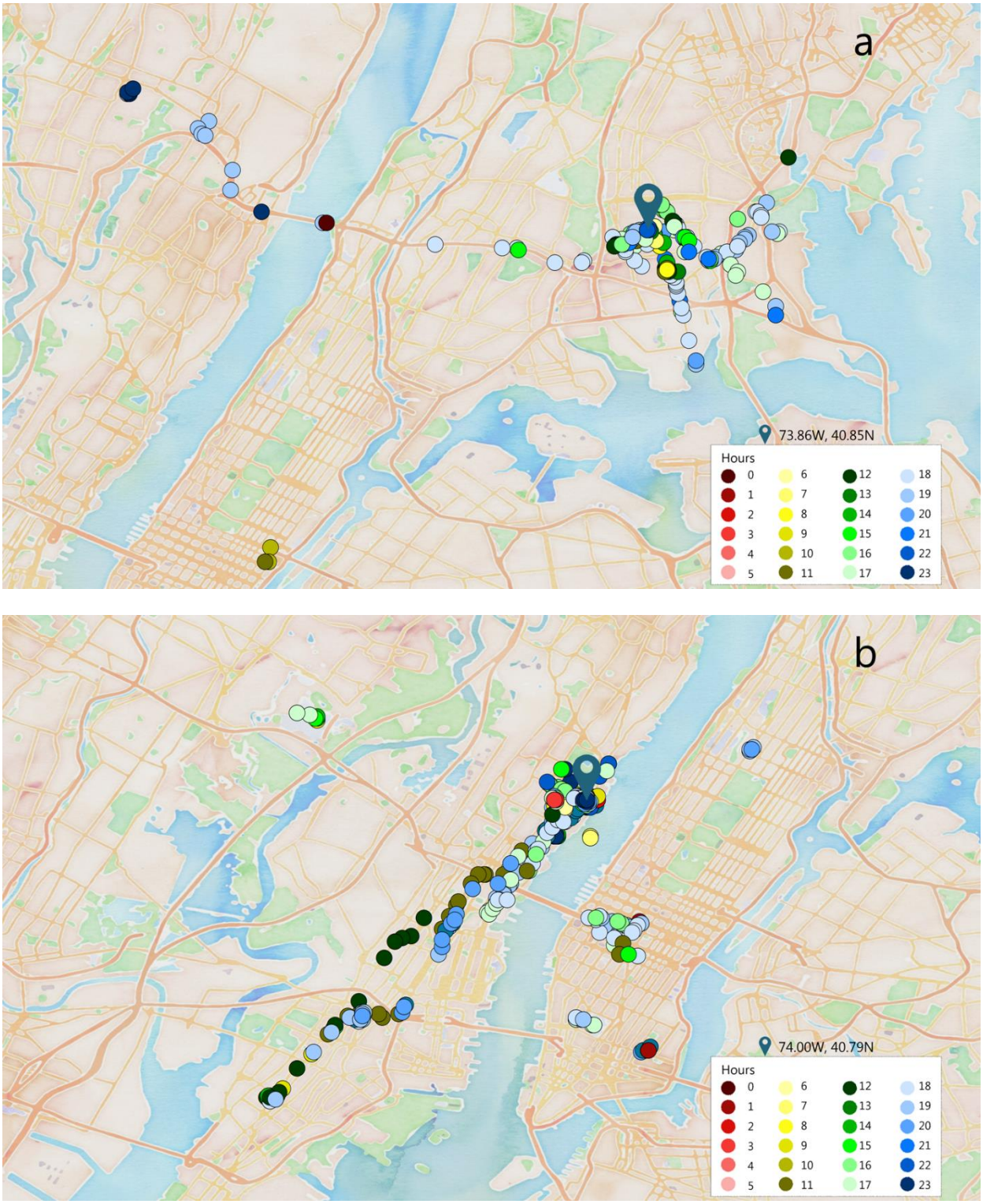

Figure 5: Periodic Movement Routines of Two Individuals
(© OpenStreetMap contributors)

2.6 Discussion

The current study found that Twitter could potentially provide more human mobility data for research, thus reduce the statistical bias possibly existing in human mobility studies with lower quantities of data. In Cho et al.'s study (2011), Gowalla provided about 305,000 location data points monthly, and the number from Brightkite was about 145,000. In Noulas et al. (2012) study, 371,502 displacements were collected from FourSquare during a six-month period in NYC which includes 43,681 individuals. Comparably, Twitter provided a much larger quantity of human mobility data. The movement data was about 19 times greater to the volume of displacement data from Noulas et al. (2012). Additionally, the number of Twitter users was more than 2 times greater compared to FourSquare in NYC if we assumed no new individuals would post geotagged tweets or about 13 times otherwise. This substantially larger volume of data was also collected over a much shorter period, further emphasizing the potential of Twitter to be used to understand, model and predict human mobility.

The results from our second analysis showed that power law dominated human mobility in NYC. The *p*-values derived from the comparison between power law distribution and other distributions confirmed that truncated power law distribution could best capture the human mobility pattern. Thus, human movements followed a Lévy flight model. This finding aligned with results from other research from proprietary data (Brockmann et al. 2006; González et al. 2008; Hawelka et al. 2014), and confirmed Twitter, as an open access social networking platform, can be used to study human mobility in urban areas. However, we did observe certain inconsistencies. Existing research showed that the β values ranged from 1.59 to 1.88, while our β value is 1.09. Such difference might be owing to the fact that our value was derived from higher-resolution data within a constrained geographical area.

The analysis on individuals' locations showed that although human movements could diffuse to a large area, the majority of their movements are limited to several primary locations. In fact, 12 primary locations of each individual covered more than 90% of all the locations he/she visited during the month on average. Such results aligned with the claim from the Schneider et al. (2013) study which found 7 locations cover roughly 90% of all the placements. A larger value reported in this study, i.e. 12 locations covered more than 90% of locations, might be the result of a smaller area of each location; a location covered about 0.01 km^2 in this study while it was 1 to 3 km^2 in Schneider et al. (2013). It also confirmed the findings from Song et al. (2010a) that human mobility are characterized by a decreasing tendency to visit new locations but a high probablity to return to the same locations (e.g. home, office, etc.).

The study's final analysis showed that periodic modulations characterize human mobility. People followed inherent routines and kept returning to their primariy locations at certain times in a day. Such a finding supported the results from previous studies (Cho et al. 2011; Liang et al. 2012), and confirmed that human movements are governed by the 24 hour and 7 day temporal circles. However, periodicities differed among individuals, and thus, their predictability varied. The comparison between user A and user B demonstrated that movements of some people could be predicted with higher accuracy than others (89% vs. 35%). Such inherent complexity deserves more investigation in the future.

2.7 Limitations and Future Study

The study has several potential limitations. First, people with higher degrees of education are more represented among Twitter users, and thus there is a possibility that the collected data are more representative of the mobility of people with higher education. Second, the study is limited by its

data sample. We only used 30 days of Twitter data to analyze its potential application in human mobility research. Some long-term patterns may only be observed by analyzing a database from an extended time scale. Also, our analysis was limited to one urban area, NYC. Human mobility patterns observed in one might not apply to other cities owing to their different urban layouts, and civil infrastructures. We plan to collect data for a longer time period and from more cities in future studies. Data from different cities will be compared to examine if daily urban movements show any consistencies.

Validating the applicability of Twitter to study human mobility has opened multiple future research avenues including epidemic spread, civil infrastructure development, and disaster response and evacuation, among other avenues. Human mobility and, in particular, human interactions through close contact can be studied in relation to the spread of contagious diseases, such as the international spread of the Ebola virus occurring in 2014. In civil infrastructure development, studying human mobility dynamics can potentially discover new trends in the diffusion of human locations and guide the future development of transportation systems and utility systems to meet or adapt to growth. Also, human mobility analysis can improve our understanding of the dynamics of energy demand and carbon emissions in urban areas which traditional static models do not address, and thus guide the development of the smart grid (Amin and Wollenberg 2005). In disaster response and evacuation, building evacuation models could be developed using empirical human movement data. Using human mobility data before, during and after natural and/or man-made disasters, researchers can build a human mobility model by integrating agent-based modeling and GIS technology. The model can be used to simulate different scenarios involving damages and failure of civil infrastructures (e.g. road damage, tunnel flooding, etc.) to identify the best strategies for disaster evacuation and response.

2.8 Conclusion

The interdependence and mutual influence of human mobility and civil infrastructure profoundly impact urban development in cities. Therefore, understanding, quantifying, and predicting human movements in urban areas is of critical importance to policy making in transportation, energy and power supply, disaster evacuation and response, and even epidemic control (Bengtsson et al. 2011; González et al. 2008; Song et al. 2010a, b; Wang and Taylor 2014; Wesolowski et al. 2012). Unfortunately, although researchers have developed models to understand and predict patterns of movement trajectories, civil applications for these models are limited. A major reason for this is data scarcity. Historically, collecting human movement data was difficult and few scientists had access to human movement data of high quantity and quality. Although researchers have used geosocial networking platforms, including Twitter, to study human mobility, few studies have introduced a comprehensive approach to collecting human mobility data. Additional research is needed to explore the viability of Twitter by comparing its data structures and analytical results to those of existing studies.

This study has contributed first steps toward (1) developing a comprehensive methodology for collecting human mobility data; and (2) demonstrating that Twitter can be a viable resource in the study of human mobility. A process map was developed comprising four innovative Python modules. It was executed for one month and tweets posted in NYC were retrieved. The data were analyzed to validate the applicability of Twitter for human mobility research. Study findings demonstrated that (1) twitter can provide a much larger quantity of human mobility data compared with other social networking platforms, with potentially higher precision and accuracy; (2) human mobility is governed by power law distribution; and (3) NYC dwellers exhibit periodic modulations.

This study has also extended previous research on geosocial networking platforms (Cho et al. 2011; Noulas et al. 2012; Noulas et al. 2011) to Twitter, one of the most popular social networking platforms in the world. Its results demonstrate that Twitter is able to deliver a large volume of data with more users owing to its enormous user base and open design. The analysis results were compared with those of existing studies (Brockmann et al. 2006; Cho et al. 2011; González et al. 2008; Hawelka et al. 2014; Liang et al. 2012; Schneider et al. 2013; Song et al. 2010a, b). The results of displacement distribution, primary locations, and periodicity aligned with those of previous studies and thus validated the suitability of Twitter for such analyses.

Future studies will (1) collect additional mobility data from multiple cities and over longer time scales to validate the methodology internally and externally; (2) develop algorithms that emulate the mobility patterns identified; and (3) use the data to build and validate an agent-based human mobility simulation model. This expanded approach will enable investigation of several of the recently identified civil engineering grand challenges (Becerik-Gerber et al. 2014). Moreover, it is hoped that the model will provide key insights and powerful predictability for policymakers in large cities globally and potentially help inform key urban issues and policies, such as those relating to disaster evacuation, response and relief, and the spread of epidemics.

2.9 Acknowledgement

This study is supported by the National Science Foundation under Grant No. 1142379 and by the Virginia Tech BioBuild Interdisciplinary Graduate Education Program (IGEP) grant. Any opinions, findings, and conclusions or recommendations expressed in this material are those of the authors and do not necessarily reflect the views of the National Science Foundation or Virginia Tech. Human mobility data were collected using the open API provided by Twitter. Because of

Twitter policy, the data are not available for distribution. The maps used in this paper were developed by OpenStreetMap under CC BY SA and tiled by Stamen Design under CC BY 3.0.

CHAPTER 3: QUANTIFYING HUMAN MOBILITY PERTURBATION AND RESILIENCE IN HURRICANE SANDY[3]

3.1 Abstract

Human mobility is influenced by environmental change and natural disasters. Researchers have used trip distance distribution, radius of gyration of movements, and individuals' visited locations to understand and capture human mobility patterns and trajectories. However, our knowledge of human movements during natural disasters is limited owing to both a lack of empirical data and the low precision of available data. Here, we studied human mobility using high-resolution movement data from individuals in NYC during and for several days after Hurricane Sandy in 2012. We found the human movements followed truncated power-law distributions during and after Hurricane Sandy, although the β value was noticeably larger during the first 24 hours after the storm struck. Also, we examined two parameters: the center of mass and the radius of gyration of each individual's movements. We found that their values during perturbation states and steady states are highly correlated, suggesting human mobility data obtained in steady states can possibly predict the perturbation state. Our results demonstrate that human movement trajectories experienced significant perturbations during hurricanes, but also exhibited high resilience. We expect the study will stimulate future research on the perturbation and inherent resilience of human mobility under the influence of hurricanes. For example, mobility patterns in coastal urban areas could be examined as hurricanes approach, gain or dissipate in strength, and as the path of the storm changes. Understanding nuances of human mobility under the influence of such disasters

[3] This paper was co-authored with Professor John E. Taylor and was published in the Journal of PLOS ONE.
Wang Q., Taylor J. E. (2014) Quantifying Human Mobility Perturbation and Resilience in Hurricane Sandy. *PLoS ONE* 9(11): e112608. doi:10.1371/journal.pone.0112608.

will enable more effective evacuation, emergency response planning and development of strategies and policies to reduce fatality, injury, and economic loss.

Keywords: *Geosocial networking; Human mobility; Infrastructure development; Twitter; Urban development*

3.2 Introduction

Natural disasters can cause extensive damage, economic loss and human suffering. According to the United Nations Office for Disaster Risk Reduction, over the period from 2000 through 2012 natural disasters have been responsible for killing 1.2 million people and affected the lives of 2.9 billion people (UNISDR 2013). Tropical cyclones, which include hurricanes and typhoons, are among the most severe natural disasters that cause tremendous loss of life and suffering (CWS, 2013). This calls for a better understanding of human mobility during typhoons and hurricanes to aid evacuation, emergency response and immediate post-disaster relief (Adger et al. 2005; Candia et al. 2008; González et al. 2008). Improved knowledge about human mobility can be used to reduce traffic jams (Pan et al. 2007), establish temporary communication networks (Chaintreau et al. 2007; Feeley et al. 2004), and deliver critical information to reduce injuries, fatalities, and economic loss (Kleinberg 2007; Vespignani 2010).

Recent research has improved our understanding of general human mobility patterns but unfortunately we know comparatively little about human movements during disasters. Research has shown that human movements follow power-law distributions with scaling parameter values ranging from 1.59 to 1.75 (Brockmann et al. 2006; González et al. 2008). Individual movement trajectories exhibited similar shapes after being rescaled by the radius of gyration (González et al. 2008). But, movement trajectories demonstrate uneven visitation frequency of different locations,

repeatedly returning to certain locations while being less likely to visit new ones (Song et al. 2010a, b). At the city scale, movements follow similar distributions in different urban areas (Noulas et al. 2012) and exhibit characteristics of periodicity to return to primary locations and unusual bursts during special events (Liang et al. 2012). Also, human movements have been shown to follow highly efficient trajectory configurations during their daily movements (Schneider et al. 2013). While human mobility studies have improved our knowledge about general mobility patterns, it is intuitive to assume that disasters may perturb such routine movements (Bagrow et al. 2011; Horanont et al. 2013; Morrow-Jone and Morrow-Jone 1991) and even cause population migration (Bengtsson et al. 2011). Therefore, human mobility trajectories during disasters would deviate from steady states. Research on the topic of human mobility under the influence of disasters is limited perhaps owing to the inherent unpredictability of disasters and resulting data scarcity. Moreover, much empirically grounded human mobility research utilizes mobile phones to track human mobility (González et al. 2008; Schneider et al. 2013; Song et al. 2010a, b; Wesolowski et al. 2012). The data precision of these studies is limited to the coverage area of each mobile phone tower, which is typically around 3km2. While such precision has been instrumental in developing an understanding of general patterns of human mobility over larger scales (e.g., a state or a country), it may lack the necessary precision to capture mobility changes caused by disasters and other extreme events that unfold at smaller scales (e.g., a building or a city). The necessity of high-resolution data cannot be ignored because many of those caught in the storm surge during hurricanes and typhoons may have been spared if they had evacuated a short distance to higher ground.

3.3 Methodology

We study the perturbation and resilience of human mobility patterns during and after Hurricane Sandy—one of the largest tropical storms recorded in the Atlantic Ocean that affected millions of people (Ferris et al. 2013; OCHA 2012)—which struck the northeastern seaboard of the United States leading to significant injury and loss of human life in October 2012. The study used high-resolution data from Twitter which were collected from 4pm Oct. 29, 2012—the day Hurricane Sandy landed in NYC—through 4pm Nov. 10, 2012. During the 12-day data collection period, a total of 702,188 tweets were collected from a total of 53,934 distinct individuals. The volume of data collected each day is provided in Table A1. We located each user using geolocation information attached to each tweet which contains a longitude and latitude geographical coordinate. The coordinates are high resolution with accuracy to approximately 10 meters.

3.4 Results and Discussion

After mapping each recorded location during every 24-hour period, we observed that movement locations covered nearly the entire mapped area and showed similar geographical distribution to 24-hour periods soon after the hurricane (Figure 6A, 6C, and 6E). This observation suggests that NYC residents were relatively resilient in terms of human mobility during Hurricane Sandy. While such resilience could be vital for the city's post-disaster response and recovery, it may also be life threatening during an extreme event such as a hurricane. Overlapping the location and movement data with the mandated evacuation areas reveals that human activities were still observed in evacuation zones although people were ordered to evacuate, (Figure 6A and 6B). Regrettably, several fatalities occurred in these evacuation zones.

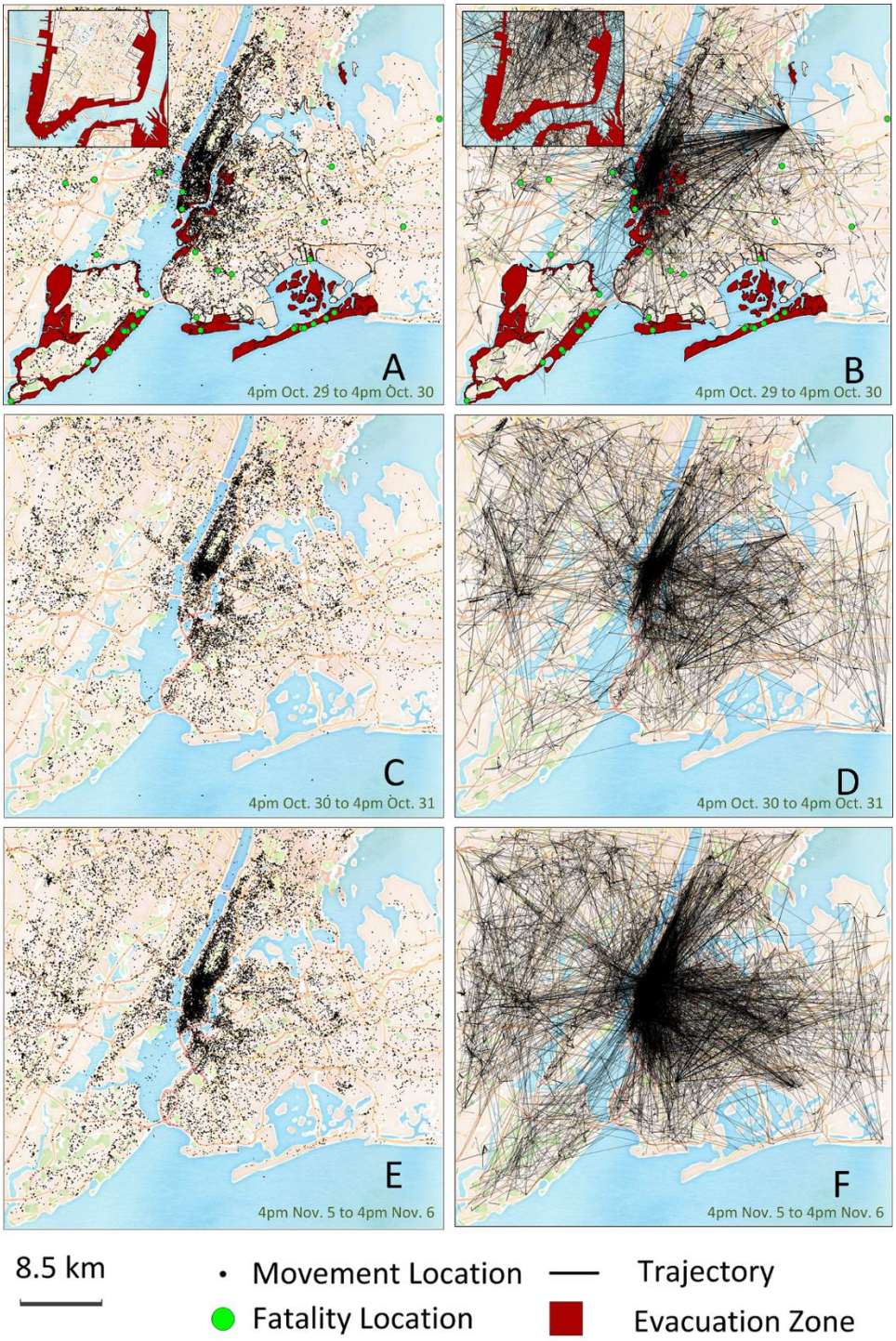

Figure 6: Geographical distribution of visited locations and movement trajectories over 24-hour periods. A, **C**, and **E**, locations visited by Twitter users. **B**, **D**, and **F**, movement trajectories of Twitter users. The insets in **A** and **B** show an enlarged map of the lower Manhattan area. Red areas indicate the evacuated zones enforced by NYC government, though some of the areas were still active with human activity/mobility in this 24-hour period. The green nodes indicate the locations where fatalities occurred.

To discover whether human movements were disrupted, we also mapped each individual's unique mobility trajectory during each 24-hour period. We found the movement trajectories in the post-disaster period exhibited similar patterns (Figure 6D and 6F), radiating from Manhattan to other areas, with the exception of the trajectories in the first 24-hour period. To test if the observed difference was mathematically significant, we posed the following hypothesis:

Hypothesis 1: During Hurricane Sandy, the human mobility distribution was significantly perturbed.

To explore this hypothesis, we calculated all the distances between consecutive locations from each distinct user. The displacement distributions for these travel ranges are provided in Table A2. We found that while short-distance trips (Δr<1km) increased during the first 24-hour period, longer-distance travels significantly decreased (Figure 7A). Also, the total displacements (Δr) for each 24-hour period followed a truncated power-law distribution, though with different values (Figure 7B). During the first 24-hour period during which Hurricane Sandy struck NYC, the scale-invariance β value of the distribution was 1.73, the exponential cutoff value λ was 2.70×10^{-5}, and the minimum fitting value κ was 591 m. During the 11 other 24-hour data collection periods, the β value was 1.19±0.06, the λ value was (6.13±0.69) $\times10^{-5}$, and the cutoff value κ was 4 m. The change of the β values is primarily the result of the larger optimized cut-off value of the first 24-hour displacement data. The reduction of longer-distance travels and the substantial difference between β and κ allowed us to reject the null hypothesis and confirm that a perturbation of human mobility occurred during Hurricane Sandy. The differences between the calculated β values here and the values reported in other studies (Brockmann et al. 2006; González et al. 2008) perhaps are owing to the fact that the values in our study were derived from higher precision location data in

a more tightly constrained geographical area. It is worth noting, however, that the truncated power-law distribution discovered here is similar to the human mobility patterns identified in those studies.

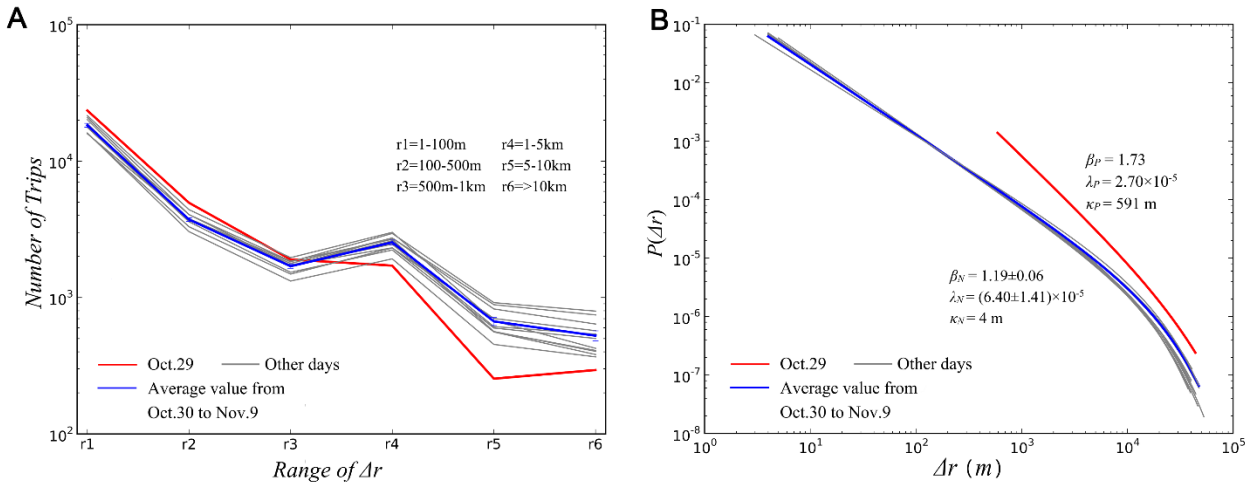

Figure 7: Human Mobility Perturbation. A, Statistical distribution of displacements for each 24-hour period. Each line represents the change of numbers of trips within different ranges of displacements. **B**, Displacement distribution for each 24-hour period. Each line represents a probability density function $P(\Delta r)$. All plotted distributions followed a truncated power-law distribution (Table A3).

The results confirm that Hurricane Sandy perturbed human mobility patterns. However, the results reveal other important insights regarding human mobility perturbation during Hurricane Sandy in NYC. First, the distribution of the perturbation bears strong similarity to daily movement distributions in the following 11-day period. We also analyzed data from November 2013—one year later—in NYC and compared the results with the 11-day period of data collected in 2012. The two sets of results showed strong similarity, which confirms that typical, steady state daily human movements follow truncated power-law distribution with the β value around 1.19. Second, the most significant human mobility perturbation appears to have lasted less than 24 hours as the β value returned to a normal level on Oct. 30, 2012. This brief change in human mobility indicates that NYC residents were resilient to the effects of Hurricane Sandy. This resilience in human mobility was the case even as most public transportation only started to resume partial or full

schedule service 36 to 72 hours after Hurricane Sandy struck (Kaufman et al. 2012) and over 1 million people in the city were still without power until 2pm Nov. 2 (McGeeham 2012).

While Figure 7A and 7B show a clear deviation between the mobility distribution of the first 24-hour period and the distributions of the other 24-hour periods, demonstrating that Hurricane Sandy perturbed human mobility in NYC, it raises new questions: how did people change their movements and do these changes correlate to movements in non-perturbed states? To explore these questions, we mapped each individual's movement trajectory over each 24-hour period to examine perturbations at the individual level. Individuals generally exhibited two perturbation trends: shifting their movements to a different place or places, and changing their travel distances. To quantify the observed perturbation, we calculated the center of mass ($\vec{r}_{CM}$) and the radius of gyration (r_g) for each active individual's trajectory during the 24-hour perturbation state (P) and the relatively steady state from Nov. 3 to Nov. 9 (N). An individual is considered active if the user had at least 5 data entries during both the perturbation state and the steady state. We found that 2,241 individuals qualified as active users during these periods and they transmitted 34,386 entries during the perturbation state and 128,904 entries during the steady state period. The mobility perturbation can be defined by two parameters: the shifting distance of the center of mass $\Delta d_{CM} = \vec{r}_{CM}^{P} - \vec{r}_{CM}^{N}$, and the radius of gyration in perturbation state r_g^P. To examine whether the values of these parameters can be projected using the values from steady states or whether disasters make human movements chaotic, we tested two additional hypotheses:

Hypothesis 2a: Δd_{CM} positively correlates with r_g^N.

Hypothesis 2b: r_g^P positively correlates with r_g^N.

We first analyzed Δd_{CM} and found that the values followed a stretched exponential distribution (see Materials S1). We also found the values strongly correlate with r_g^N (correlation coefficient = 0.59, p<0.001). Larger values of r_g^N can result in larger shifting distances in the center of movements for individuals. The shifting distance Δd_{CM} follows $\Delta d = 4.09 r_g^{N^{0.45}}$ (Figure 8A red line). The fitting results for this are provided in Table A4. The green line in Figure 8A shows where Δd_{CM} equals r_g^N. We can see that with the increase of r_g^N, Δd_{CM} converges toward the green line. Therefore, we can reject the null hypothesis for Hypothesis 2a, finding support that r_g^N can possibly be used to predict the shift of the center of movements. This implies that a person needs to move to a safer place during a hurricane in order to sustain their mobility.

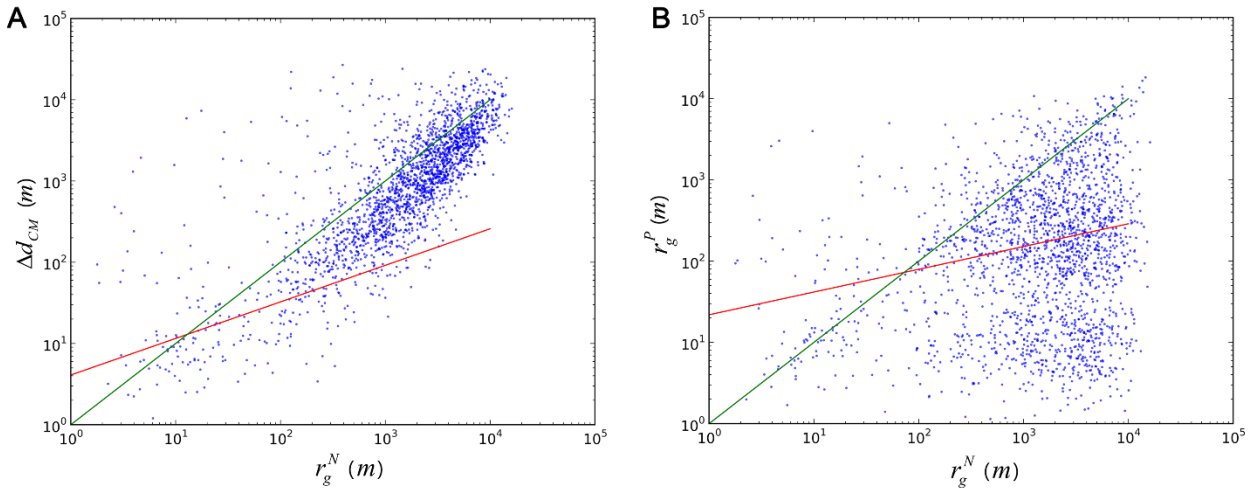

Figure 8: Relation between perturbation states and steady states. A, Δd_{CM} versus r_g^N. The correlation coefficient between the two parameters is 0.59 (p<0.001). The red line is the fitted function of the correlation where $\Delta d = 4.09 r_g^{N^{0.45}}$ (m). The green line in Figure 8A shows where Δd_{CM} equals r_g^N. **B,** r_g^P versus r_g^N. The notations are the same as in **A**. The correlation coefficient between these two parameters is 0.25 (p<0.001) with fitted function $r_g^P = 21.88 r_g^{N^{0.28}}$ (m).

We then examined whether a correlation exists between r_g^P and r_g^N. We found that r_g^P follows a truncated power-law distribution (see Materials S1). The value of r_g^P was 1.19, approximating the value reported in a previous study (González et al. 2008) (~1.20). However, we did not find such

a property in r_g^N. This finding implies that cutting the heavy tails of long-distance travels could change the general pattern found in the radius of gyration in human movements. Pairing r_g^P and r_g^N, we found their correlation can be captured with the function $r_g^P = 21.88 r_g^{N^{0.28}}$ (Figure 8B). The green line in Figure 8B shows where r_g^P equals r_g^N. Most people decreased their r_g^P, i.e., scaled down their areas of movement, during Hurricane Sandy. With the increase of r_g^N, this trend became more evident. The correlation between the two parameters resulted in a correlation coefficient of 0.25 (p<0.001), and therefore, the null hypothesis for Hypotheses 2b can be rejected. This implies that r_g^N can be used to predict r_g^P.

Our results demonstrate that, although Hurricane Sandy did impact the mobility patterns of individuals in NYC, the perturbation was surprisingly brief and the mobility patterns encouragingly resilient. This resilience occurred even in the large-scale absence of mobility infrastructure. While human movements followed truncated power-law distributions in perturbed and steady states, their mobility-related behaviors did exhibit important changes. That is, people changed the center of their movements and their travel distances as they sought shelter.

3.5 Conclusions

Our finding that steady state shifts in the center of mass (Δd_{CM}) and the radius of gyration (r_g^N) of daily individual trajectories correlate with perturbed states is particularly interesting. Human mobility appears to possess an inherent resilience—even in perturbed states—such that movement deviations, in aggregate, follow predictable patterns in hurricanes. Therefore, it may be possible to use human mobility data collected in steady states to predict perturbation states during extreme events and, as a result, develop strategies to improve evacuation effectiveness and speed critical disaster response to minimize loss of life and human suffering.

3.6 Acknowledgement

Human mobility data were collected using the open API provided by Twitter. Due to Twitter's policy, the longitudes of the data were modified so the locations are shown in an area close to Beijing, China instead of NYC where the data were actually collected. We conducted additional analyses and confirmed that the results calculated by the Haversine formula based on the modified data had no difference from the ones based on the original data. The maps used in this paper are developed by OpenStreetMap under CC BY SA, and tiled by Stamen Design under CC BY 3.0. Correspondence and requests for material should be addressed to J.E.T (jet@vt.edu).

3.7 Data Availability

The authors confirm that, for approved reasons, some access restrictions apply to the data underlying the findings. Due to Twitter's policy, the longitudes of the data were modified so the locations are shown in an area close to Beijing, China, instead of NYC where the data were actually collected. The authors conducted additional analyses and confirmed that the results calculated by the Haversine formula based on the modified data had no difference from the ones based on the original data. The displacement data from each day and the locations of active users during perturbed and steady states are available from DRYAD using the DOI doi:10.5061/dryad.jv577.

3.8 Funding

This study is supported by the National Science Foundation under Grant No. 1142379 and by the Virginia Tech BioBuild Interdisciplinary Graduate Education Program (IGEP) grant. Any opinions, findings, and conclusions or recommendations expressed in this material are those of the authors and do not necessarily reflect the views of the National Science Foundation. Open access

publication of this article was supported by Virginia Tech's Open Access Subvention Fund. The funders had no role in study design, data collection and analysis, decision to publish, or preparation of the manuscript.

CHAPTER 4: GETTING OUT OF DODGE: URBAN HUMAN MOBILITY RESILIENCE UNDER THE INFLUENCE OF MULTIPLE TYPES OF NATURAL DISASTERS[4]

4.1 Abstract

Natural disasters pose serious threats to large urban areas, therefore understanding and predicting human movements is critical for evaluating a population's vulnerability and resilience and developing plans for disaster evacuation, response and relief. However, only limited research has been conducted into the effect of natural disasters on human mobility. This study examines how natural disasters influence human mobility patterns in urban populations using individuals' movement data collected from Twitter. We selected fifteen significant cases across five types of natural disaster and analyzed the human movement data before, during, and after each event, comparing the perturbed and steady state movement data. The results suggest that the power-law continues to govern human mobility in most cases and that human mobility patterns observed in steady states are often correlated with those in perturbed states, highlighting their inherent resilience. However, this resilience has its limits and can fail in more powerful natural disasters. The findings from this study will deepen our understanding of the interaction between urban dwellers and civil infrastructure, improve our ability to predict human movement patterns during natural disasters, and facilitate contingency planning by policymakers.

Keywords: *Geo-social networking; Human mobility; Natural disasters; Perturbation; Resilience.*

[4] This journal-length manuscript was co-authored with Professor John E. Taylor and will be submitted to a peer-reviewed journal.

4.2 Introduction

Natural disasters have a severe impact on human societies. A recent report from UNISDR (2013) revealed that natural disasters caused 1.2 million deaths, affected 2.9 billion people, and resulted in a total of US $1.7 trillion of economic loss globally from 2000 to 2012. This situation is not expected to improve; the climate change caused by human activities means that the frequency of natural disasters will continue to increase for the foreseeable future (EM-DAT 2012).

Governments and communities have developed a range of coping mechanisms to fight natural disasters, among which disaster response and evacuation plans are important components. These plans evaluate the potential risks posed by different types of disasters and attempt to control and minimize the consequences. However, the effectiveness of these top-down plans is often questioned, because they often lack sufficient understanding and do not take into account real-world human behaviors (Chakraborty et al. 2005; Drabek 2000; Wolshon and Marchive III 2007). Prior to Hurricane Sandy making landfall in New Jersey in October 2012, although 71 percent of the people living in evacuation areas were aware of a mandatory order to move inland, more than 50 percent failed to do so (Schuerman 2013). Regrettably, most of the fatalities occurred in these evacuation areas (CDC, 2013). Even those who evacuated were not entirely safe: data from the US Federal Emergency Management Agency (FEMA) revealed that the flooded areas were actually much larger than the designated evacuation areas and several people who stayed in the assumed safe areas also lost their lives (Rosenzweig and Solecki 2014). In the aftermath of the hurricane, NYC updated its mandatory evacuation zones based on this experience. A similar situation occurred in the Philippines a year later when Typhoon Haiyan struck the city of Tacloban. Although the government ordered city residents to evacuate and seek shelter prior to the typhoon's arrival, instead of moving to higher ground, many took refuge in concrete buildings that were

unable to withstand the strength of the wind and the accompanying floodwaters and many lives were lost when the buildings collapsed (Teves and Bodeen 2013). Tragedies such as these highlight the importance of developing a better understanding of how people actually react, especially in terms of their mobility and evacuation behaviors, during natural disasters and extreme events.

Human mobility plays a critical role in disaster response and evacuation strategies. First, and possibly most importantly, it determines the effectiveness of evacuation efforts. As Pan et al. (2007) pointed out, overcrowding and crushing during emergency situations can cause incidents and thus injuries and the unnecessary loss of lives. Alarmed by the approach of a severe snow storm in December 2013, the U.S. city of Atlanta, Georgia, issued a snow storm warning and advised people to leave school and work early and return home. The unfortunate consequence of this warning was that residents all crammed onto the city's roads and highways at the same time, causing a city-wide traffic jam. Many were still stuck on the roads when the storm hit, forcing them to abandon their vehicles and seek shelter (Beasley 2014). Without a deeper understanding of human movements during natural disasters, the same situation is bound to occur again. Human mobility also has an impact on the effectiveness of information communications during emergencies. When a region's communications infrastructure is damaged by a natural disaster, human mobility effectively determines the bandwidth of emergency information networks and thus the speed and width of information diffusion (Kleinberg 2007). In this situation, peer-to-peer connections can create 'Mobile ad-hoc networks' (MANETs) or 'Pocket switched networks' (PSNs) using mobile communication devices such as cell phones (Chaintreau et al. 2007; Feeley et al. 2004). These temporary networks can provide critical information and hence reduce injuries, fatalities, and economic loss (Vespignani 2010). Accurate human mobility predictions can also potentially save lives. In both Hurricane Sandy and Typhoon Haiyan, if it had been possible to identify vulnerable

individuals and provide them with detailed instructions, their lives might have been spared. The critical roles of human mobility related to all three of these aspects call for in-depth investigations to build our understanding of how best to work with real-world human behaviors in disaster situations.

Despite its importance little research into human mobility has been reported, especially related to human mobility under the influence of natural disasters, i.e. in perturbed states. While several fundamental characteristics of generic human mobility have been identified, research on perturbed human mobility is fragmented and little has been done to discover fundamental patterns. Also, these studies mostly focus on one case or one type of natural disaster due to the limitations imposed by the difficulty of utilizing large amounts of empirical data. It is therefore unclear whether the findings of these narrowly focused studies can be extended to other extreme events. Their failure to seek universal patterns in perturbed human mobility under the influences of different types of natural disasters thus limits the contributions and potential applications of these studies.

To overcome this gap in the research, this study attempts to take the first step towards identifying patterns in perturbed human mobility by examining human mobility under the influence of multiple types of natural disasters. This study is based on the use of a large quantity of human movement data collected from Twitter. This data collection effort has taken almost two years, providing us with human mobility data for a number of different natural disasters around the world, including tropical cyclones, winter storms, wild fires, earthquakes, and severe thunderstorms. By analyzing and comparing the data from these events, we attempted to uncover universal patterns in the movements of a perturbed human society.

The paper is organized as follows. After reviewing related work about human mobility and how it could potentially be influenced by disasters and environmental change, we propose three hypotheses based on the information uncovered. This is followed by sections introducing our data collection and analytical methods. After presenting the results, the findings and their implications are discussed. The paper concludes by addressing the study's limitations and presenting our conclusions.

4.3 Background

There has been a great deal of research into general human mobility patterns. Using both currency circulation data and mobile phone data, researchers have confirmed that human movements follow a power-law distribution, with β values ranging from 1.59 to 1.88 (Brockmann et al. 2006; Cheng et al. 2011; González et al. 2008; Hawelka et al. 2014). This means that human movements can generally be described by the Lévy flight model, which is typically found in animals' movement patterns (Ramos-Fernandez et al. 2004). Research has also shown that individual movement trajectories exhibited similar shapes after being rescaled by the radius of gyration (González et al. 2008). Song et al. (2010a) investigated a large dataset containing a year's worth of location information for 1 million mobile phone users and observed three unique characteristics of human mobility which both the Lévy flight model (Brockmann et al. 2006) and the continuous-time random-walk model (Kimura and Saito 2006; Saltelli 2008) failed to explain. These characteristics were: (1) a decreasing tendency for a person to visit new locations; (2) an uneven visitation frequency for different locations; and (3) an ultraslow diffusion, which meant people tended to return to the same locations (e.g. home, office, etc.). Based on these observations, Song et al. (2010b) developed a new individual-mobility model that incorporated two unique generic mechanisms: exploration and preferential return. However, although this new model is more

representative of human mobility patterns than previous models, it still only captures long-term spatial and temporal scaling patterns.

Human movement at the city scale has also been investigated. At this level, periodic modulations characterize human mobility (Song et al. 2010a). Noulas et al. (2012) studied human mobility in 31 large cities around the world, and found that the global movements followed a power-law distribution. They also found human mobility in all the cities studied followed almost the same pattern. Perhaps unsurprisingly, several studies have also found that people exhibit characteristics of periodicity governed by 24 hour and 7 day temporal cycles in returning to primary locations (Cho et al. 2011; Liang et al. 2012). Human movements have also been shown to follow highly efficient trajectory configurations during their daily movements. Schneider et al. (2013) reported that people are highly efficient when performing their daily trips, following only 17 trajectory configurations out of over a million possible trajectories.

While these human mobility studies have improved our knowledge about general mobility patterns, it seems likely that a change in the environment, particularly a major event such as a natural disaster, will significantly perturb these routine patterns. Bagrow et al. (2011) used mobile phone billing data to track people's communication in 8 emergency events (including bombings and earthquakes) and 8 non-emergency events (such as sports events and concerts). Their results showed that the emergency information tends to diffuse globally while the non-emergency information is more spatially constrained. Horanont et al. (2013) studied the relationship between weather conditions and people's everyday activities and discovered that some types of weather conditions can significantly influence human movements, although the level of influence on individuals varied highly. These findings indicate that unusual events and changes in the natural environment will indeed influence people's activities. Natural disasters can cause major population

migration. Morrow-Jones and Morrow-Jones (1991) studied an 8-year dataset and confirmed that natural disasters do cause involuntary migration. This can occur on a large scale; Bengtsson et al. (2011) tracked population movements in Haiti using cell phone data and found that earthquake and disease infection caused as much as 20% of the population to leave the capital city, Port-au-Prince.

While these studies demonstrate that human movement trajectories during disasters do deviate from their normal steady states, research in this area is fragmented and not enough effort has been devoted to discovering fundamental patterns in human mobility under the influences of natural disasters. Many factors have constrained more extensive and in-depth research, but a key issue is the inherent unpredictability of natural disasters. Current technology is still ineffective in predicting the occurrence of natural disasters such as earthquakes and tornadoes, and even though we now have some advance warning of some types of natural disasters, particularly tropical cyclones, winter storms, and thunder storms, researchers and practitioners are still unable to accurately forecast their precise paths, strength, and influence. Hurricane Sandy had already caused extensive damage in Jamaica and Cuba before it arrived in the U.S. several days later, but the nation still suffered 73 deaths and about $65 billion of economic loss (Ferris et al. 2013). The failure of one of the world's most highly developed countries to minimize the damage from a significant impending natural disaster when the devastation it had already wreaked in two other countries had been featuring on the evening news for days highlights the challenges involved in protecting urban dwellers from natural disasters. This unpredictability also makes it difficult to collect empirical human movement data from multiple types of natural disasters, and thus researchers have limited data at their disposal when seeking to examine the fundamental attributes of perturbed human mobility.

One of these fundamental attributes is resilience. Understanding and quantifying the resilience of human mobility could provide a key indicator for measuring the vulnerability and adaptability of human society when facing natural disasters (Adger 2006; Brooks et al. 2005; Folke 2006). It could help predict human movements in urban areas and shed new light on the interdependence between human mobility and civil infrastructure, providing invaluable knowledge that will help define the shape of the decision-making landscape for socio-ecological systems (Adger 2006). However, there has been only limited research into understanding and quantifying the resilience of human mobility. A recent study by Wang and Taylor (2014) examined human movement under the influence of Hurricane Sandy and discovered that human mobility does indeed possess inherent resilience. The study's findings revealed that the power-law still governed New Yorkers' movements under the attack of Hurricane Sandy and that the values for the center of movement and the radius of gyration were correlated with their values during a steady state. This correlation suggests the possibility of predicting the pattern of perturbed human mobility. Despite the importance of these findings, the study did not examine whether this resilience can withstand the pressures of other types of disasters or disasters with more extensive impacts and damages. There is a critical gap in research on human mobility perturbation and resilience under the influence of multiple types of natural disasters. Such research is critical for predicting human movements during natural disasters and exploring the interdependence between human mobility and civil infrastructure. Ultimately, a better understanding of human mobility in highly stressful disaster situations will promote public safety by identifying the most effective ways to predict human locations and travel patterns, thus facilitating the protection of vulnerable individuals from potential harm and injury during natural disasters.

4.4 Hypotheses Development

Based on the results from previous studies, we posited several hypotheses to examine human mobility resilience. Resilience in human mobility means the ability of human movement to absorb shocks, maintain its fundamental attributes, and return to its steady state equilibrium in response to natural disasters (Cutter et al. 2008). The hypotheses were then tested for each natural disaster case. As mentioned earlier, human mobility is governed by a power-law (Brockmann et al. 2006; González et al. 2008) and although extreme weather can significantly influence human movements (Bagrow et al. 2011; Horanont et al. 2013), this power-law holds even during a strong hurricane (Wang and Taylor 2014). Therefore, we propose our first hypothesis:

Hypothesis 1: A power law governs human mobility in multiple types of natural disasters.

Researchers have found that the center of mass of human movements and the radius of gyration can fundamentally describe individual human movements (González et al. 2008). As already mentioned, Wang and Taylor (2014) found the values of these two factors during the perturbation state to be correlated to their values during the steady state; people tend to seek refuge in areas that are already familiar to them. We therefore extended this finding to multiple types of natural disasters, and proposed the following two hypotheses:

Hypothesis 2: Shifts in the distances of centers of movement during natural disasters are positively correlated with the values of the radius of gyration in steady states.

Hypothesis 3: Values of radius of gyration during natural disasters are positively correlated with the ones in steady states.

4.5 Data Collection

Much empirically grounded human mobility research utilizes mobile phones to track human mobility (González et al. 2008; Schneider et al. 2013; Song et al. 2010a, b; Wesolowski et al. 2012). The data precision of these studies is limited to the coverage area of each mobile phone tower, which is typically around 1~3km2. While such precision has been instrumental in developing an understanding of general patterns of human mobility over larger scales (e.g., a state or a country), it may lack the necessary precision to capture mobility changes caused by disasters and other extreme events that unfold at smaller scales (e.g., a city).

To overcome this limitation, Twitter was used to collect high-resolution human mobility data in this study. Twitter is an online social networking media that allows people to post statuses that are limited to 140 characters, called tweets. It has over 645 million active users (Statistic Brain 2014) and they post about 500 million tweets per day (Weber 2010). Users can enable a function which automatically adds location information, called a geotag, to each tweet they post. Each geotag contains the exact coordinate at which the tweet was posted. Numerous studies have adopted the platform to study communication and geo-social networking (Folke 2006; Schwarz et al. 2011). Using the Twitter public API, we developed a method to collect geotagged tweets around the world. Refer to Wang and Taylor (2015) for details about the data collection systems.

Human mobility data before, during and after fifteen natural disaster events from five types of natural disasters were used to conduct this study. We collected data over a two-year period. Then we reviewed natural disasters that occurred during the period and retrieved human mobility data from affected areas. While many natural disasters happened globally, we selected fifteen events that provided sufficient data for analysis. These fifteen events divide into the following groups:

four typhoons, three winter storms, three earthquakes, two wild fires, and three thunderstorms. They included a total of 3,673,626 geo-tagged tweets from 212,735 individuals. The summary of these events and data can be found in Table 2.

Table 2: Summary of Natural Disasters and Collected Data

Type	Name	Location	No. of Tweets	No. of Users
Typhoon	Wipha	Tokyo, Japan	849,173	73,451
	Halong	Okinawa, Japan	166,325	5,124
	Kalmaegi	Calasiao, Philippines	21,698	1,063
	Rammasun	Manila, Philippines	408,760	27,753
Earthquake	Bohol	Bohol, Philippines	114,606	7,942
	Iquique	Iquique, Chile	15,297	1,470
	Napa	Napa, USA	38,019	1,850
Winterstorm	Xaver	Norfolk, Britain	115,018	8,498
	Xaver	Hamburg, Germany	15,054	2,745
	-*	Atlanta, USA	157,179	15,783
Rainstorm	-*	Phoenix, USA	579,735	23,132
	-*	Detroit, USA	765,353	15,949
	-*	Baltimore, USA	328,881	14,582
Wildfire	New South Wales**	New South Wales, Australia (1)	64,371	9,246
	New South Wales**	New South Wales, Australia (2)	34,157	4,147

*No specific names were assigned to the natural disasters.
**The wildfire covered 290,000 acres, and we picked the two most severe areas that were close to urban areas.

4.6 Data Analysis and Results

To explore the proposed hypotheses, we conducted multiple analyses on the human mobility data collected from Twitter. To test the first hypothesis and determine whether natural disasters changed the fundamental power law that governs human mobility, we first calculated the displacements. A displacement is the distance over two consecutive points from one individual. It was calculated using the Haversine formula (Robusto 1957):

$$d = 2r \times \sin^{-1}\left(\sqrt{\sin^2\left(\frac{\phi_2 - \phi_1}{2}\right) + \cos\phi_1\phi_2 \sin^2\left(\frac{\varphi_2 - \varphi_1}{2}\right)}\right)$$

Where r is the earth radius, which approximately equals to 6,367,000 meters, ϕ is the latitude, and φ is the longitude

We fitted the displacement data into truncated power-law distribution (Clauset et al. 2009; González et al. 2008; Klaus et al. 2011). The truncated power-law distribution can be captured by the following equation:

$$P(\Delta r) \propto \Delta r^{-\beta} e^{-\lambda \Delta r}$$

Where Δr is the displacement, β is the scaling parameter, and λ is the exponential cutoff value.

To test the goodness of fit, we conducted the Maximum Likelihood Estimation test to compare the truncated power-law distribution to both the exponential distribution and lognormal distribution. Maximum Likelihood Estimation is a statistical method to estimate which statistical model has higher goodness of fit to the empirical data (Amundsen and Klemetsen 1988; Anderson et al. 2014;

Chakraborty et al. 2005; Dow and Cutter 1998). The Python package powerlaw was used for fitting and Maximum Likelihood Estimation.

The results of the fitting are shown in Figure 9. The red circles represent the movements during the 24-hour period when the disaster happened. The green circles represent the movements before the disasters happened, while the blue circles represent the aftermath. The red, green and blue lines are the fitting results. The Maximum Likelihood Estimation test results are provided in Appendix B Table B1. The results show that the power-law still dominates human mobility in most cases across different types of disasters. In all cases, each daily displacement data fits with the power-law distribution better than the exponential distribution (p-value<0.001). Out of 471 days, we found that 455 days followed the power-law distribution better than the lognormal distribution. Therefore, we found support for Hypothesis 1 in all the cases.

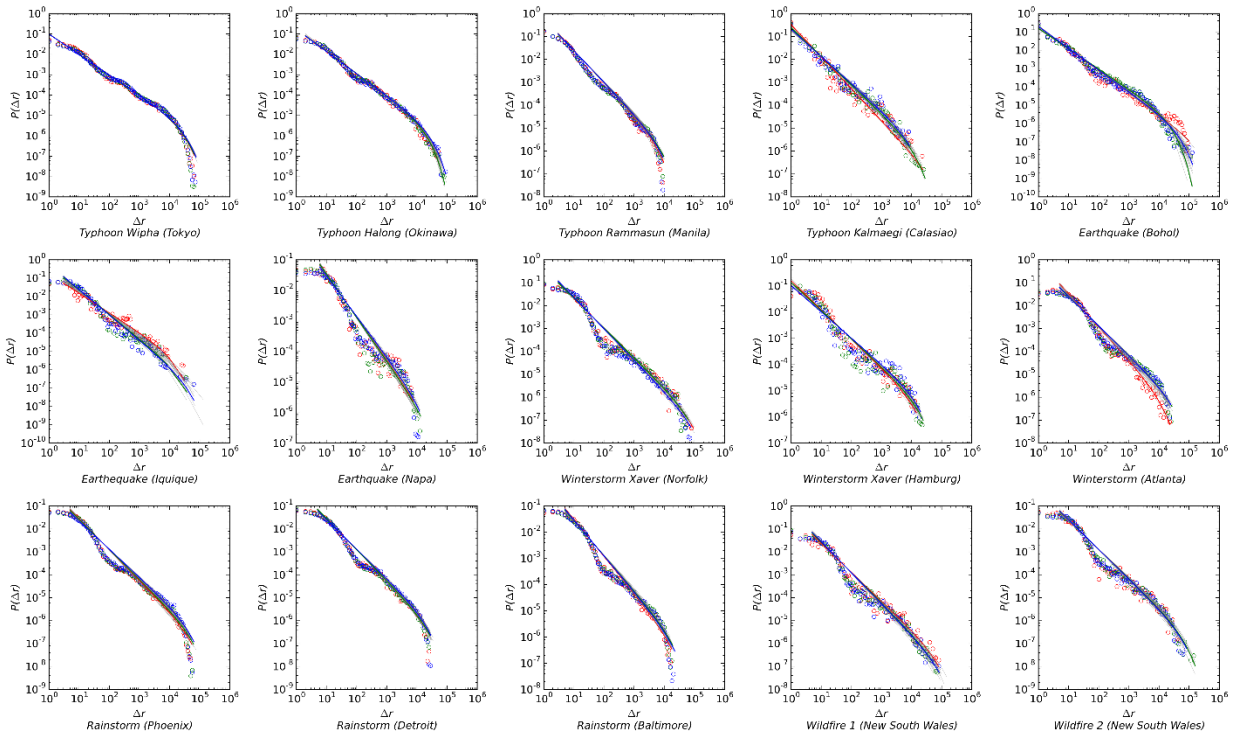

Figure 9: Human Movement Data Fitting Results

To test Hypothesis 2 and Hypothesis 3, we analyzed the shifting distances of the centers of human movement trajectories during the natural disasters in each affected city. We also documented the changes of the radius of gyrations of human movements from the steady states to the perturbation states. We first calculated each individual's center of mass of movements from both perturbation states $\vec{r}_{CM}^{P}$ and steady states $\vec{r}_{CM}^{S}$ using the following equation:

$$\vec{r}_{CM} = \frac{1}{n(t)} \sum_{i=1}^{n(t)} \vec{r}_i$$

Where $\vec{r}_i$ was a coordinate, and *n(t)* was the number of places one visited within the 24-hour period. The perturbation state was set as the 72-hour period when a natural disaster occurred, and the steady state was set as another 72-hour period which occurred two weeks before the perturbation state. Using the center of mass in the steady state and in the perturbation state, the shifting distance Δd_{CM} was calculated using the following equation:

$$\Delta d_{CM} = \left| \vec{r}_{CM}^{P} - \vec{r}_{CM}^{N} \right|$$

We also calculated the radius of gyration in both the perturbation states r_g^P and the steady states r_g^S using the following equation:

$$r_g = \sqrt{\frac{1}{n(t)} \left[2r \times \sin^{-1} \left(\sqrt{\sin^2 \left(\frac{\phi_2 - \phi_1}{2} \right) + \cos \phi_1 \cos \phi_2 \sin^2 \left(\frac{\varphi_2 - \varphi_1}{2} \right)} \right) \right]^2}$$

The states were the same periods we used to calculate the center of mass.

Analytic results demonstrated that Δd_{CM} are strongly correlated with r_g^S in thirteen out of the fifteen cases. The correlation coefficients and *p*-values are presented in Table 3. Therefore, Hypothesis 2 was supported in thirteen cases.

Table 3: Correlation between Δd_{CM} and r_g^S

Type	Name/Location	Correlation Coefficient
Typhoon	Wipha (Tokyo)	0.539672692***
	Halong (Okinawa)	0.399066158***
	Kalmaegi (Calasiao)	0.412774447*
	Rammasun (Manila)	0.57926189***
Earthquake	Bohol (Bohol)	0.270450514***
	Iquique (Iquique)	0.15591484
	Napa (Napa)	0.463082337***
Winterstorm	Xaver (Norfolk)	0.555180382***
	Xaver (Hamburg)	0.257535062
	- (Atlanta)	0.678411423***
Rainstorm	- (Phoenix)	0.533596975***
	- (Detroit)	0.452612074***
	- (Baltimore)	0.413542843***
Wildfire	New South Wales (1)	0.896617706***
	New South Wales (2)	0.292383392*

*significant at $p< 0.05$; ** significant at $p<0.01$; ***significant at $p<0.001$

We also tested the correlation between r_g^P and r_g^S. The correlation coefficients were positive and significant in eleven out of fifteen cases, as shown in Table 4. Therefore, Hypothesis 3 was supported in eleven cases.

Table 4: Correlation between r_g^P and r_g^S

Type	Name/Location	Correlation Coefficient
Typhoon	Wipha (Tokyo)	0.524405***
	Halong (Okinawa)	0.215695***
	Kalmaegi (Calasiao)	0.149604
	Rammasun (Manila)	0.288469***
Earthquake	Bohol (Bohol)	0.031066
	Iquique (Iquique)	-0.08923
	Napa (Napa)	0.33824*
Winterstorm	Xaver (Norfolk)	0.332673***
	Xaver (Hamburg)	0.198529
	Storm (Atlanta)	0.250897***
Rainstorm	Storm (Phoenix)	0.341179***
	Storm (Detroit)	0.245938***
	Storm (Baltimore)	0.243112***
Wildfire	New South Wales (1)	0.799249***
	New South Wales (2)	0.507008***

*significant at $p< 0.05$; ** significant at $p<0.01$; ***significant at $p<0.001$

4.7 Discussion

Our results, in aggregate, demonstrate that natural disasters do indeed influence human movements in urban areas, although the impact can vary in terms of severity and duration. In this section we discuss the results of each of our hypotheses in relation to previous research and its implications for future research and practice. These findings add to our understanding of the perturbation and resilience of human mobility during natural disasters.

In our first hypothesis, we assumed that natural disasters would not fundamentally change human mobility patterns and that the power-law distribution would continue to govern human movements. Results from data fitting and Maximum Likelihood Estimation tests show that although perturbed by different types of natural disasters, human movements in almost all the cases were still governed by the power-law. This finding aligns with previous studies that showed general human mobility follows a power-law distribution, with beta values ranging from 1.59 to 1.88 (Brockmann et al. 2006; Cheng et al. 2011; González et al. 2008; Hawelka et al. 2014). The differences between the calculated β values here and the values reported in other studies may be due to the fact that the values in our study were derived from higher precision location data in more tightly constrained geographical areas.

In our second hypothesis, we assumed that the values of the shifts in the distances of the centers of individual movements (Δd_{CM}) are correlated with the values of the radius of gyration in steady states (r_g^S). Our analysis demonstrates that while the correlation is supported in most cases, this correlation was not statistically significant in either the 2014 Iquique earthquake or the 2013 Xaver winter storm in Hamburg. Similarly, while we observed strong correlations between the values of the radius of gyration in perturbed states (r_g^P) and those in steady states (r_g^S) in eleven cases, we did not find such correlations in four cases. In addition to the same two identified in the previous analysis, no statistical correlations were supported in either the 2013 Bohol earthquake or 2014's Typhoon Kalmaegi.

The findings from both Hypothesis 2 and Hypothesis 3 are critical to understand human mobility under the influence of natural disasters. While previous research has discovered that the radius of gyration can be used to capture individual human mobility patterns (González et al. 2008), an individual's radius of gyration could significantly change under the influence of natural disasters

and extreme events. In cases where natural disasters have a relatively mild impact, the radius of gyration can indeed be used to understand and even predict human movement patterns, as noted in a previous study (Wang and Taylor 2014). However, if the impact is severe enough, human mobility patterns observed in steady states can be significantly changed. Thus, they can no longer be used to predict human movements in their perturbed states. Further research is needed to determine the point after which the resilience in human mobility can no longer be predicted.

4.8 Limitations

While Twitter is widely adopted in some countries, it is less prevalent in other places. For this study a substantial amount of empirical data was collected from Tokyo, Manila, Okinawa, Norfolk, Hamburg, Napa, Atlanta, Phoenix, Detroit and Baltimore, but less data was available from places such as Iquique, where we were able to collect less than 300 displacements (the suggested value for comparing the goodness of fit between a lognormal distribution and a power-law distribution) for several days after the Iquique earthquake. The limited number of data points could potentially influence the results, resulting in a better fit for the lognormal distribution for several days. However, we were able to retrieve more than 100 displacements each day for all the cases, and overall the number is sufficient to distinguish whether a power-law distribution or an exponential distribution fitted the data better.

4.9 Conclusion

Human mobility in urban areas is inevitably influenced by natural and man-made disasters. Existing research has reported that changes in the natural environment can cause behavioral change and temporary, or even permanent, human migrations (Bengtsson et al. 2011; Morrow-Jone and Morrow-Jone 1991). In this study we collected empirical human movement data using Twitter to

discover whether human mobility is indeed perturbed by different natural disasters, and whether the human mobility patterns observed in steady states are correlated with those during natural disasters. The data were analyzed to identify and quantify human mobility perturbation from the steady state in each case.

Our findings demonstrate that: (1) human mobility patterns are unlikely to deviate from the fundamental power-law during a natural disaster; (2) human mobility in perturbed states generally shows strong correlations with those in steady states; and (3) in the event of a particularly severe natural disaster, human mobility can change become more eratic and this correlation is lost.

The results from the empirical data revealed that power-law continues to govern human mobility during a natural disaster. This result supports the findings from several studies of general human mobility patterns (Brockmann et al. 2006; Cheng et al. 2011; González et al. 2008; Hawelka et al. 2014). While previous research did not distinguish between human mobility patterns in perturbation states or steady states, our findings demonstrate that the power-law is still applicable even during multiple types of natural disasters, highlighting the inherent resilience and adaptability of human mobility.

The study also contributes to research into human mobility by showing that natural disasters can significantly change human mobility patterns even where the fundamental power-law still holds. An earlier study had shown that human mobility has inherent resilience; the values of the radius of gyration in perturbation states were correlated with those in steady states in NYC when Hurricane Sandy came onshore (Wang and Taylor 2014). This study extends this earlier research by examining this resilience more closely across multiple types of natural disasters, demonstrating that human mobility resilience can survive a certain level of perturbation during disasters but that

more powerful disasters could destroy this resilience and force people to adopt entirely different travel patterns.

While this study provides a first attempt to examine human mobility perturbation over a range of natural disaster types, future research can build on its findings by extending this approach to additional types of natural disasters and incorporating other influential factors as independent variables that may, or may not, be correlated with the mobility patterns (for example, the differing availability of public transportation and/or types of mobility infrastructure available). Such future research will help identify the factors that contribute significantly to human mobility perturbation. Also, given that the Lévy flight model still appears to govern human behavior even in perturbed states, future research can look to nature to identify bio-inspired solutions for coping with the disturbances brought by natural disasters. This will help policy makers and practitioners to better predict human movements and improve disaster evacuation, response, and recovery plans.

4.10 Acknowledgements

This study is supported by the National Science Foundation under Grant No. 1142379 and a Virginia Tech BioBuild Interdisciplinary Graduate Education Program grant. Any opinions, findings, and conclusions or recommendations expressed in this material are those of the authors and do not necessarily reflect the views of the National Science Foundation or the Virginia Tech Interdisciplinary Graduate Education Program.

CHAPTER 5: CONTRIBUTIONS

For my doctoral research, I led initiatives to comprehend human mobility patterns under the influence of natural disasters. I approached this goal by first developing a data collecting system that gathers data on human movements. The high quality data collected through the system enabled the study on human mobility under the influence of natural disasters. I applied knowledge and analytical methods learned from data science and geo-social networking to study human movements. Lessons and contributions associated with the three research initiatives are presented in the following sections.

5.1 The Design of Human Movement Data Collecting System

At the first stage of my doctoral research, I conducted a full review of existing avenues to collect human movement data. Human movement data had previously been collected from four resources - currency circulation, GPS, cell phone data, and geo-social networking platforms (Brockmann et al. 2006; González et al. 2008; Cho et al. 2011; Liang et al. 2012; Noulas et al. 2012). However, these resources have their complications as I reported in Chapter 2. To resolve these complications, especially the representativeness issues existing in the small to medium size geo-social networking platforms, I developed a novel data collecting system. While this system was influenced by earlier systems, several fresh concepts were integrated into its design to facilitate human mobility study.

The system was designed to collect large scale data of human movements from massive online social networking platforms. Although my doctoral research implemented Twitter, the design is compatible with any geo-social networking platform with open APIs. My system provides several advantages over other platforms. It collects human movement data with much larger quantity in

comparison to other smaller platforms used in existing studies (Cho et al. 2011; Noulas et al. 2012). Therefore, it provides more data for analysis and potentially reduces the effect of data bias. My system also provides human mobility data with higher resolution. The high-resolution data enables human mobility research on the city-level and identifies travel perturbation on a finer scale. Moreover, the demographical information of Twitter users shows that the users of this large-scale social network are representative of the broader population. This information makes it possible to generalize the findings further than previous studies. Finally, the system only relies on social networking platforms with open APIs. The open design not only reduces the barriers of human mobility study, but it also makes it possible for researchers to validate findings from previous studies.

Beyond the improvements to previous data collecting systems, my system also incorporates a flexible design in order to support a wide range of geo-social networking platforms. The system was designed using only Python. Therefore, the system can be transplanted on most operational systems. Additionally, while the system has primarily been used to collect human location data, it can be applied to collect social relations, communication, information diffusions, etc. Such information can be integrated into the human mobility research and can reveal the driving forces of human traveling under the influences of natural disasters.

5.2 The Understanding and Quantification of Human Mobility Perturbation

My doctoral research focused on understanding and quantifying human mobility perturbation. While human mobility research has discovered some fundamental patterns (Brockmann et al. 2006; González et al. 2008; Song et al. 2010a, b), previous research has seldom considered how environmental change can impact human movements. Although it is intuitive to assume extreme

events and weather changes could influence human mobility (Bagrow et al. 2011; Horanont et al. 2013), to the best of my knowledge, no studies have attempted to quantify the perturbation, perhaps due to difficulties associated with collecting high resolution data. There is a pressing need to quantify such perturbation so we can better predict human mobility during extreme events.

My research takes initial steps to gain a ground-truth understanding of human mobility perturbation. I used both geographical analysis and statistical analysis to demonstrate how human movements deviated from their steady state patterns, transferring into a perturbation pattern. For example, in Hurricane Sandy's case, residents in NYC reduced their long-distance travels and increased their short-distance travels. I also developed a methodology to quantify human mobility perturbation using key concepts and analytical methods borrowed from geo-social networking research. The quantification relies on three key parameters: the scaling parameter of the power-law distribution, the center of mass of movements, and the radius of gyration of movements. While they are confirmed as the key parameters to capture general human mobility, I demonstrate that they are also the key factors to quantify the perturbation that human mobility experienced during natural disaster events. Comparing the values of the three parameters between steady states and perturbation states, I am able to quantify the perturbation strength and identify more powerful influence across different disaster events.

5.3 The Discovery of Resilience in Human Mobility

Evaluating resilience is a key task during natural disasters and extreme events (Adger 2006; Cutter et al. 2008). While previous research has concentrated on the resilience in infrastructure systems in natural disasters (Pan et al. 2007; Rosenzweig and Solecki 2014), my research discovered resilience in human travel behaviors. As I demonstrated in Chapter 3, mobility resilience is an

inherent attribute of human behaviors. But such resilience can be a double-edged sword. Resilience can help individuals withstand the impact of natural disasters to a certain extent and return back to routines quickly after perturbation. However, it can also make people reluctant to take prompt and effective actions to avoid potential dangers caused by natural disasters.

I examined resilience by quantifying the correlation of human mobility patterns between steady states and perturbation states. I not only showed in what cases human mobility resilience can withstand the impact of natural disasters, but also I revealed the limitation of that resilience. Extremely powerful natural disasters can weaken the correlation, destroy human mobility resilience, and even force human mobility into a rather chaotic state. The discovery of resilience, as well as the loss of resilience, has significant implications. It improves our understanding about the complexity of the phenomenon. Such understanding is a key component of analyzing human behaviors during natural disasters and emergencies. Additionally, it aids in predicting human mobility during natural disasters. Such prediction is of critical importance for policy makers and practitioners to solve infrastructure related issues during natural disasters such as traffic jams, accidents and crashes, road blockages, etc.

CHAPTER 6: FUTURE RESEARCH

My doctoral research lies at the intersection of human mobility and natural disasters, motivated by the fact that the human race is facing an increasingly critical challenge regarding natural disasters. I explore and quantify perturbation and resilience in human travel behaviors under the influence of extreme events by applying recent technological advancements in geo-social networking and data science. Currently, I am expanding my research focus from hurricanes to other types of natural disasters, including earthquakes, tsunamis, storms, wildfires, etc., in an effort to identify a universal pattern that governs human movements in a perturbation state. In the future, my research will extend to investigate the coupled systems that link human mobility and social networks. My ultimate goal is to promote public safety and health by finding the most effective way to predict human locations and travel patterns, thus facilitating the protection of vulnerable individuals from potential harms and injuries during disasters.

Recent advances in geo-social networking technologies have opened up new opportunities to uncover the hidden forces that drive human mobility and its perturbation. Over the next few years, my research will build on my PhD studies in three areas: (1) simulating and visualizing large-scale human mobility in urban areas under the influence of natural disasters; (2) exploring the existence of a universal pattern that governs human mobility perturbation; and (3) developing a disaster response and feedback system.

6.1 Simulating Large-Scale Human Mobility in Urban Areas under the Influence of Natural Disasters[5]

While the findings from my doctoral research provides considerable insight into the phenomenon of human mobility perturbation, this future project aims to apply these findings to visualize human movements in a virtual environment and simulate the mobility of humans facing the approach and/or occurrence of natural disasters. Such simulations will improve the predictability of human movements during extreme events, and influence both local and regional policies on disaster response, evacuation, and relief plans.

Human mobility research originated from animal mobility studies. Researchers have attempted to describe animal movement patterns for over one hundred years. Pearson (1905) first proposed a mathematical model to capture human and animal movements. The model assumed each individual moves consistently, and each move has a set distance though a randomly different angle from its previous movements. Such model is called a random walk model. Later, Lévy modified the model and made the distances of steps follow a heavy-tailed probability distribution such as power-law (Mandelbrot 1983). This model was called Lévy flight. Research has shown that the movements of many types of animals follow Lévy flight (Bartumeus 2007, Benhamou 2007, Viswanathan et al. 1996).

Undoubtedly an important discovery, Lévy flight may not always be the best model to describe animal movements. An assumption of Lévy flight, though it may not be explicitly pointed out by

[5] Preliminary results of this future study have been developed into a conference paper titled "Examining and Simulating Human Mobility under the Influence of Tropical Cyclones," which was submitted to the 5th International/11th Construction Specialty Conference, Vancouver, British Columbia, Canada.

researchers, is that animal movements happen in a continuous space without any constraints. However, in reality animals habitats and foraging spaces have boundaries. It is also evident that human activities have imposed more constraints and limitations to animal spaces. All of these constraints can make Lévy flight an inappropriate model to describe animal movements.

One of the examples that human activity influences animal movements is habitat fragmentation. Habitat fragmentation is a process that a large habitat is transformed into several smaller patches. These patches isolate from each other and the total area of these patches is always smaller than the original habitat (Wilcove, McLellan, and Dobson 1986). Habitat fragmentation was observed to be associated with different types of long-term effects such as population reduction and extinction, edge effects, reduced gene flows and so on (Wolff, Schauber, and Edge 1997). Research has shown that habitat fragmentation can dramatically change animal movements as a short-term effect (Diffendorfer, Gaines, and Holt 1995). Laurance et al. (2004) studied how roads and human clearing influenced birds' movements. They found while there were no physical constraints that prevented birds from flying near or crossing the roads built inside of forests, birds avoid doing so due to edge and gap avoidances. In fact, comparing two areas of the same size, one in a forest and one crossed by a road, the number of movements reduced by 50% in the latter case.

While mainly observed in animals, similar fragmentation can happen in human societies as well. As aforementioned, such fragmentation are particularly common during the occurrence of natural disasters. Different situations, such as road blocks, traffic jams, evacuation zones, disaster damaged areas, etc., can all fragment urban spaces. In these emergency situations, urban dwellers might find it difficult to cross these gaps, be forced to reduce their activities in a smaller area, and/or be denied to the primary locations they visit in ordinary days. All these can cause constraints to human movements.

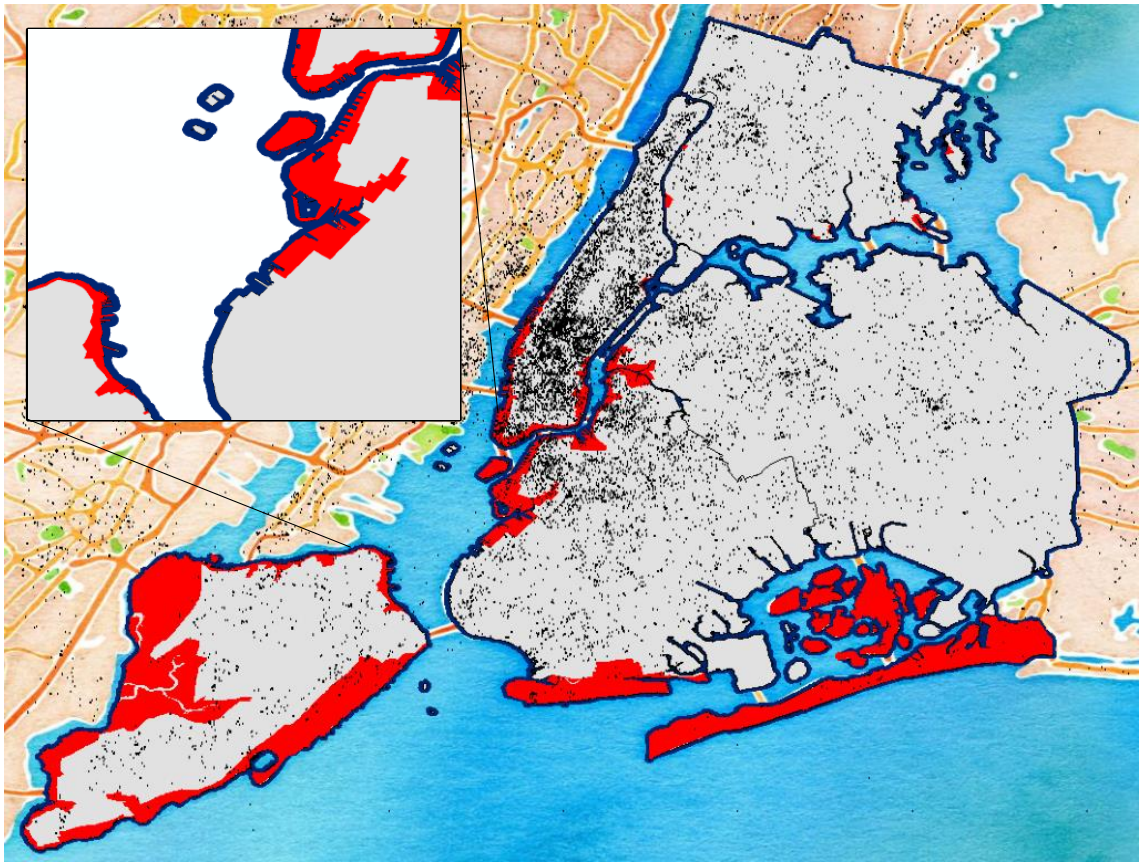

Figure 10: Geographical Data from New York City

Inspired by habitat fragmentation and its influence on animal movements, this future study examines whether such phenomenon in built environment has similar influence on human movements. A preliminary study re-examined the human mobility data collected from Twitter. I used ArcGIS and its associated Python package arcpy to conduct my initial analysis. The grey area in Figure 10 shows the shapefile of NYC. Each black point was a geographical coordinate retrieved from a geo-tagged tweet. The read areas are the mandatory evacuation zones. The accuracy of each location is 3 to 8 meters depending on the geo-tagging devices. To minimize the possible errors caused by both the shapefile and devices, I created a buffer of 200 meters around the original shapefile (blue areas in Figure 10). A crossing displacement needs to have one point inside the original shapefile, and the other point outside of the buffered shapefile.

Table 5 shows the total displacements and crossing displacements in different days. I found no significant changes of total displacements during the strike of Hurricane Sandy. In fact, the total displacements increased by 19% during the first 24-hours after the landfall of Hurricane Sandy. However, the crossing displacements were dramatically reduced, and the reduction was up to 50%.

Table 5: Total Displacements and Crossing Displacements

Day	Total Displacements	Crossing Displacements
1	51185	310
2	38438	321
3	42746	373
4	40457	353
5	51894	466
6	46863	421
7	41764	495
8	43184	615
9	43367	576
10	45220	521
11	37879	474
12	41168	612

The crossing displacements gradually recovered to a normal level. The phenomenon reflected the infrastructural situations in New York City. Hurricane Sandy caused flooding to several tunnels and widespread power outage. After the strike of Hurricane Sandy, most public transportation only started to resume partial or full schedule service 36 to 72 hours after Hurricane Sandy struck

(Kaufman et al. 2012) and over 1 million people in the city were still without power until 2pm Nov. 2 (McGeeham 2012).

Geographical analysis highlighted the impact of habitat fragmentation on human mobility. Figure 11 shows that crossing displacements usually radiate from the lower Manhattan area to other places. During the emergency, areas surrounding this area became evacuation zones and separated Manhattan from New Jersey. Comparing the three panels in Figure 11, one can observe that the separation substantially reduced human mobility crossing New York City to its adjacent areas.

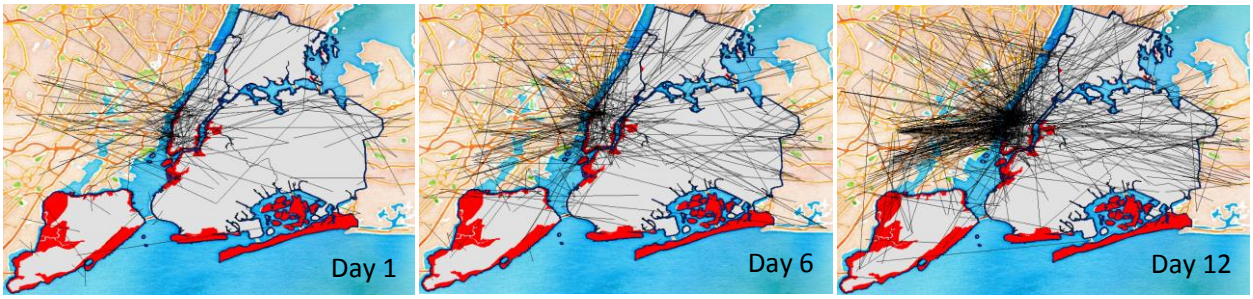

Figure 11: Geographical Distribution of Crossing Displacements

Research has shown that agent-based simulation plays a key role in the study of human mobility in emergency situations (González, Hidalgo, and Barabási 2008). The analytical results and the large-scale data of human movements enable the possibility to build an agent-based model to simulate human mobility during the occurrences of tropical cyclones. Therefore, in the future I will develop an agent-based GIS model with a structure of three levels: an individual level, an aggregate level and an environment level (Figure 12). On the individual level, an agent represents a person in NYC. The analytical results from the human movement data will be used to create algorithms that govern each agent's attributes, decision-making, behaviors, and interactions with other agents. Each agent will have its own center of movement, radius of gyration, trajectory, primary visiting locations, traveling routes, etc. An agent will also have its own preference to deal

with the risk when the environment changes, i.e. hurricane approaching and striking. On the aggregate level, I will simulate the aggregate properties and patterns from all the agents. Following a pattern-oriented modeling approach (Grimm et al. 2005), distributions found in human displacements, shifting of movement centers, radius of gyration, and social degree will be used to govern the aggregate properties in the model. On the environment level, GIS data of the NYC urban setting and road system will serve as the context for agents' movements and behaviors.

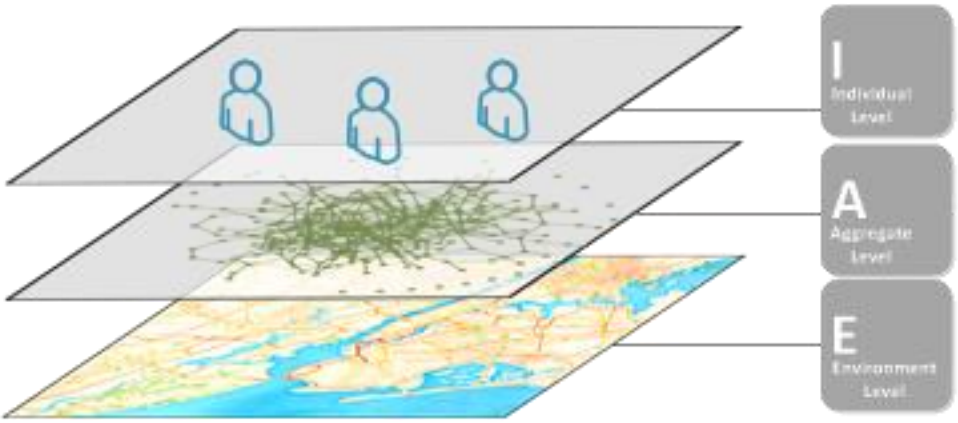

Figure 12: Agent-Based GIS Model

Computational experiments will be conducted to test three scenarios using the agent-based GIS model. These three scenarios are (1) the imposition of evacuation orders, (2) the occurrences of flooding, and (3) the abrupt failure of infrastructure that cause certain road blockage. In each scenario, I will test how human movements perturb and how human mobility patterns differ in different scenarios. The model will help us explore the impact of habitat fragmentation in urban areas to improve our understanding human mobility patterns under the influence of tropical cyclones. The results will support the decision-making of policymakers in different emergency situations.

6.2 Exploring Universal Pattern of Human Mobility Perturbation[6]

Drawing inspiration from the findings related to human mobility in multiple disasters, I am interested in exploring the possibility of a universal pattern that dominates human mobility perturbation across different types of natural disasters. My research has been focusing on comparable studies to identify the changes of human mobility. I plan to extend the effort to include a broader spectrum of natural disasters. The study will aim to discover fundamental parameters, equations or algorithms to describe human mobility perturbation during emergencies. The findings could contribute to the development of a deeper understanding of common coping mechanisms across human societies, regardless of their demographics, geographies, and economic status.

A preliminary study has examined the loss of resilience of human mobility under the influence of typhoons. The examination was based on high-resolution empirical human mobility data collected from 8 areas under the influences of 5 Typhoons. These cases are (1) Tokyo, Japan (Typhoon Wipha, 2013), (2) Tacloban, Philippines (Typhoon Haiyan, 2013), (3) Cebu, Philippines (Typhoon Haiyan, 2013), (4) Antipolo, Philippines (Typhoon Rammasun, 2014), (5) Manila, Philippines (Typhoon Rammasun, 2014), (6) Okinawa, Japan (Typhoon Halong, 2014), (7) Nakagami, Japan (Typhoon Phanfone, 2014), and (8) Calasiao, Philippines (Typhoon Kalmaegi, 2014). I collected human mobility data from continuously streaming global geo-tagged tweets. After a typhoon occurred, I retrieved the 24-hour human mobility data from the impacted areas, as well as, 15-day data before the landing of the typhoon and 17-day data after the landing of the typhoon. In total, I collected 1,688,319 geo-tagged tweets from 123,938 individuals in the eight cases. To test if the

[6] Preliminary results of this future study have been developed into a conference paper for the 2015 Engineering Project Organization Conference – Engineering Growth, Edinburgh, Scotland. The paper is titled "Loss of Resilience in Human Mobility under the Influence of Natural Disasters".

occurrences of human mobility perturbation were caused by the typhoons, I compared the human movements of different days. I assumed that the day each typhoon made landfall was day 0 and retrieved displacement data on that day. Displacement data was also retrieved from 15 days before the landfall (-) and 17 days after the landfall (+). Each day was assumed to start at 3am in the morning at local time. I assumed that the perturbation state ($\mathbf{D}_p$) was the 24-hour period after a typhoon made landfall. The steady state ($\mathbf{D}_s$) was considered the normal days that were at least one week before or after the landing of the typhoon.

I analyzed the perturbation strength for each case by examining the changes in the distributions of displacements. First, I calculated the probability distributions for both $\mathbf{D}_p$ and $\mathbf{D}_s$, and let $\boldsymbol{d}_E = [d_E^{(1)}, d_E^{(2)}, \ldots, d_E^{(dmax)}]$ be the Euclidean distances between the two distributions. Therefore, $\boldsymbol{d}_E$ demonstrates the perturbation strength between human mobility in a perturbation state and a steady state for each case. I collected wind speed data from reports and weather station records and conducted the Pearson test between the strength of human mobility perturbation and wind speed. The results show that the median values of $\boldsymbol{d}_E$ are were weakly correlated with wind speeds ($r = 0.69$, $p<0.1$).

The analysis of displacements demonstrated three patterns for human mobility while influenced by tropical cyclones. While displacements from all cases suffered temporary fluctuations, the three cases with smaller $\boldsymbol{d}_E$ absorbed the perturbations quickly (Pattern 1). However, with the increasing of perturbation degree, it became increasingly difficult to absorb the shocks. Human mobility experienced a higher magnitude of fluctuation and required a longer time period to return to equilibrium (Pattern 2). In the case of Typhoon Haiyan in Tacloban, human mobility collapsed and the movements dropped to an extremely low level (Pattern 3).

To understand the perturbation and loss of resilience, I tested two sets of hypotheses. First, perturbations follow the same pattern in different cases only with different magnitudes (**Hypothesis 1A**) or stronger perturbations are caused by entirely different patterns (**Hypothesis 1B**). Second, the loss of resilience could come from a fundamental deviation from power-law (**Hypothesis 2A**) or from the aggregate effects of individuals changing their radii of gyrations (**Hypothesis 2B**).

The analysis on the first set allowed me to find that stronger perturbations in human mobility exhibit significantly different patterns from the weaker ones. Low-magnitude perturbation often exhibits mild fluctuations in travel frequencies and distances and returns to its equilibrium in a short-time period. High-magnitude perturbation, on the other hand, forces human movements to significantly deviate from their balance with stronger perturbations, taking a significantly longer time to return to equilibrium. While low-magnitude perturbation is linear and shows a clear pattern of oscillation, high-magnitude perturbation is non-linear, chaotic, and more difficult to predict.

These findings highlight the possibility that human mobility can lose its resilience in extreme conditions. When experiencing mild influences from tropical cyclones, human mobility suffers temporary perturbation but strives to return to its state of equilibrium. However, powerful influences from tropical cyclones, or natural disasters in general, can destroy established resilience in human mobility, forcing individuals to deviate from their routines and adapt to new environments. The process is often more time-consuming, unpredictable, and associated with the collapse of established equilibriums.

After analyzing the second set of hypotheses, I found that although tropical cyclones can trigger different patterns of human mobility perturbation, a truncated power-law governs human mobility

universally, even when influenced by extremely powerful natural disasters, such as Typhoon Haiyan. While this finding confirms that the power-law is the fundamental pattern in human mobility (Brockmann, Hufnagel, and Geisel, 2006; González, Hidalgo, and Barabási, 2008), it also suggests the perturbation and collapse of human mobility are not caused by the deviation from power-law. The scaling parameter β is an insensitive factor and cannot be used to capture these phenomena in human movements.

Instead, the perturbation and loss of resilience of human mobility are more likely to be the results of individuals changing their radii of gyrations. I found that the radius of gyration is not only a key parameter to describe the fundamental patterns on the individual level (González, Hidalgo, and Barabási, 2008), but also the key factor to capture and analyze perturbations in aggregate human mobility. This links human mobility perturbation from the micro-level to the macro-level, enabling more accurate location and travel predictions during the occurrence of natural disasters to minimize loss of life and human suffering.

6.3 Developing a Disaster Response and Feedback System

I also plan to develop a real-time disaster response and feedback system. While geo-social networking data can be used to analyze the aftermath of a natural disaster, the data is collected in real-time. The real-time data is valuable because the lack of such data has critically hindered research on disaster evacuation and relief plans. Until now, the majority of the real-time evacuation studies have been simulation studies. Very limited studies have focused on real-time human travels, and the available ones primarily focus on ontology and visualization after a disaster event. Developing a real-time evacuation feedback system is limited by (1) the lack of real-time data; (2)

the available real-time data is insufficient to allow patterns to emerge; and/or (3) the data has low-resolution.

Massive social networking platforms can potentially overcome these limitations and contribute to study on real-time feedback systems. Take Twitter as an example. A tweet during an emergency could provide several types of information: (1) if this individual was safe and could report a safe location; (2) if he/she suggested a dangerous location, such as failure of infrastructure, flooding, road block, and traffic jams; (3) if he/she suggested a place to evacuate; (4) if he/she suggested a route to evacuate and the conditions of the route; and (5) what means he/she used to evacuate (bus, cars or on foot). All this information could be integrated into a live interactive map to provide critical, real-time information. Such a feedback system could potentially provide more accurate, prompt information for individuals to make decisions in emergencies.

REFERENCES

Adger, W. N. (2006). "Vulnerability." *Global Environmental Change*, 16(3), 268-281.

Adger, W. N., Hughes, T. P., Folke, C., Carpenter, S. R., and Rockström, J. (2005). "Social-ecological resilience to coastal disasters." *Science*, 309(5737), 1036-1039.

Amin, S. M., and Wollenberg, B. F. (2005). "Toward a smart grid: Power delivery for the 21st century." *IEEE Power Energ. Mag.*, 3(5), 34–41.

Amundsen, P., and Klemetsen, A. (1988). "Diet, gastric evacuation rates and food consumption in a stunted population of Arctic charr, Salvelinus alpinus L., in Takvatn, northern Norway." *Journal of Fish Biology*, 33(5), 697-709.

Anderson, K., Lee, S., and Menassa, C. (2014). "Impact of Social Network Type and Structure on Modeling Normative Energy Use Behavior Interventions." *Journal of Computing in Civil Engineering*, 28(1), 30-39.

Badland, H., and Schofield, G. (2005). "Transport, urban design, and physical activity: an evidence-based update." *Transportation Research Part D: Transport and Environment*, 10(3), 177-196.

Bagrow, J. P., Wang, D., and Barabasi, A.-L. (2011). "Collective response of human populations to large-scale emergencies." *PLoS ONE*, 6(3), e17680.

Bartumeus, F. (2007). "Lévy processes in animal movement: an evolutionary hypothesis." *Fractals*, 15(02), 151-162.

Bartumeus, F., da Luz, M. G. E., Viswanathan, G., and Catalan, J. (2005). "Animal search strategies: a quantitative random-walk analysis." *Ecology*, 86(11), 3078-3087.

Bassett, D. R., Cureton, A. L., and Ainsworth, B. E. (2000). "Measurement of daily walking distance-questionnaire versus pedometer." *Medicine and Science in Sports and Exercise*, 32(5), 1018-1023.

Beasley, D. (2014). "Deadly ice storm turns Atlanta into parking lot, strands thousands." <http://www.reuters.com/article/2014/01/29/us-usa-weather-idUSBREA0Q1DK20140129>. (December 10, 2014).

Becerik-Gerber, B., Siddiqui, M., Brilakis, I., El-Anwar, O., El-Gohary, N., Mahfouz, T., Jog, G., Li, S., and Kandil, A. (2014). "Civil Engineering Grand Challenges: Opportunities for Data Sensing, Information Analysis, and Knowledge Discovery." *Journal of Computing in Civil Engineering*, 28(4). <10.1061/(ASCE)CP.1943-5487 .0000290, 04014013>.

Bengtsson, L., Lu, X., Thorson, A., Garfield, R., and von Schreeb, J. (2011). "Improved response to disasters and outbreaks by tracking population movements with mobile phone network data: a post-earthquake geospatial study in Haiti." *PLoS Medicine*, 8(8), e1001083.

Benhamou, S. (2007). "How many animals really do the Levy walk?" *Ecology*, 88(8), 1962-1969.

Bennett, S. (2013). "Facebook, Twitter, Instagram, Pinterest, LinedIn: 2013 social media demographics." <http://www.mediabistro.com/alltwitter/ social-demographics-2013_b53515>. (Dec. 15, 2014).

Bland, H., and Frost, J. (2012). "Opportunities and Considerations for Smartphone Applications and Mobile Social Media in Post Extreme Event Reconnaissance Data Collection." *Proc., 6th Congress on Forensic Engineering (CD-ROM),* San Francisco, 505–514.

Brockmann, D., Hufnagel, L., and Geisel, T. (2006). "The scaling laws of human travel." *Nature*, 439(7075), 462-465.

Brooks, N., Neil Adger, W., and Mick Kelly, P. (2005). "The determinants of vulnerability and adaptive capacity at the national level and the implications for adaptation." *Global Environmental Change*, 15(2), 151-163.

Byers, J. A. (2001). "Correlated random walk equations of animal dispersal resolved by simulation." *Ecology*, 82(6), 1680-1690.

Candia, J., González, M. C., Wang, P., Schoenharl, T., Madey, G., and Barabási, A.-L. (2008). "Uncovering individual and collective human dynamics from mobile phone records." *Journal of Physics A: Mathematical and Theoretical*, 41(22), 224015.

CDC (Center for Disease Control and Prevention). 2013. Deaths Associated with Hurricane Sandy — October–November 2012. edited by Center for Disease Control and Prevention. Atlanta, GA. <http://www.cdc.gov/mmwr/preview/mmwrhtml/mm6220a1.htm>. (Feburary 22, 2015).

Chaintreau, A., Hui, P., Crowcroft, J., Diot, C., Gass, R., and Scott, J. (2007). "Impact of human mobility on opportunistic forwarding algorithms." *IEEE Transactions on Mobile Computing*, 6(6), 606-620.

Chakraborty, J., Tobin, G. A., and Montz, B. E. (2005). "Population evacuation: assessing spatial variability in geophysical risk and social vulnerability to natural hazards." *Natural Hazards Review*, 6(1), 23-33.

Cheng, Z., Caverlee, J., Lee, K., and Sui, D. Z. "Exploring millions of footprints in location sharing services." *Proc., 5th Int. AAAI Conf. on Weblogs and Social Media (ICWSM '11),* Barcelona, Spain, 81-88.

Cho, E., Myers, S. A., and Leskovec, J. "Friendship and mobility: user movement in location-based social networks." *Proc., Proceedings of the 17th ACM SIGKDD International Conference on Knowledge Discovery and Data Mining*, ACM, San Diego, 1082-1090.

Clauset, A., Shalizi, C. R., and Newman, M. E. (2009). "Power-law distributions in empirical data." *SIAM Review*, 51(4), 661-703.

Cutter, S. L., Barnes, L., Berry, M., Burton, C., Evans, E., Tate, E., and Webb, J. (2008). "A place-based model for understanding community resilience to natural disasters." *Global environmental change*, 18(4), 598-606.

CWS (Church World Service – Asia/Pacific) (2013) Typhoon Haiyan/Yolanda Philippines: Situation Report 19. <http://reliefweb.int/sites/reliefweb. int/files/resources/2013.12.19-Haiyan-Typhoon-Philippines-Situation-Report-19.pdf>. Accessed: 22 October 2014.

Dai, A. (2013). "Increasing drought under global warming in observations and models." *Nature Climate Change*, 3(1), 52-58.

Diffendorfer, J. E., Michael S. G., and Holt, R. D. (1995). "Habitat fragmentation and movements of three small mammals (Sigmodon, Microtus, and Peromyscus)." *Ecology*, 76 (3), 827-839.

Dow, K., and Cutter, S. L. (1998). "Crying wolf: Repeat responses to hurricane evacuation orders." *Coastal Management*, 25, 237-252.

Drabek, T. E. (2000). "Disaster evacuations: tourist-business managers rarely act as customers expect." *The Cornell Hotel and Restaurant Administration Quarterly*, 41(4), 48-57.

Du, J., and Wang, Q. (2011). "Exploring Reciprocal Influence between Individual Shopping Travel and Urban Form: Agent-Based Modeling Approach." *Journal of Urban Planning and Development*, 137(4), 390-401.

EM-DAT (2012). "Natural Disasters Trends." The International Disaster Database, Center for Research on the Epidemiology of Disaster (CRED). < http://www.emdat.be/natural-disasters-trends>. (Feburary 22, 2015).

Estabrooks, P. A., Lee, R. E., and Gyurcsik, N. C. (2003). "Resources for physical activity participation: does availability and accessibility differ by neighborhood socioeconomic status?" *Annals of Behavioral Medicine*, 25(2), 100-104.

Fan, Y., and Khattak, A. J. (2008). "Urban form, individual spatial footprints, and travel: Examination of space-use behavior." *Transportation Research Record: Journal of the Transportation Research Board*, 2082(1), 98-106.

Feeley, M., Hutchinson, N., and Ray, S. (2004). "Realistic mobility for mobile ad hoc network simulation." *Ad-Hoc, Mobile, and Wireless Networks*, Springer-Verlag Berlin Heidelberg, German, 324-329.

Ferris, E., Petz, D., and Stark, C. (2013). "*The Year of Recurring Disaster: A Review of Natural Disasters in 2012."* The Brookings Institution, London School of Economics, Project on Internal Displacement. (http://www.brookings.edu/~/media/Researc h/Files/Reports/2013/03/natural%20disasters%20review/Brookings_Review_Natural_Di sasters_2012.pdf). (October 22, 2014).

Folke, C. (2006). "Resilience: the emergence of a perspective for social–ecological systems analyses." *Global Environmental Change*, 16(3), 253-267.

González, M. C., Hidalgo, C. A., and Barabási, A.-L. (2008). "Understanding individual human mobility patterns." *Nature*, 453(7196), 779-782.

Grimm, V., Revilla,E., Berger, U., et al. (2005). "Pattern-oriented modeling of agent-based complex systems: lessons from ecology." *Science* 310(5750), 987-991.

Gulbinas, R., Jain, R., Taylor, J., Peschiera, G., and Golparvar-Fard, M. (2014). "Network Ecoinformatics: Development of a Social Ecofeedback System to Drive Energy Efficiency in Residential Buildings." *Journal of Computing in Civil Engineering*, 28(1), 89-98. 10.1061/(ASCE)CP.1943-5487.0000319.

Hauff, C., and Houben, G.-J. "Placing images on the world map: a microblog-based enrichment approach." *Proc., Proceedings of the 35th international ACM SIGIR conference on Research and development in information retrieval*, ACM, Portland, OR, 691-700.

Hawelka, B., Sitko, I., Beinat, E., Sobolevsky, S., Kazakopoulos, P., and Ratti, C. (2014). "Geo-located Twitter as proxy for global mobility patterns." *Cartography and Geographic Information Science*, 41(3), 260-271.

Hecht, B., Hong, L., Suh, B., and Chi, E. H. "Tweets from Justin Bieber's heart: the dynamics of the location field in user profiles." *Proc., Proceedings of the SIGCHI Conference on Human Factors in Computing Systems*, ACM, Vancouver, BC, Canada, 237-246.

Horanont, T., Phithakkitnukoon, S., Leong, T. W., Sekimoto, Y., and Shibasaki, R. (2013). "Weather Effects on the Patterns of People's Everyday Activities: A Study Using GPS Traces of Mobile Phone Users." *PLoS ONE*, 8(12), e81153.

Howden, L. M., and Meyer, J. A. (2010). "Age and Sex Composition: 2010. 2010 Census Briefs.", <http://www.census.gov/prod/cen2010/briefs/c2010br-03.pdf.>. (Dec. 15, 2014)

Huang, S., Sadek, A., and Guo, L. (2013). "Computational-Based Approach to Estimating Travel Demand in Large-Scale Microscopic Traffic Simulation Models." *Journal of Computing in Civil Engineering*, 27(1), 78-86.

Huberman, B. A. (2012). "Sociology of science: Big data deserve a bigger audience." *Nature*, 482(7385), 308-308. 10.1061/(ASCE)CP.1943-5487.0000202.

Ikawa, Y., Enoki, M., and Tatsubori, M. "Location inference using microblog messages." *Proc., Proceedings of the 21st international conference companion on World Wide Web*, ACM, Lyon, France, 687-690.

Isaac, M. (2013). "With a Slew of Updates, Google+ Makes Its Photography Pitch." <http://allthingsd.com/20131029/with-a-slew-of-updates-google-makes-its-photography-pitch/>. (Dec. 15, 2014).

Johansen, S., and Juselius, K. (1990). "Maximum likelihood estimation and inference on cointegration—with applications to the demand for money." *Oxford Bulletin of Economics and statistics*, 52(2), 169-210.

Kareiva, P., and Shigesada, N. (1983). "Analyzing insect movement as a correlated random walk." *Oecologia*, 56(2-3), 234-238.

Kaufman, S., Qing, C., Levenson, N., and Hanson, M. (2012). "*Transportation During and After Hurricane Sandy."* New York City: Rudin Center for Transportation NYU Wagner Graduate School of Public Service. < https://wagner.nyu.edu/files/faculty/publications/sandytransportation.pdf>. (October 22, 2014).

Kimura, M., and Saito, K. "Tractable models for information diffusion in social networks." *Proc., Knowledge Discovery in Databases: PKDD 2006*, Springer, 259-271.

Kinsella, S., Murdock, V., and O'Hare, N. "I'm eating a sandwich in Glasgow: modeling locations with tweets." *Proc., Proceedings of the 3rd international workshop on Search and mining user-generated contents*, ACM, Scotland, U.K., 61-68.

Klaus, A., Yu, S., and Plenz, D. (2011). "Statistical analyses support power law distributions found in neuronal avalanches." *PLoS ONE*, 6(5), e19779.

Kleinberg, J. (2007). "Computing: The wireless epidemic." *Nature*, 449(7160), 287-288.

Knutson, T. R., McBride, J. L., Chan, J., Emanuel, K., Holland, G., Landsea, C., Held, I., Kossin, J. P., Srivastava, A., and Sugi, M. (2010). "Tropical cyclones and climate change." *Nature Geoscience*, 3(3), 157-163.

Kwak, H., Lee, C., Park, H., and Moon, S. (2010). "What is Twitter, a social network or a news media?" *Proc., Proceedings of the 19th international conference on World wide web*, ACM, Raleigh, NC, 591-600.

Landsea, C. W., Vecchi, G. A., Bengtsson, L., and Knutson, T. R. (2010). "Impact of Duration Thresholds on Atlantic Tropical Cyclone Counts." *Journal of Climate*, 23(10), 2508-2519.

Laurance, S. W., Stouffer, P. C., and Laurance, W. F. (2004). "Effects of road clearings on movement patterns of understory rainforest birds in central Amazonia." *Conservation Biology*. 18(4), 1099-1109.

Lee, R., and Sumiya, K. "Measuring geographical regularities of crowd behaviors for Twitter-based geo-social event detection." *Proc., Proceedings of the 2nd ACM SIGSPATIAL international workshop on location based social networks*, ACM, San Jose, CA, 1-10.

Lee, R., Wakamiya, S., and Sumiya, K. (2011). "Discovery of unusual regional social activities using geo-tagged microblogs." *World Wide Web*, 14(4), 321-349.

Liang, X., Zheng, X., Lv, W., Zhu, T., and Xu, K. (2012). "The scaling of human mobility by taxis is exponential." *Physica A: Statistical Mechanics and its Applications*, 391(5), 2135-2144.

Lindqvist, J., Cranshaw, J., Wiese, J., Hong, J., and Zimmerman, J. "I'm the mayor of my house: examining why people use foursquare-a social-driven location sharing application."

Proc., Proceedings of the SIGCHI Conference on Human Factors in Computing Systems, ACM, Vancouver, BC, Canada, 2409-2418.

Mandelbrot, B. B. (1983). *The fractal geometry of nature*, New York: W.H. Freeman.

Mao, H., Shuai, X., and Kapadia, A. "Loose tweets: an analysis of privacy leaks on twitter." *Proc., Proceedings of the 10th annual ACM workshop on Privacy in the electronic society*, ACM, Chicago, 1-12.

Markoff, J. (2012). "Troves of personal data, forbidden to researchers." *New York Times*, New York Times, New York City, D1.

McGeeham, P. (2012). *"Wait for Power May Linger for Some. The New York Times. New York City."* **A20**. <http://www.nytimes.com/2012/11/02/nyregion/power-restoration-after-hurricane-sandy-may-take-longer-than-expected.html?_r=0>. (October 22, 2014).

Meehl, G. A., Washington, W. M., Collins, W. D., Arblaster, J. M., Hu, A., Buja, L. E., Strand, W. G., and Teng, H. (2005). "How much more global warming and sea level rise?" *Science*, 307(5716), 1769-1772.

Menassa, C., Kamat, V., Lee, S., Azar, E., Feng, C., and Anderson, K. (2014). "Conceptual Framework to Optimize Building Energy Consumption by Coupling Distributed Energy Simulation and Occupancy Models." *Journal of Computing in Civil Engineering*, 28(1), 50-62. 10.1061/(ASCE)CP.1943-5487.0000299.

Metzler, R., and Klafter, J. (2000). "The random walk's guide to anomalous diffusion: a fractional dynamics approach." *Physics Reports*, 339(1), 1-77.

Montroll, E. W., and Weiss, G. H. (1965). "Random walks on lattices. II." *Journal of Mathematical Physics*, 6(2), 167.

Morrow-Jone, H. A., and Morrow-Jone, C. R. (1991). "Mobility due to natural disaster: Theoretical considerations and preliminary analyses." *Disasters*, 15(2), 126-132.

NCO (2014). "GPA Accuracy." <http://www.gps.gov/governance/excom/nco/>. (April 17, 2014).

Nik Bakht, M., and El-Diraby, T. E. (2013). "Analyzing Infrastructure Discussion Networks: Order of "Influence" in Chaos of "Followers." *4th Construction Speciaty Conf.*, Canadian Society of Civil Engineers (CSCE), Montréal, Canada.

Noulas, A., Scellato, S., Lambiotte, R., Pontil, M., and Mascolo, C. (2012). "A tale of many cities: universal patterns in human urban mobility." *PLoS ONE*, 7(5), e37027.

Noulas, A., Scellato, S., Mascolo, C., and Pontil, M. (2011). "An Empirical Study of Geographic User Activity Patterns in Foursquare." *Proc., 5th Int. AAAI Conf. on Weblogs and Social Media*, Barcelona, Spain, 570–573.

OCHA (Office for the Coordination of Humanitarian Affairs). (2012). The Caribbean: Hurricane Sandy Situation Report No.2. (http://reliefweb.int/sites/reliefweb.int /files/resources/Situation_Report_351.pdf). (October 22, 2014).

Oerlemans, J. (1994). "Quantifying global warming from the retreat of glaciers." *Science*, 264(5156), 243-245.

Pan, X., Han, C. S., Dauber, K., and Law, K. H. (2007). "A multi-agent based framework for the simulation of human and social behaviors during emergency evacuations." *Ai & Society*, 22(2), 113-132.

Pearson, K. (1905). "The problem of the random walk." *Nature*, 72(1865), 294.

Ramos-Fernandez, G., Mateos, J. L., Miramontes, O., Cocho, G., Larralde, H., and Ayala-Orozco, B. (2004). "Lévy walk patterns in the foraging movements of spider monkeys (Ateles geoffroyi)." *Behavioral Ecology and Sociobiology*, 55(3), 223-230.

Ravetz, J. (2012). "Sociology of science: Keep standards high." *Nature*, 481(7379), 25-25.

Robusto, C. (1957). "The cosine-haversine formula." *The American Mathematical Monthly*, 64(1), 38-40.

Rosenzweig, C., and Solecki, W. (2014). "Hurricane Sandy and adaptation pathways in New York: Lessons from a first-responder city." *Global Environmental Change*, 28(0), 395-408.

Russell, M. (2011). *Mining the Social Web: Analyzing Data from Facebook, Twitter, LinkedIn, and Other Social Media Sites*, O'Reilly Media, Sebastopol, CA.

Russell, M. A. (2011). *21 Recipes for Mining Twitter*, O'Reilly Media, Sebastopol, CA.

Saltelli, A. (2008). *Global Sensitivity Analysis : The Primer*, Chichester, England; Hoboken, NJ: John Wiley.

Sampson, R. J. (2012). *Great American city: Chicago and the enduring neighborhood effect*. Chicago: University of Chicago Press.

Sandercock, G., Angus, C., and Barton, J. (2010). "Physical activity levels of children living in different built environments." *Preventive Medicine*, 50(4), 193-198.

Scellato, S., Mascolo, C., Musolesi, M., and Crowcroft, J. (2011). "Track globally, deliver locally: improving content delivery networks by tracking geographic social cascades." *Proceedings of the 20th international conference on World wide web*, ACM, Hyderabad, India, 457-466.

Scellato, S., Mascolo, C., Musolesi, M., and Latora, V. (2010). "Distance matters: geo-social metrics for online social networks." *Proceedings of the 3rd Wonference on Online social networks*, USENIX Association, Boston, MA, 8-8.

Scellato, S., Noulas, A., Lambiotte, R., and Mascolo, C. (2011). "Socio-Spatial Properties of Online Location-Based Social Networks." *Proc., 5th Int. AAAI Conf. on Weblogs and Social Media (ICWSM '11),* Barcelona, Spain, 329–336..

Schneider, C. M., Belik, V., Couronné, T., Smoreda, Z., and González, M. C. (2013). "Unravelling daily human mobility motifs." *Journal of The Royal Society Interface*, 10(84), 20130246.

Schuerman, M. (2013). "City: Evacuation Rate During Sandy Dangerously Low." <http://www.wnyc.org/story/291228-highs-and-lows-citys-sandy-response/>. (December 10, 2014).

Schwarz, A.-M., Béné, C., Bennett, G., Boso, D., Hilly, Z., Paul, C., Posala, R., Sibiti, S., and Andrew, N. (2011). "Vulnerability and resilience of remote rural communities to shocks and global changes: Empirical analysis from Solomon Islands." *Global Environmental Change*, 21(3), 1128-1140.

Smith, C. (2014). "How Many People Use 415 of the Top Social Media, Apps and Tools? (March 2014)." <http://expandedramblings.com/index.php/resource-how-many-people-use-the-top-social-media/3/#.U011P_ldU0M>. (Dec. 15, 2014).

Song, C., Koren, T., Wang, P., and Barabasi, A.-L. (2010a). "Modelling the scaling properties of human mobility." *Nature Physics*, 6(10), 818-823.

Song, C., Qu, Z., Blumm, N., and Barabási, A.-L. (2010b). "Limits of predictability in human mobility." *Science*, 327(5968), 1018-1021.

Spitzer, F., Spitzer, F., Spitzer, F., and Mathematician, A. (1964). *Principles of random walk*, Van Nostrand, Princeton.

Statistic Brain (2014). "Twitter Statistics." <http://www.statisticbrain.com/twitter-statistics/>. (January 10, 2014).

Stocker, T. F., Qin, D., Plattner, G.-K., Tignor, M., Allen, S. K., Boschung, J., Nauels, A., Xia, Y., Bex, V., and Midgley, P. M. (2013). "Climate change 2013: The physical science basis." *Intergovernmental Panel on Climate Change, Working Group I Contribution to the IPCC Fifth Assessment Report (AR5)(Cambridge Univ Press, New York)*.

Sutton, J., Hansard, B., and Hewett, P. "Changing channels: Communicating tsunami warning information in Hawaii." *Proc., Proceedings of the 3rd International Joint Topical Meeting on Emergency Preparedness and Response, Robotics, and Remote Systems*. Curran Associates, Red Hook, NY.

Sutton, J., Spiro, E., Butts, C., Fitzhugh, S., Johnson, B., and Greczek, M. (2013). "Tweeting the Spill: Online Informal Communications, Social Networks, and Conversational Microstructures during the Deepwater Horizon Oilspill." *International Journal of Information Systems for Crisis Response and Management (IJISCRAM)*, 5(1), 58-76.

Sutton, J., Spiro, E. S., Johnson, B., Fitzhugh, S., Gibson, B., and Butts, C. T. (2013). "Warning tweets: serial transmission of messages during the warning phase of a disaster event." *Information, Communication & Society*, 17(6), 765-787.

Sutton, J. N. (2009). "Social media monitoring and the democratic national convention: New tasks and emergent processes." *Journal of Homeland Security and Emergency Management*, 6(1), 1-20.

Sutton, J. N. (2010). "*Twittering Tennessee: Distributed networks and collaboration following a technological disaster", Proc., 7th Int. ISCRAM Conf.,* Information Systems for Crisis Response and Management, Brussels, Belgium.

Teves, O., and Bodeen, C. (2013). "Haiyan Storm Surges Caught Philippines by Surprise." <http://bigstory.ap.org/article/haiyan-storm-surges-caught-philippines-surprise>. (November 18, 2014).

Toole, J. L., Colak, S., Alhasoun, F., Evsukoff, A., and Gonzalez, M. C. (2014). "The path most travelled: Mining road usage patterns from massive call data." *arXiv:1403.0636vl*, <http://arxiv.org/pdf/1403 .0636v1.pdf>.

UNISDR (The United Nations Office for Disaster Risk Reduction). (2013). "*Disasters Impacts 2000–2012*". < http://www.preventionweb.net/files/31737 _20130312disaster20002012copy.pdf>. (October 22, 2014).

United Nations (2009). "Urban and Rural Areas 2009." United Nations, Department of Economic and Social Affairs, Population Division, United Nations, New York.

USCB (2012). "Age and Sex Composition in the United States: 2012. Table 1. Population by Age and Sex: 2012.", <http://www.census.gov/population/age/data/files/2012/2012gender_table1.xls>. (Dec. 15, 2014)

USCB (2012). "Income, Expenditures, Poverty, & Wealth: Household Income.", <http://www.census.gov/compendia/statab/cats/income_expenditures_poverty_wealth/household_income.html>. (Dec. 15, 2014).

USCB (2013). "Educational Attainment in the United States: 2013 – Detailed Tables. ." <https://www.census.gov/hhes/socdemo/education/data/cps/2013/tables.html>. (Dec. 15, 2014)

USCB (2014). "People QuickFacts." <http://quickfacts.census.gov/qfd/states/00000.html.>. (Dec. 15, 2014)

Van Dyck, D., Cardon, G., Deforche, B., and De Bourdeaudhuij, I. (2011). "Urban–rural differences in physical activity in belgian adults and the importance of psychosocial factors." *Journal of Urban Health*, 88(1), 154-167.

Vespignani, A. (2010). "Complex networks: The fragility of interdependency." *Nature*, 464(7291), 984-985.

Vicente, C. R., Freni, D., Bettini, C., and Jensen, C. S. (2011). "Location-related privacy in geo-social networks." *IEEE Internet Computing*, 15(3), 20-27.

Viswanathan, G., Afanasyev, V., Buldyrev, S., Murphy, E., Prince, P., and Stanley, H. E. (1996). "Lévy flight search patterns of wandering albatrosses." *Nature*, 381(6581), 413-415.

Wakamiya, S., Lee, R., and Sumiya, K. (2013). "Analyzing Distortion of Geo-social Proximity using Massive Crowd Moving Logs over Twitter." *IEICE technical report. Data engineering*, 113(105), 23-28.

Walker, R., Pettitt, J., Scruggs, K., and Mlakar, P. (2014). "Data Collection and Organization by Smartphone for Infrastructure Assessment." *Journal of Infrastructure Systems*, 20(1), 06013001. <10.1061/(ASCE)IS.1943-555X.0000166>.

Wang, F., and Landau, D. P. (2001). "Efficient, multiple-range random walk algorithm to calculate the density of states." *Phys. Rev. Lett.*, 86(10), 2050.

Wang, P., Hunter, T., Bayen, A. M., Schechtner, K., and González, M. C. (2012). "Understanding road usage patterns in urban areas." *Scientific reports*, 2. , <http://www.nature.com/srep/2012/121220/srep01001/pdf/ srep01001.pdf>.

Wang, P., Liu, L., Li, X., Li, G., and González, M. C. (2014). "Empirical study of long-range connections in a road network offers new ingredient for navigation optimization models." *New Journal of Physics*, 16(1), 013012.

Wang, Q., and Taylor, J. E. (2014). "Energy saving practice diffusion in online networks." *Energy and Buildings*, 76(0), 622-630.

Wang, Q., and Taylor, J. E. (2014). "Quantifying Human Mobility Perturbation and Resilience in Hurricane Sandy." *PLoS ONE*, 9(11), e112608.

Wang, Q., and Taylor, J. E. (2015). "Process Map for Urban-Human Mobility and Civil Infrastructure Data Collection Using Geosocial Networking Platforms." *Journal of Computing in Civil Engineering*, 0(0), 04015004.

Weber, E. U. (2010). "What shapes perceptions of climate change?" *Wiley Interdisciplinary Reviews: Climate Change*, 1(3), 332-342.

Wesolowski, A., Eagle, N., Tatem, A. J., Smith, D. L., Noor, A. M., Snow, R. W., and Buckee, C. O. (2012). "Quantifying the impact of human mobility on malaria." *Science*, 338(6104), 267-270.

Wilcove, D. S., McLellan C. H., and Dobson, A. P. (1986). "Habitat fragmentation in the temperate zone." *Conservation biology*. 6, 237-256.

White, H. (1982). "Maximum likelihood estimation of misspecified models." *Econometrica: Journal of the Econometric Society*, 1-25.

Wolff, J. O., Schauber E. M., and Edge, W. D. (1997). "Effects of habitat loss and fragmentation on the behavior and demography of gray‐tailed voles." *Conservation Biology*. 11 (4), 945-956.

Wolshon, B., and Marchive III, E. (2007). "Emergency planning in the urban-wildland interface: Subdivision-level analysis of wildfire evacuations." *Journal of Urban Planning and Development*, 133(1), 73-81.

World Bank (2013). "*World Development Indicator: Urban Population.*" The World Bank Group, New York City, New York.

APPENDIX A: SUPPLEMENTARY INFORMATION FOR CHAPTER 3[7]

A1 Supplementary Information Methods

This section presents the detailed description of methods used for data collection and analysis. This also includes supporting findings, figures and tables relating to the analytical results of the shifting distance of the center of movements and radius of gyrations.

A1.1 Data Collection

Human mobility data were collected from Twitter. We used the open API from Twitter to create a continuous connection between a computer in our research lab and a streaming endpoint at a Twitter server. The connection continuously downloaded tweets in real-time. Each public tweet was collected if the tweet had geolocation information, also called being geotagged, and if the coordinate was within 74˚15'W to 73˚40'W longitude and 40˚30'N to 40˚57'N latitude. Thus, the data collection was ensured coverage of the entirety of NYC. Every tweet included the text information, the tweet's ID, the name and ID of the user who posted the tweet, the time stamp when it was posted, and the coordinate. A reconnecting mechanism was coded so that if the streaming was lost for 30 seconds, a restart message was displayed and a new streaming connection established. We observed no reconnections during the 12 days of data collection. Despite power outages, we observed no break in our data. In fact, the number of tweets recorded during the first 24-hours after Hurricane Sandy struck the city was the second largest daily number of tweets collected over the 12 day data collection period, at 12 percent more than the average number of

[7] Appendix A was co-authored with Professor John E. Taylor and was published as the supporting information of Chapter 3 in the Journal of PLOS ONE.

geotagged tweets sent during the ensuing 11 days. The amount of data collected each 24-hour period can be found in Table A1.

We analyzed the time elapsed between every two consecutive tweets from each individual, and found the time followed a truncated power-law distribution with the scale-invariance β value only slightly larger than 1, which is in line with the β=0.9±0.1 reported in a previous study (González et al. 2008). The exponential cutoff λ was 3.93×10-6, and the minimum fitting value κ was 10 seconds. This distribution is plotted in Figure A1.

A1.2 Displacements Distribution Analysis

We found all the displacements using the retrieved movement trajectories. The distance between two coordinates was calculated using the Haversine formula:

$$d = 2r \times \sin^{-1}\left(\sqrt{\sin^2\left(\frac{\phi_2 - \phi_1}{2}\right) + \cos\phi_1 \cos\phi_2 \sin^2\left(\frac{\varphi_2 - \varphi_1}{2}\right)}\right)$$

Where r is the earth radius, which approximately equals to 6,367,000 meters, ϕ is the latitude, and φ is the longitude. We counted the numbers of trips within different ranges of distances, and results are shown in Figure 7A and Table A2.

Then we fitted the displacement data to truncated power-law distribution:

$$P(\Delta r) \propto \Delta r^{-\beta} e^{-\lambda \Delta r}$$

Where Δr is the displacement, β is the scaling parameter, λ is the exponential cutoff value. We found the displacement data in each 24-hour period followed a truncated power-law distribution. The results are shown in Figure 7B and Table A2. To test if the truncated power-law distribution

was the best fit, we conducted two tests: the Kolmogorov-Smirnov (*KS*) test, and Maximum Likelihood Estimation (MLE) to compare truncated power-law distribution to both exponential distribution and lognormal distribution. The results are shown in Table A3. For each 24-hour period, the data sample passed the *KS* test, and therefore, the truncated power-law distribution had a high-level of goodness of fit. Also, the comparison results confirmed that the truncated power-law distribution is a better fit compared to both lognormal and exponential distributions.

A1.3 Estimating the Shifting Distance of Center of Mass

The first parameter we used to capture the perturbation in human movement trajectory was the shift of center of mass. We first calculated the center of mass of movement trajectories $\vec{r}_{CM}^{\,P}$ during Hurricane Sandy using the following equation:

$$\vec{r}_{CM}^{\,P} = \frac{1}{n(t)} \sum_{i=1}^{n(t)} \vec{r}_i$$

where *n(t)* was the number of locations an individual visited in the 24-hour period, $\vec{r}_i$ was the coordinate. Then we calculated the center of mass for each 24-hour period from Oct. 30, 2012 to Nov. 10, 2012 using the equation listed above. Using the average center of mass in the normal state and the center of mass in perturbation state, the shifting distance Δd_{CM} was calculated using the following equation:

$$\Delta d_{CM} = \left| \vec{r}_{CM}^{\,P} - \vec{r}_{CM}^{\,N} \right|$$

Where $\vec{r}_{CM}^{\,P}$ is the center of mass of a movement trajectory in the perturbation state, and $\vec{r}_{CM}^{\,N}$ is the center of mass in the normal state. Using both the KS test and distribution comparison, we found

that the distribution of Δd_{CM} followed a stretched exponential distribution and the results are shown in Figure A2.

$$P(\Delta d_{CM}) = e^{-\Delta d_{CM}^{0.655}}$$

A1.4 Estimating the Radius of Gyration

The second parameter to describe perturbation of movement trajectories is the radius of gyration. Similar to the center of mass, we calculated the radius of gyration in each 24-hour period using the following equation (2)

$$r_g = \sqrt{\frac{1}{n(t)} \sum_{i=1}^{n(t)} (\vec{r} - \vec{r}_{CM})^2}$$

Where $\vec{r}_i$ was the coordinate, and $\vec{r}_{CM}$ was the center of mass of a movement trajectory in the each 24-hour period.

The radius of gyration in the perturbation states was calculated using 2241 active users from the first 24-hour period, and the radius of gyration in the steady states was the average values from Nov. 3 to Nov. 9. Both r_g^P and r_g^N followed truncated power-law distributions. The results of the fitting of the distributions are shown in Figure A3.

A1.5 Estimating Predictability

To understand if the perturbation of movement trajectories can be predicted, we first plotted Δd_{CM} and r_g^N with logarithmic axes (Figure 8A). The two parameters showed a positive correlation. To quantify the relation, we conducted a *t*-test between Δd_{CM} and r_g^N to find the correlation coefficient. We also conducted linear regression to develop the equation between the two parameters. Results

are shown in Figure 8A and Table A4. We followed a similar procedure to find the relation between $r_g{}^N$ and $r_g{}^N$. The results are shown in Figure 8B and Table A4.

A2 Supplementary Information Figures

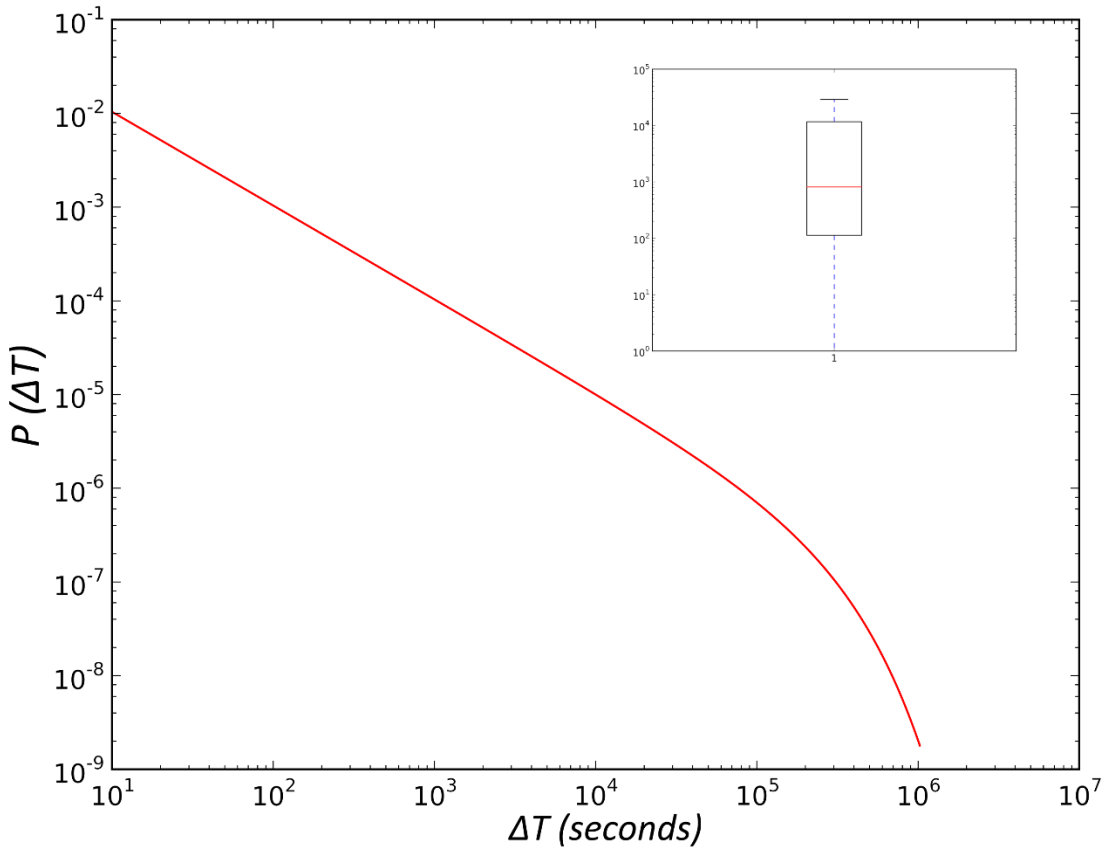

Figure A1: Distribution of Time Intervals. ΔT is the time interval between two consecutive tweets from the same individual. The distribution has β=1+6.3×10^{-9}, λ=3.93×10^{-6}, and κ=10 seconds. The inset is the box-and-whisker-plot of ΔT. The minimum value was 1 second, and the maximum value was 1,026,563 seconds (11.88 days). The median value was 813 seconds (13.55 minutes), the first quartile was 113 seconds (1.88 minutes), and third quartile was 11,677 seconds (3.24 hours). The whiskers show the 1.5 interquartile ranges.

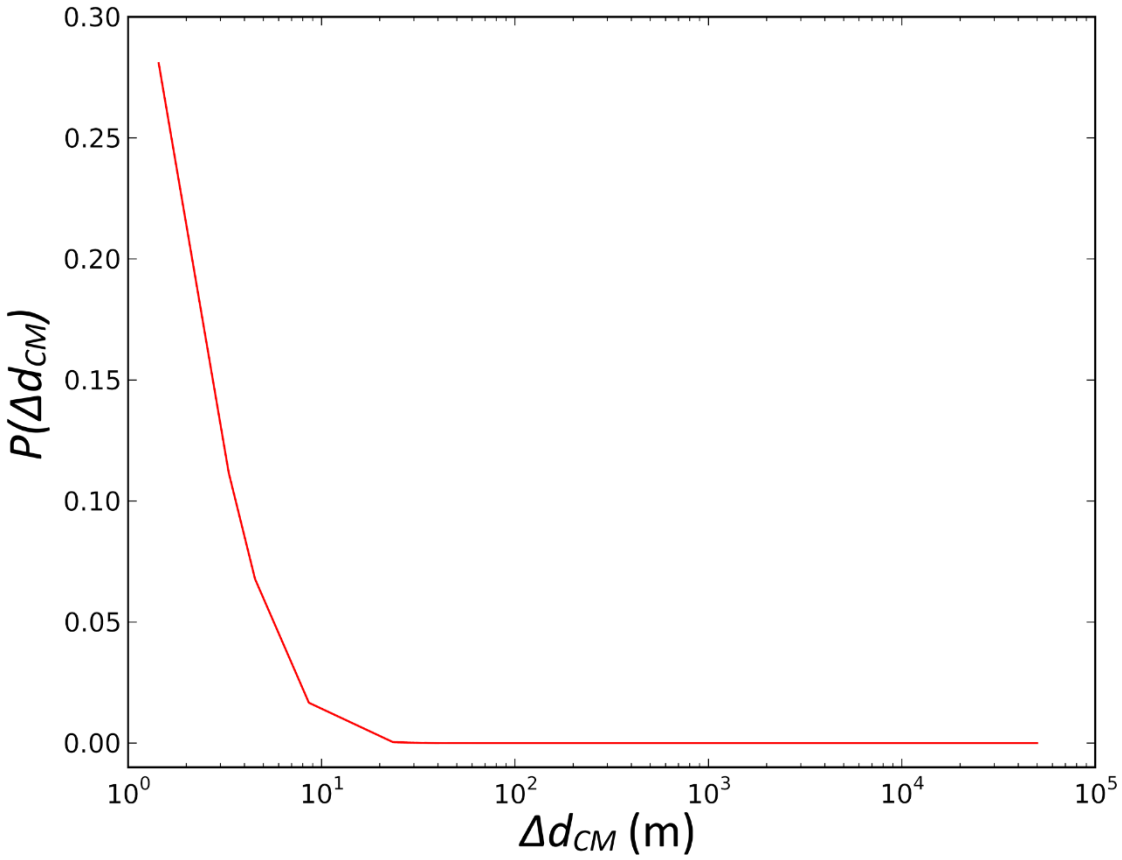

Figure A2: Distribution of Δd_{CM}. The distribution followed a stretched exponential distribution. Distribution comparison between lognormal distribution and stretched exponential distribution returned R=-233.13 (p<0.001) which favors the latter. Also, the comparison between truncated power-law and stretched exponential distributions returned R=-1042.49 (p<0.001) which favors the latter as well.

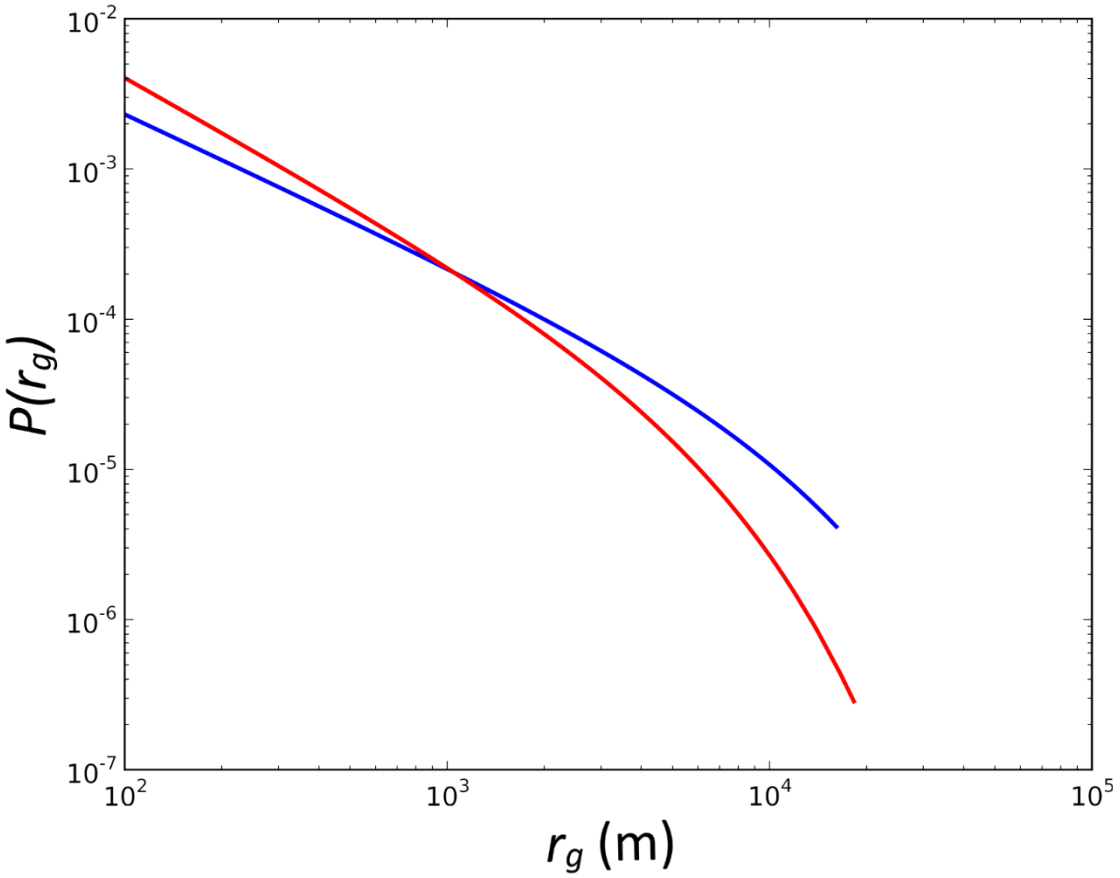

Figure A3: Distribution of r_g. r_g^P followed truncated power-law distributions (red line). It has β=1.19 which is close to the β value (1.20) reported in [1], λ=1.84×10^{-4}, and κ=100 m. However, r_g^N showed no such attribute (blue line).

A3 Supplementary Information Tables

Table A1: Data Volume for Each 24-Hour Period

Time Period	Number of Tweets
Day 1	63,086
Day 2	49,373
Day 3	55,864
Day 4	52,448
Day 5	65,800
Day 6	60,230
Day 7	54,403
Day 8	57,575
Day 9	57,813
Day 10	58,769
Day 11	50,543
Day 12	55,730

Table A2: Displacement Distribution

Days	1-100m	100-500m	500m-1km	1-5km	5-10km	>10km
1	23494	4949	1900	1713	254	294
2	16080	3040	1320	1920	453	367
3	18136	4057	1722	2602	563	403
4	17661	3593	1530	2230	559	382
5	21547	4407	1960	3004	674	424
6	20819	4051	1846	2671	561	409
7	18532	3725	1728	2313	597	501
8	18243	3711	1779	2731	886	745
9	18769	3681	1710	2730	824	639
10	20144	3689	1729	2458	612	538
11	15961	3302	1485	2310	702	571
12	15875	3782	1827	2948	917	795

Table A3: Displacement Fitting Results

Period	β Value	λ Value	κ Value (m)	*KS*-test	Lognormal Comparison	Exponential Comparison
Day 1	1.73	2.70E-05	591	0.025***	26.58***	1251.28***
Day 2	1.24	5.56E-05	4	0.023***	556.90***	43925.59***
Day 3	1.20	5.23E-05	4	0.022***	598.50***	36351.78***
Day 4	1.13	6.01E-05	3	0.015**	816.76***	39808.21***
Day 5	1.25	5.78E-05	4	0.025***	446.96***	34612.09***
Day 6	1.20	7.79E-05	4	0.022**	621.02***	36960.03***
Day 7	1.23	6.44E-05	4	0.022*	492.43***	37638.76***
Day 8	1.21	7.40E-05	4	0.021*	663.75***	44210.40***
Day 9	1.25	6.63E-05	5	0.030*	621.45***	39790.81***
Day 10	1.22	6.10E-05	4	0.022***	528.08***	40092.48***
Day 11	1.20	4.98E-05	4	0.030***	822.63***	42010.51***
Day 12	1.21	5.31E-05	4	0.021***	722.15***	42531.20***

* *p*-value<0.05, ** *p*-value<0.01, *** *p*-value<0.001

Table A4: Fitting Results between the Center of Mass and the Radius of Gyration

Relation	Coefficient Estimation		Std. Error	*t*-value
Δd_{CM}	Intercept Value	0.611	0.0595	10.28^{***}
	r_g^N coefficient	0.456	0.0276	16.55^{***}
r_g^P	Intercept Value	1.345	0.296	4.54^{***}
	r_g^N coefficient	0.276	0.087	3.16^{***}

* p-value<0.05, ** p-value <0.01, *** p-value <0.001

APPENDIX B: SUPPLEMENTARY INFORMATION FOR CHAPTER 4[8]

B1 Supplementary Information Table

Table B1: Complete Data Fitting Results

Case	Day	Scaling Parameter	Xmin[1]	Lognormal Comparison[2]	Exponential Comparison[3]
Wipha	1	1.00	1	522.46***	15890.04***
Wipha	2	1.00	1	540.51***	17419.26***
Wipha	3	1.00	1	602.09***	17523.11***
Wipha	4	1.00	1	573.39***	17315.68***
Wipha	5	1.00	1	493.87***	16332.13***
Wipha	6	1.00	1	625.35***	18314.91***
Wipha	7	1.00	1	596.34***	18740.83***
Wipha	8	1.00	1	463.86***	16025.27***
Wipha	9	1.00	1	464.58***	15316.92***
Wipha	10	1.00	1	494.3***	15364.37***
Wipha	11	1.00	1	448.48***	15511.45***
Wipha	12	1.00	1	455.47***	14414.25***
Wipha	13	1.00	1	394.69***	16635.77***
Wipha	14	1.00	1	405.43***	17240.04***
Wipha	15	1.00	1	537.36***	18700.86***
Wipha	16	1.00	1	676.01***	18692.28***
Wipha	17	1.00	1	646.42***	21682.6***
Wipha	18	1.00	1	440.99***	15117.24***
Wipha	19	1.00	1	431.45***	14248.4***
Wipha	20	1.00	1	491.23***	17291.01***
Wipha	21	1.00	1	671.23***	19332.81***
Wipha	22	1.00	1	655.87***	16304.15***
Wipha	23	1.00	1	460.14***	15364.21***
Wipha	24	1.00	1	496.5***	15778.3***
Wipha	25	1.00	1	609.73***	18214.82***
Wipha	26	1.00	1	589.23***	16092.69***
Wipha	27	1.00	1	496.33***	17740.77***
Wipha	28	1.00	1	448.44***	18613.65***
Wipha	29	1.00	1	470.9***	15129.74***
Wipha	30	1.00	1	556.44***	15561.4***

[8] Appendix B was co-authored with Professor John E. Taylor and serves as the supporting information of Chapter 4.

Case	Day	Scaling Parameter	Xmin[1]	Lognormal Comparison[2]	Exponential Comparison[3]
Wipha	31	1.00	1	192.57***	14770.86***
Wipha	32	1.00	1	470.05***	16946.51***
Wipha	33	1.00	1	408.12***	15875.09***
Wipha	34	1.00	1	329.19***	16348.15***
Halong	1	1.08	2	56.34***	5505.09***
Halong	2	1.09	2	67.05***	5211.8***
Halong	3	1.10	2	68.03***	5087.1***
Halong	4	1.06	2	109.86***	4484.07***
Halong	5	1.11	2	83.65***	5229.3***
Halong	6	1.11	2	73.82***	5546.28***
Halong	7	1.10	2	54.37***	5264.73***
Halong	8	1.09	2	74.58***	4737.1***
Halong	9	1.14	2	69.1***	6005.99***
Halong	10	1.16	2	74.06***	6868.52***
Halong	11	1.11	2	92.59***	6269.46***
Halong	12	1.10	2	73.49***	5430.27***
Halong	13	1.10	2	105.72***	5376.0***
Halong	14	1.06	2	99.85***	5009.56***
Halong	15	1.11	2	41.38***	4213.7***
Halong	16	1.09	2	78.29***	5885.46***
Halong	17	1.10	2	68.71***	5547.58***
Halong	18	1.08	2	75.97***	6179.17***
Halong	19	1.08	2	93.99***	5767.33***
Halong	20	1.06	2	82.08***	5807.33***
Halong	21	1.08	2	126.12***	4984.1***
Halong	22	1.10	2	80.55***	5904.64***
Halong	23	1.07	2	77.8***	4669.98***
Halong	24	1.10	2	88.1***	5713.79***
Halong	25	1.07	2	69.15***	4866.53***
Halong	26	1.10	2	87.7***	6209.91***
Halong	27	1.07	2	56.76***	5316.41***
Halong	28	1.09	2	97.22***	6250.5***
Halong	29	1.10	2	51.99***	6206.2***
Halong	30	1.11	2	58.2***	6190.21***
Halong	31	1.09	2	52.82***	5376.95***
Halong	32	1.11	2	89.8***	6414.53***
Halong	33	1.08	2	64.13***	5415.26***
Rammasun	1	1.40	3	115.37***	12973.6***
Rammasun	2	1.43	3	98.08***	13639.57***

Case	Day	Scaling Parameter	Xmin[1]	Lognormal Comparison[2]	Exponential Comparison[3]
Rammasun	3	1.34	3	149.47***	13407.53***
Rammasun	4	1.35	3	157.9***	14362.26***
Rammasun	5	1.30	3	163.62***	12541.22***
Rammasun	6	1.39	3	134.25***	15138.92***
Rammasun	7	1.43	3	101.99***	15440.3***
Rammasun	8	1.34	3	139.76***	14925.73***
Rammasun	9	1.33	3	161.43***	13559.84***
Rammasun	10	1.36	3	131.48***	14173.97***
Rammasun	11	1.31	3	138.91***	12288.75***
Rammasun	12	1.32	3	163.35***	13792.23***
Rammasun	13	1.38	3	149.73***	16137.91***
Rammasun	14	1.42	3	130.32***	17333.32***
Rammasun	15	1.36	3	170.21***	17620.49***
Rammasun	16	1.41	3	191.12***	23310.79***
Rammasun	17	1.32	3	96.26***	11943.99***
Rammasun	18	1.39	3	134.38***	17151.55***
Rammasun	19	1.34	3	152.82***	14906.02***
Rammasun	20	1.38	3	145.42***	17952.44***
Rammasun	21	1.40	3	121.69***	17349.34***
Rammasun	22	1.35	3	154.43***	14653.08***
Rammasun	23	1.33	3	137.51***	14823.2***
Rammasun	24	1.32	3	160.55***	14108.83***
Rammasun	25	1.32	3	168.09***	14820.26***
Rammasun	26	1.32	3	181.81***	13917.71***
Rammasun	27	1.38	3	153.75***	17093.03***
Rammasun	28	1.43	3	106.01***	17565.41***
Rammasun	29	1.37	3	140.13***	14694.57***
Rammasun	30	1.43	3	111.61***	17549.01***
Rammasun	31	1.33	3	152.28***	14782.05***
Rammasun	32	1.33	3	140.47***	15427.2***
Rammasun	33	1.32	3	162.89***	15268.24***
Rammasun	34	1.41	3	138.03***	18930.48***
Kalmaegi	1	1.25	1	15.09***	1358.09***
Kalmaegi	2	1.23	1	19.81***	1360.07***
Kalmaegi	3	1.26	1	15.49***	1881.58***
Kalmaegi	4	1.21	1	16.2***	1210.52***
Kalmaegi	5	1.28	1	9.47***	1364.42***
Kalmaegi	6	1.16	1	22.79***	1073.37***
Kalmaegi	7	1.35	1	5.97**	1919.13***

Case	Day	Scaling Parameter	Xmin[1]	Lognormal Comparison[2]	Exponential Comparison[3]
Kalmaegi	8	1.24	1	11.89***	1188.82***
Kalmaegi	9	1.41	1	5.3**	1935.71***
Kalmaegi	10	1.20	1	18.7***	1061.85***
Kalmaegi	11	1.24	1	7.99***	746.2***
Kalmaegi	12	1.21	1	11.2***	722.52***
Kalmaegi	13	1.31	1	4.54*	813.5***
Kalmaegi	14	1.10	1	12.39***	420.08***
Kalmaegi	15	1.13	1	23.15***	825.2***
Kalmaegi	16	1.40	1	-1	1852.92***
Kalmaegi	17	1.28	1	17.05***	2389.73***
Kalmaegi	18	1.30	1	8.82**	1721.6***
Kalmaegi	19	1.23	1	18.26***	1341.14***
Kalmaegi	20	1.28	1	9.86***	1533.66***
Kalmaegi	21	1.20	1	17.74***	975.47***
Kalmaegi	22	1.22	1	15.3***	1298.1***
Kalmaegi	23	1.29	1	19.05***	1962.5***
Kalmaegi	24	1.22	1	32.6***	2454.46***
Kalmaegi	25	1.27	1	13.47**	1465.49***
Kalmaegi	26	1.28	1	5.73**	838.39***
Kalmaegi	27	1.15	1	16.47***	630.19***
Kalmaegi	28	1.13	1	19.64***	620.27***
Kalmaegi	29	1.16	1	28.82***	1091.75***
Kalmaegi	30	1.25	1	12.46**	1736.08***
Kalmaegi	31	1.13	1	41.48***	1296.58***
Kalmaegi	32	1.25	1	8.37**	904.67***
Kalmaegi	33	1.16	1	21.63***	848.72***
Kalmaegi	34	1.19	1	17.22***	875.95***
Bohol	1	1.12	1	71.11***	3544.69***
Bohol	2	1.08	1	75.93***	2719.24***
Bohol	3	1.11	1	60.23***	2896.21***
Bohol	4	1.08	1	72.04***	2910.26***
Bohol	5	1.09	1	81.69***	3377.03***
Bohol	6	1.10	1	104.64***	3978.45***
Bohol	7	1.15	1	82.04***	4438.49***
Bohol	8	1.10	1	68.9***	3046.07***
Bohol	9	1.11	1	53.44***	3563.82***
Bohol	10	1.09	1	67.34***	2745.31***
Bohol	11	1.10	1	71.39***	3494.55***
Bohol	12	1.07	1	83.1***	2892.98***

Case	Day	Scaling Parameter	Xmin[1]	Lognormal Comparison[2]	Exponential Comparison[3]
Bohol	13	1.11	1	76.68***	3981.62***
Bohol	14	1.16	1	74.21***	5168.08***
Bohol	15	1.13	1	57.04***	2954.24***
Bohol	16	1.21	1	87.28***	12052.22***
Bohol	17	1.21	1	54.65***	8646.87***
Bohol	18	1.22	1	51.86***	6694.7***
Bohol	19	1.19	1	65.68***	5373.59***
Bohol	20	1.14	1	71.3***	4608.66***
Bohol	21	1.20	1	61.73***	8685.52***
Bohol	22	1.23	1	44.04***	6676.7***
Bohol	23	1.23	1	46.88***	5834.97***
Bohol	24	1.22	1	44.53***	5231.74***
Bohol	25	1.19	1	46.19***	4857.74***
Bohol	26	1.18	1	61.75***	4705.8***
Bohol	27	1.16	1	67.2***	4103.95***
Bohol	28	1.22	1	42.97***	4922.36***
Bohol	29	1.22	1	44.02***	6122.71***
Bohol	30	1.21	1	47.64***	4787.69***
Bohol	31	1.21	1	37.65***	5647.93***
Iquique	1	1.43	3	0.56	216.18***
Iquique	2	1.30	3	3.48*	462.83***
Iquique	3	1.32	3	3.66**	346.26***
Iquique	4	1.21	3	0.15	309.43***
Iquique	5	1.18	3	-0.56	409.82***
Iquique	6	1.28	3	-2.02	345.18***
Iquique	7	1.32	3	-9.04*	459.31***
Iquique	8	1.20	3	5.7*	547.9***
Iquique	9	1.16	3	8.5***	284.93***
Iquique	10	1.11	3	9.16***	220.76***
Iquique	11	1.16	3	5.95***	174.12***
Iquique	12	1.07	3	9.35***	187.97***
Iquique	13	1.24	3	2.41	255.43***
Iquique	14	1.37	3	0.73	330.84***
Iquique	15	1.15	3	8.33***	337.83***
Iquique	16	1.07	3	6.61**	204.82***
Iquique	17	1.12	3	-4.76	428.9***
Iquique	18	1.23	3	6.5***	535.66***
Iquique	19	1.32	3	5.02***	976.68***
Iquique	20	1.31	3	5.39***	540.19***

Case	Day	Scaling Parameter	Xmin[1]	Lognormal Comparison[2]	Exponential Comparison[3]
Iquique	21	1.26	3	5.39***	460.8***
Iquique	22	1.25	3	6.24***	402.64***
Iquique	23	1.36	3	2.61*	394.95***
Iquique	24	1.32	3	3.74**	628.69***
Iquique	25	1.32	3	4.05**	522.83***
Iquique	26	1.35	3	2.58**	488.06***
Iquique	27	1.34	3	-4.71	445.09***
Iquique	28	1.43	3	1.46	538.78***
Iquique	29	1.35	3	6.46***	833.31***
Iquique	30	1.28	3	12.27***	1369.89***
Iquique	31	1.35	3	10.22***	1410.85***
Napa	1	1.42	6	7.15***	1272.13***
Napa	2	1.47	6	5.83***	1038.89***
Napa	3	1.38	6	11.81***	1118.2***
Napa	4	1.34	6	15.61***	1054.13***
Napa	5	1.49	6	6.99***	1539.98***
Napa	6	1.43	6	8.56***	1119.93***
Napa	7	1.41	6	11.46***	1266.87***
Napa	8	1.49	6	6.78***	1280.35***
Napa	9	1.49	6	6.62***	1457.53***
Napa	10	1.39	6	9.58***	1111.43***
Napa	11	1.35	6	13.28***	896.88***
Napa	12	1.47	6	6.53***	1088.76***
Napa	13	1.44	6	8.13***	1243.46***
Napa	14	1.47	6	7.29***	1252.18***
Napa	15	1.37	6	16.05***	1149.79***
Napa	16	1.38	6	13.69***	1018.2***
Napa	17	1.33	6	19.2***	1050.78***
Napa	18	1.35	6	13.45***	970.62***
Napa	19	1.45	6	6.86***	1026.65***
Napa	20	1.38	6	11.79***	1107.22***
Napa	21	1.36	6	13.8***	980.09***
Napa	22	1.38	6	14.52***	1190.63***
Napa	23	1.34	6	16.61***	1058.66***
Napa	24	1.28	6	21.57***	873.68***
Napa	25	1.43	6	9.94***	1376.51***
Napa	26	1.23	6	65.3***	2241.0***
Napa	27	1.38	6	18.88***	1485.56***
Napa	28	1.42	6	16.3***	1690.35***

Case	Day	Scaling Parameter	Xmin[1]	Lognormal Comparison[2]	Exponential Comparison[3]
Napa	29	1.35	6	16.17***	989.29***
Napa	30	1.32	6	19.14***	949.33***
Napa	31	1.28	6	19.36***	848.0***
Norfolk	1	1.30	3	41.95***	5292.83***
Norfolk	2	1.31	3	40.04***	4960.98***
Norfolk	3	1.28	3	36.43***	3958.71***
Norfolk	4	1.35	3	27.48***	5166.28***
Norfolk	5	1.37	3	21.29***	5388.42***
Norfolk	6	1.29	3	41.26***	4524.78***
Norfolk	7	1.28	3	40.61***	4498.48***
Norfolk	8	1.30	3	33.79***	4280.03***
Norfolk	9	1.30	3	33.17***	3991.5***
Norfolk	10	1.23	3	54.12***	3775.52***
Norfolk	11	1.30	3	26.63***	4055.89***
Norfolk	12	1.37	3	20.7***	5284.65***
Norfolk	13	1.28	3	38.35***	4076.61***
Norfolk	14	1.32	3	30.54***	4376.95***
Norfolk	15	1.31	3	36.82***	4905.99***
Norfolk	16	1.30	3	39.55***	5049.72***
Norfolk	17	1.29	3	36.3***	4299.86***
Norfolk	18	1.32	3	30.72***	4363.66***
Norfolk	19	1.40	3	14.13***	5444.36***
Norfolk	20	1.28	3	39.54***	4495.37***
Norfolk	21	1.28	3	39.19***	4184.33***
Norfolk	22	1.30	3	31.86***	4333.82***
Norfolk	23	1.29	3	35.5***	4203.18***
Norfolk	24	1.27	3	40.11***	4376.94***
Norfolk	25	1.35	3	25.43***	5344.27***
Norfolk	26	1.42	3	13.53***	6591.65***
Norfolk	27	1.33	3	26.8***	4825.96***
Norfolk	28	1.35	3	21.51***	4851.11***
Norfolk	29	1.32	3	28.36***	4399.09***
Norfolk	30	1.31	3	31.18***	4600.62***
Norfolk	31	1.29	3	39.69***	4575.32***
Hamburg	1	1.12	1	16.42***	621.79***
Hamburg	2	1.05	1	17.73***	453.31***
Hamburg	3	1.05	1	11.89***	404.06***
Hamburg	4	1.11	1	5.89*	395.68***
Hamburg	5	1.12	1	4.76	488.16***

Case	Day	Scaling Parameter	Xmin[1]	Lognormal Comparison[2]	Exponential Comparison[3]
Hamburg	6	1.06	1	13.29***	510.73***
Hamburg	7	1.04	1	13.17***	509.95***
Hamburg	8	1.02	1	18.81***	389.85***
Hamburg	9	1.03	1	9.19**	359.7***
Hamburg	10	1.00	1	17.22***	426.04***
Hamburg	11	1.07	1	6.53*	475.63***
Hamburg	12	1.07	1	5.29*	324.77***
Hamburg	13	1.00	1	13.85***	206.52***
Hamburg	14	1.00	1	11.87***	355.13***
Hamburg	15	1.01	1	15.7***	371.85***
Hamburg	16	1.11	1	1.37	658.46***
Hamburg	17	1.06	1	10.12**	500.3***
Hamburg	18	1.06	1	5.54	392.94***
Hamburg	19	1.16	1	3.32	384.85***
Hamburg	20	1.06	1	11.66***	387.39***
Hamburg	21	1.00	1	16.05***	223.67***
Hamburg	22	1.01	1	12.83***	350.58***
Hamburg	23	1.07	1	12.95***	456.78***
Hamburg	24	1.00	1	20.39***	296.3***
Hamburg	25	1.01	1	11.44***	295.37***
Hamburg	26	1.07	1	6.32**	278.46***
Hamburg	27	1.00	1	22.29***	224.28***
Hamburg	28	1.00	1	17.06***	205.88***
Hamburg	29	1.00	1	18.0***	307.77***
Hamburg	30	1.04	1	10.35***	301.97***
Hamburg	31	1.00	1	17.94***	332.82***
Atlanta	1	1.29	5	47.51***	3912.13***
Atlanta	2	1.30	5	48.89***	3706.45***
Atlanta	3	1.26	5	62.1***	3604.21***
Atlanta	4	1.29	5	56.81***	3686.4***
Atlanta	5	1.37	5	31.23***	4042.66***
Atlanta	6	1.32	5	49.09***	3710.96***
Atlanta	7	1.32	5	43.36***	4029.07***
Atlanta	8	1.31	5	51.45***	4202.53***
Atlanta	9	1.33	5	35.54***	3929.05***
Atlanta	10	1.27	5	63.22***	4273.64***
Atlanta	11	1.28	5	63.96***	4381.42***
Atlanta	12	1.25	5	74.01***	4484.44***
Atlanta	13	1.39	5	28.19***	5187.56***

Case	Day	Scaling Parameter	Xmin[1]	Lognormal Comparison[2]	Exponential Comparison[3]
Atlanta	14	1.28	5	60.27***	4281.44***
Atlanta	15	1.30	5	76.06***	6736.03***
Atlanta	16	1.45	5	-22.6**	5395.63***
Atlanta	17	1.43	5	26.24***	5538.64***
Atlanta	18	1.30	5	61.89***	4674.06***
Atlanta	19	1.27	5	74.23***	4608.4***
Atlanta	20	1.38	5	33.99***	5263.23***
Atlanta	21	1.34	5	44.02***	4575.93***
Atlanta	22	1.31	5	60.59***	4791.65***
Atlanta	23	1.30	5	53.82***	4041.89***
Atlanta	24	1.24	5	72.12***	3582.09***
Atlanta	25	1.23	5	82.96***	4097.88***
Atlanta	26	1.25	5	65.32***	4061.39***
Atlanta	27	1.36	5	36.14***	4929.58***
Atlanta	28	1.26	5	72.13***	4738.58***
Atlanta	29	1.42	5	22.51***	5702.91***
Atlanta	30	1.54	5	-19.62**	6075.7***
Atlanta	31	1.45	5	11.82***	5463.94***
Phoenix	1	1.37	5	153.65***	25988.16***
Phoenix	2	1.28	5	309.86***	22205.19***
Phoenix	3	1.28	5	339.11***	23940.53***
Phoenix	4	1.24	5	349.67***	20177.3***
Phoenix	5	1.23	5	406.02***	21228.94***
Phoenix	6	1.21	5	437.94***	19006.33***
Phoenix	7	1.31	5	241.63***	23106.08***
Phoenix	8	1.34	5	212.37***	26660.57***
Phoenix	9	1.41	5	123.89***	28031.78***
Phoenix	10	1.30	5	308.21***	26497.92***
Phoenix	11	1.29	5	317.96***	23911.48***
Phoenix	12	1.29	5	327.89***	25244.33***
Phoenix	13	1.21	5	439.64***	19173.58***
Phoenix	14	1.30	5	270.64***	22604.58***
Phoenix	15	1.42	5	122.23***	29565.39***
Phoenix	16	1.34	5	326.38***	36424.54***
Phoenix	17	1.30	5	301.39***	23966.43***
Phoenix	18	1.27	5	335.89***	22357.02***
Phoenix	19	1.26	5	341.7***	21486.78***
Phoenix	20	1.19	5	463.78***	17837.27***
Phoenix	21	1.29	5	275.61***	21919.64***

Case	Day	Scaling Parameter	Xmin[1]	Lognormal Comparison[2]	Exponential Comparison[3]
Phoenix	22	1.40	5	145.52***	28327.03***
Phoenix	23	1.29	5	315.77***	23951.23***
Phoenix	24	1.23	5	445.82***	25741.24***
Phoenix	25	1.25	5	315.34***	18815.52***
Phoenix	26	1.23	5	268.62***	13802.69***
Phoenix	27	1.17	5	339.66***	12313.97***
Phoenix	28	1.27	5	208.94***	14869.42***
Phoenix	29	1.36	5	132.07***	18912.31***
Phoenix	30	1.29	5	200.42***	15388.26***
Phoenix	31	1.27	5	221.81***	15441.31***
Detroit	1	1.37	5	307.41***	36677.93***
Detroit	2	1.36	5	279.44***	31541.65***
Detroit	3	1.33	5	323.61***	31137.64***
Detroit	4	1.34	5	312.75***	31350.02***
Detroit	5	1.29	5	361.37***	27063.4***
Detroit	6	1.24	5	510.72***	30125.61***
Detroit	7	1.31	5	379.34***	34327.56***
Detroit	8	1.38	5	215.45***	32300.68***
Detroit	9	1.39	5	235.14***	34447.59***
Detroit	10	1.38	5	254.73***	31710.3***
Detroit	11	1.33	5	349.79***	31395.0***
Detroit	12	1.30	5	409.6***	30399.96***
Detroit	13	1.27	5	419.26***	27414.83***
Detroit	14	1.40	5	204.05***	32676.09***
Detroit	15	1.38	5	234.61***	30693.32***
Detroit	16	1.35	5	269.08***	29431.99***
Detroit	17	1.34	5	318.81***	29393.67***
Detroit	18	1.32	5	354.77***	31516.87***
Detroit	19	1.30	5	356.54***	27722.4***
Detroit	20	1.29	5	357.94***	26077.83***
Detroit	21	1.33	5	266.64***	25613.08***
Detroit	22	1.39	5	108.64***	15689.28***
Detroit	23	1.32	5	159.81***	14285.39***
Detroit	24	1.30	5	168.76***	12445.07***
Detroit	25	1.28	5	191.85***	12479.36***
Detroit	26	1.24	5	222.52***	11473.54***
Detroit	27	1.29	5	161.17***	11317.58***
Detroit	28	1.34	5	119.71***	12266.16***
Detroit	29	1.30	5	180.34***	13461.11***

Case	Day	Scaling Parameter	Xmin[1]	Lognormal Comparison[2]	Exponential Comparison[3]
Detroit	30	1.31	5	145.59***	12267.05***
Detroit	31	1.34	5	162.21***	14211.81***
Baltimore	1	1.34	5	120.86***	9411.18***
Baltimore	2	1.35	5	103.34***	9793.81***
Baltimore	3	1.36	5	107.42***	10306.4***
Baltimore	4	1.34	5	121.75***	9723.51***
Baltimore	5	1.31	5	144.88***	9963.87***
Baltimore	6	1.29	5	112.26***	8728.37***
Baltimore	7	1.38	5	91.37***	10223.88***
Baltimore	8	1.36	5	101.02***	9747.42***
Baltimore	9	1.32	5	108.61***	8556.41***
Baltimore	10	1.36	5	112.14***	10365.85***
Baltimore	11	1.33	5	133.76***	10430.14***
Baltimore	12	1.27	5	177.03***	10137.35***
Baltimore	13	1.27	5	149.61***	9112.38***
Baltimore	14	1.32	5	113.53***	9856.63***
Baltimore	15	1.35	5	109.67***	10673.02***
Baltimore	16	1.42	5	82.13***	12484.44***
Baltimore	17	1.34	5	117.45***	10083.22***
Baltimore	18	1.35	5	107.56***	9287.11***
Baltimore	19	1.29	5	129.47***	8353.46***
Baltimore	20	1.32	5	125.04***	8700.17***
Baltimore	21	1.42	5	69.1***	10340.08***
Baltimore	22	1.40	5	89.44***	11581.29***
Baltimore	23	1.40	5	77.54***	11956.29***
Baltimore	24	1.37	5	111.48***	11455.12***
Baltimore	25	1.32	5	118.46***	8854.2***
Baltimore	26	1.34	5	114.61***	9238.23***
Baltimore	27	1.36	5	92.9***	8990.97***
Baltimore	28	1.41	5	74.74***	10126.66***
Baltimore	29	1.33	5	129.08***	9752.21***
Baltimore	30	1.31	5	135.56***	9439.43***
Baltimore	31	1.24	5	166.69***	7244.04***
AuFire1	1	1.38	5	8.32***	1128.1***
AuFire1	2	1.36	5	7.22***	1126.33***
AuFire1	3	1.28	5	15.99***	1425.95***
AuFire1	4	1.34	5	8.5***	1271.22***
AuFire1	5	1.30	5	13.3***	1398.02***
AuFire1	6	1.42	5	4.51***	1250.05***

Case	Day	Scaling Parameter	Xmin[1]	Lognormal Comparison[2]	Exponential Comparison[3]
AuFire1	7	1.34	5	6.79***	824.3***
AuFire1	8	1.34	5	7.6***	996.69***
AuFire1	9	1.29	5	7.97***	993.17***
AuFire1	10	1.29	5	15.17***	1480.55***
AuFire1	11	1.26	5	12.68***	1046.9***
AuFire1	12	1.31	5	7.29***	742.98***
AuFire1	13	1.33	5	6.75***	846.97***
AuFire1	14	1.39	5	6.42***	1312.8***
AuFire1	15	1.28	5	7.07***	770.35***
AuFire1	16	1.25	5	11.53***	995.34***
AuFire1	17	1.23	5	13.5***	782.51***
AuFire1	18	1.24	5	13.23***	864.82***
AuFire1	19	1.35	5	7.82***	1395.08***
AuFire1	20	1.45	5	5.93***	1758.1***
AuFire1	21	1.36	5	7.88***	1488.44***
AuFire1	22	1.37	5	7.01***	1362.07***
AuFire1	23	1.35	5	8.51***	1502.27***
AuFire1	24	1.29	5	14.75***	1313.13***
AuFire1	25	1.41	5	6.95***	1605.14***
AuFire1	26	1.39	5	1.48	1368.14***
AuFire1	27	1.34	5	10.04***	1151.24***
AuFire1	28	1.33	5	10.93***	1269.62***
AuFire2	1	1.35	5	19.77***	2412.84***
AuFire2	2	1.25	5	28.99***	2312.84***
AuFire2	3	1.26	5	34.63***	2446.69***
AuFire2	4	1.24	5	33.47***	2146.04***
AuFire2	5	1.21	5	29.11***	1693.35***
AuFire2	6	1.34	5	14.29***	2026.56***
AuFire2	7	1.25	5	27.37***	1702.49***
AuFire2	8	1.24	5	29.71***	1656.73***
AuFire2	9	1.23	5	33.11***	1640.66***
AuFire2	10	1.21	5	45.57***	2165.76***
AuFire2	11	1.21	5	35.37***	1752.44***
AuFire2	12	1.20	5	32.07***	1506.98***
AuFire2	13	1.31	5	21.51***	1819.72***
AuFire2	14	1.31	5	25.51***	2549.98***
AuFire2	15	1.27	5	28.06***	2000.29***
AuFire2	16	1.27	5	32.64***	2263.94***
AuFire2	17	1.21	5	35.68***	1809.06***

Case	Day	Scaling Parameter	Xmin[1]	Lognormal Comparison[2]	Exponential Comparison[3]
AuFire2	18	1.22	5	38.94***	1807.62***
AuFire2	19	1.29	5	31.14***	2437.33***
AuFire2	20	1.39	5	15.12***	2918.18***
AuFire2	21	1.31	5	24.01***	2338.01***
AuFire2	22	1.27	5	27.53***	1867.91***
AuFire2	23	1.26	5	31.47***	2155.15***
AuFire2	24	1.22	5	41.03***	2040.38***
AuFire2	25	1.33	5	22.44***	2546.69***
AuFire2	26	1.32	5	19.84***	2294.59***
AuFire2	27	1.26	5	35.66***	2172.5***
AuFire2	28	1.30	5	25.89***	2438.27***

[1] Xmin is the minimum distance that was used to fit to the truncated power-law distribution

[2] Positive value means the fitting favored truncated power-law. Negative means the fitting favored lognormal distribution

[3] Positive value means the fitting favored truncated power-law. Negative means the fitting favored exponential distribution

*significant at $p< 0.05$; ** significant at $p<0.01$; ***significant at $p<0.001$